Metaorganism Metabolomics: *Hydra* as a tool for understanding the role of bacterial metabolites in shaping the metabolic landscape of the host

Dissertation

zur Erlangung des Doktorgrades der Mathematisch-Naturwissenschaftlichen Fakultät der Christian-Albrechts-Universität zu Kiel

vorgelegt von

Danielle M. M. Harris

Kiel, im Mai 2020

First reader: Prof. Dr. Dr. h. c. Thomas C.G. Bosch

Second reader: Prof. Dr. Thomas Roeder

Date of oral examination: June 23, 2020

Table of Contents

Abstract

With increased focus on host-microbe dynamics over the past decade, evidence that resident microbes affect host behaviour has mounted. Bacteria may be responsible for some of these effects as they produce a number of neuroactive compounds that could influence nervous system structure and function, leading to changes in behavioural phenotype. In the fresh water cnidarian *Hydra*, two behaviours are altered by microbiota: contraction frequency and feeding response duration. Here, I investigate the potential of resident microbiota to influence the structure and function of the nervous system in the early metazoan *Hydra vulgaris* AEP.

I assess changes to nervous system structure by looking for altered neurogenesis and nerve cell density in adult polyps and find both unaltered in germ-free animals. This does not rule out the possibility of early-life alterations or smaller-scale changes to nervous system anatomy. Next, I present a metabolomics pipeline to aid in the identification of bacterially-derived, contraction-regulating compounds. Future work in identifying these compounds can take advantage of the new extraction process detailed here, which can easily be reproduced from the isolated stocks of *Hydra*'s five main colonizing bacterial strains.

I demonstrate the utility of the metabolomics pipeline in bioactive molecule identification by identifying a dipeptide potentially responsible for the increased chemotaxis of bacterial colonizers towards germ-free *Hydra*. This may be a new mechanism for host-led shaping of microbial community composition.

Finally, I assess the potential role of *Hydra* microbiota in influencing nervous system function by searching for in vitro neurotransmitter production by *Hydra*-associated microbes and find that the microbial community produces gamma-aminobutyric acid (GABA). Metabolic modelling confirmed the presence of GABA-synthesizing enzymes in the genomes of all five main colonizers, though only *Duganella* seems to possess secretory ability via a GABA transporter. Both GABA and *Hydra* microbiota are reported to increase the duration of the feeding response, so microbial GABA production may play a role in increasing feeding response duration. As GABA feeds into central carbon metabolism, I further analyse the role of the *Hydra* metabolite and GABA precursor putrescine on the growth of the bacterial colonizers, and find all colonizers are able to grow in a medium that contains putrescine as a

sole carbon and nitrogen source. This suggests that any microbial manipulation of behaviour via GABA is a by-product of core metabolic processes in the bacteria. The work presented here demonstrates the utility of untargeted metabolomics for approaching a mechanistic understanding of host-microbe interactions.

Zusammenfassung

Mit zunehmender Forschung an Wirt-Mikroben-Interaktionen in den letzten Jahren zeigt sich mehr und mehr, dass Mikroben das Verhalten ihres Wirtes beeinflussen können. Bakterien produzieren eine Reihe neuroaktiver Verbindungen, die Einfluss auf Struktur und Funktion des Nervensystems haben und zu Änderungen im Verhalten führen können. Im Süßwasserpolypen *Hydra* werden zwei Verhalten durch die Mikrobiota verändert: die Kontraktionsfrequenz und die Dauer der Nahrungsaufnahme. In dieser Promotion untersuche ich das Potenzial der Mikrobiota die Struktur und Funktion des Nervensystems des frühen Metazoen-*Hydra vulgaris* AEP zu beeinflussen.

Ich untersuche Veränderungen der Struktur des Nervensystems durch Analyse von Neurogenese und Nervenzelldichte in adulten Polypen, und finde beides unverändert in keimfreien im Vergleich zu konventionell angezogenen Tieren. Dies schließt kleinere anatomische Unterschiede oder Veränderungen zu früheren Zeitpunkten in der Entwicklung nicht aus.

Als nächstes stelle ich eine Metabolomik-Pipeline vor, die bei der Identifizierung von bakteriellen, kontraktionsregulierenden Verbindungen helfen soll. Obwohl kein einzelnes Molekül für diese Verhalten verantwortlich zu sein scheint, zeige ich den Nutzen der Pipeline bei der Identifizierung bioaktiver Moleküle auf. Mithilfe der Pipeline konnte ich ein Dipeptid identifizieren, das möglicherweise für die erhöhte Chemotaxis von Bakterien in Richtung keimfreier *Hydra* verantwortlich ist. Dies könnte ein neuer Mechanismus für den Einfluss des Wirtes auf die Zusammensetzung der Mikrobiota sein.

Zuletzt untersuche ich die potenzielle Rolle der *Hydra*-Mikrobiota im Einfluss auf das Nervensystems, indem ich die Neurotransmitterproduktion durch *Hydra*-assoziierte Bakterien in vitro quantifiziere. Dies zeigt, dass die Mikrobiota von *Hydra* den Neurotransmitter Gamma-Aminobuttersäure (GABA) produziert. Stoffwechselmodellierungen bestätigen GABA-synthetisierende Enzymen in den Genomen aller fünf Hauptmitglieder der Mikrobiota, obwohl nur *Duganella* über einen GABA-Antiporter sekretionsfähig scheint. Da sowohl GABA als auch die Mikrobiota von *Hydra* Fressdauer des Polypenverlängern können, ist es möglich,

dass die die mikrobielle GABA-Produktion hier eine Rolle spielt. Da GABA Teil des zentralen Kohlenstoffmetabolismus ist, analysiere ich darüber hinaus die Rolle von Putrescin, einem GABA-Vorläufer und Teil des Metabolismus von *Hydra*, im Hinblick auf das Wachstum von Mikrobiotamitgliedern in vitro. Da alle untersuchten Bakterien in der Lage sind mit Putrescin als einziger Energiequelle zu wachsen, legt nahe, dass jede mikrobielle Manipulation des Verhaltens durch GABA ein Nebenprodukt der Kernstoffwechselprozesse der Bakterien ist.

Introduction

Our understanding of host-microbe interactions has expanded greatly in the past decade, with an astonishing, and seemingly ever-mounting, array of aspects of host biology affected. From metabolism[1] and fertility[2], to pathogen defense[3] and even behaviour[4], the breadth of these effects is so vast that they call into question the very concept of self[5]. Reflecting this change in perception, the term "metaorganism" is often used in connection with host-microbe interactions, defining the eukaryotic host within the context of its microbiota: the prokaryotes, unicellular eukaryotes, fungi and the viruses that reside in or on the host organism[6]. When considering the challenge that the metaorganism concept imparts on our concept of self[5], one could argue that the influence that microbes appear to have on behaviour is of particular importance, for who are we if not the sum of our actions?

The microbiome and nervous system anatomy

Microbiota could induce structural changes to the nervous system by impacting neurogenesis and/or apoptosis rates, ultimately influencing neuronal density. Indeed, neurogenesis is regulated in part by brain-derived neurotrophic factor (BDNF), and BDNF expression levels are reduced in germ-free animals[7]. Similar to germ-free mice, chronically stressed mice have low levels of BDNF. Probiotic supplementation did not simply restore the expression levels of BDNF, but increased BDNF expression levels such that they were higher than expression levels in sham-treated control mice[8]. In the same study, probiotic treatment prevented stress-induced decreases in hippocampal neurogenesis.

Several research groups found an impact of the gut microbiota on adult hippocampal neurogenesis in mice, albeit the direction of the effect differed between the experiments. Möhle et al. uncovered a decrease in hippocampal neurogenesis in antibiotic-treated mice that could be corrected with probiotic supplementation[9]. Conversely, adult germ-free mice (germ-free from birth) have increased rates of hippocampal neurogenesis when compared to conventionally colonized mice[4]. The rate of neurogenesis was not restored to normal levels following recolonization of these germ-free animals, suggesting that microbial mediation of neurogenesis could occur during a critical period of development. In mammals, mediation of neurogenesis by the microbiome may occur through the vagus nerve, an important conduit through which the microbiota and brain are thought to communicate. It is a component of

the parasympathetic nervous system that influences immune responses, heart rate, digestion and mood[10]. Consistent with the findings of Ogbonnaya et al., mice with a severed vagus nerve had decreased rates of neurogenesis compared to control animals[11]. Accompanying neurogenesis changes were correlated with decreases in BDNF expression. Curiously, unlike the mouse study, vagotomy in rats did not result in altered neurogenesis[12].

Although the direction of the effect is unclear, host microbiota do appear to influence adult neurogenesis in mammals, and this could impact nerve-cell density. Assessing the ability of microbiota to mediate of nerve-cell density is important because certain cognitive diseases that are associated with dysbiosis, e.g. depression and autism[13,14], are also associated with changes to nerve-cell density.

The microbiome and nervous system function

Another way in which microbiota impact the nervous system is through functional changes. For example, application of the bacterium *Lactobacillus rhamnosus* to the intestinal tract of germ-free mice increased the constitutive firing rate of the mesenteric nerve bundle (the mesenteric nerve bundle connects with the vagus nerve, an important conduit between bacteria, the gut and the brain)[15]. There are also a variety of studies that have demonstrated the production of various neurotransmitters by bacteria. These include gamma-aminobutyric acid (GABA), serotonin, dopamine and norepinephrine[16,17]. It is not clear whether or not the production of these compounds occurs at physiologically relevant amounts in vivo, however. Besides direct neurotransmitter production, bacteria can also influence the levels of host-derived neurotransmitters; the production of colonic serotonin is stimulated by short chain fatty acids (SCFAs)[18,19], for example. By inducing host serotonin release through SCFA production or other microbial metabolites (e.g. the tryptophan derivative tryptamine), microbes are able to indirectly increase neuron excitability[20]. Microbiota can also potentially influence the response of the host to its endogenous neurotransmitters by altering the expression of genes encoding neurotransmitter receptors, like dopamine[21] or GABA receptors[22]. Considering the many ways in which microbiota influence the nervous system, it is perhaps not so surprising that a number of neurological disorders[23,24] and mental illnesses[25] are associated with dysbiosis.

Microbes influence other nervous system outputs including gut motility

Of course, the nervous system is responsible for much more than behaviour, and other nervous system outputs are also affected by microbiota. Gut motility in particular has received a lot of attention, likely due to the many lines of evidence connecting microbiota to irritable bowel diseases (Crohn's disease and ulcerative colitis) and irritable bowel syndrome[26–28]; a hallmark of these is altered gut motility. Indeed, several bacterial metabolites affect gut motility, for example the SCFAs propionate and butyrate influence colonic motility. These metabolites are produced by bacteria in the gut as a by-product of dietary fibre fermentation[29]. Direct application of propionate to isolated guinea pig colon decreased colonic contractions, while butyrate increased them[30]. As mentioned above, bacteria can also induce the production of serotonin through SCFAs, which increases gut motility[20]. Bacterially-derived tryptamine can bind directly to serotonin receptors in the gut, impacting gastrointestinal motility by inducing fluid secretion[31].

Evolutionary perspectives on microbiota-nervous system interactions

Eukaryotic life has always existed in the presence of prokaryotic life. Indeed, the existence of prokaryotes necessitated eukaryotic life, as the currently accepted theory of eukaryotic evolution states that the progenitor of the eukaryotic cell was itself a prokaryote that ingested another prokaryote, but rather than digesting it, formed a symbiotic relationship from which the entire domain Eukaryota would grow[32,33]. Since this pivotal moment, eukaryotic cells have existed alongside prokaryotic cells, providing ample time and opportunities for interdomain interactions to occur.

In light of these longstanding interactions, along with observations that (1) host microbiota affect host fitness, (2) host microbiota can be transferred between generations, and (3) nearly every animal studied seems to form symbiotic relationships with some of its resident microbiota, the hologenome theory of evolution was proposed[34]. The holobiont refers to the animal host with its microbiota as a single unit, while the hologenome refers to the combined genomes within the holobiont. The hologenome theory of evolution posits that the holobiont can act as a unit of selection. This theory isn't without its criticisms[35], however, conceptualizing the hologenome as providing material upon which selection can act can be a useful framework to guide experimental design and interpretations[36,37].

Certainly, when we consider the myriad of ways that microbiota interact with host nervous systems, it can be useful to keep this framework in mind, and it raises the question: have microbes been interacting with the nervous system since its very inception? Nervous systems help organisms to recognize and interact with their environments. Of course, microbes would be present in those environments and could have represented a friend or foe to even the earliest multicellular life. There is evidence to suggest that sponges (early metazoans of phylum Porifera) contain individual nervous system components and even have some contraction activities[38,39], it is unclear to what extent sponge microbiota interact with these components. It is in phylum Cnidaria, sister clade to Bilateria, where we find a bona fide nervous system[40] (Figure 1A). Within this phylum we have evidence of microbiota-nervous system interactions, suggesting that communications between microbiota and host nervous systems could be evolutionarily ancient interactions[41–43].

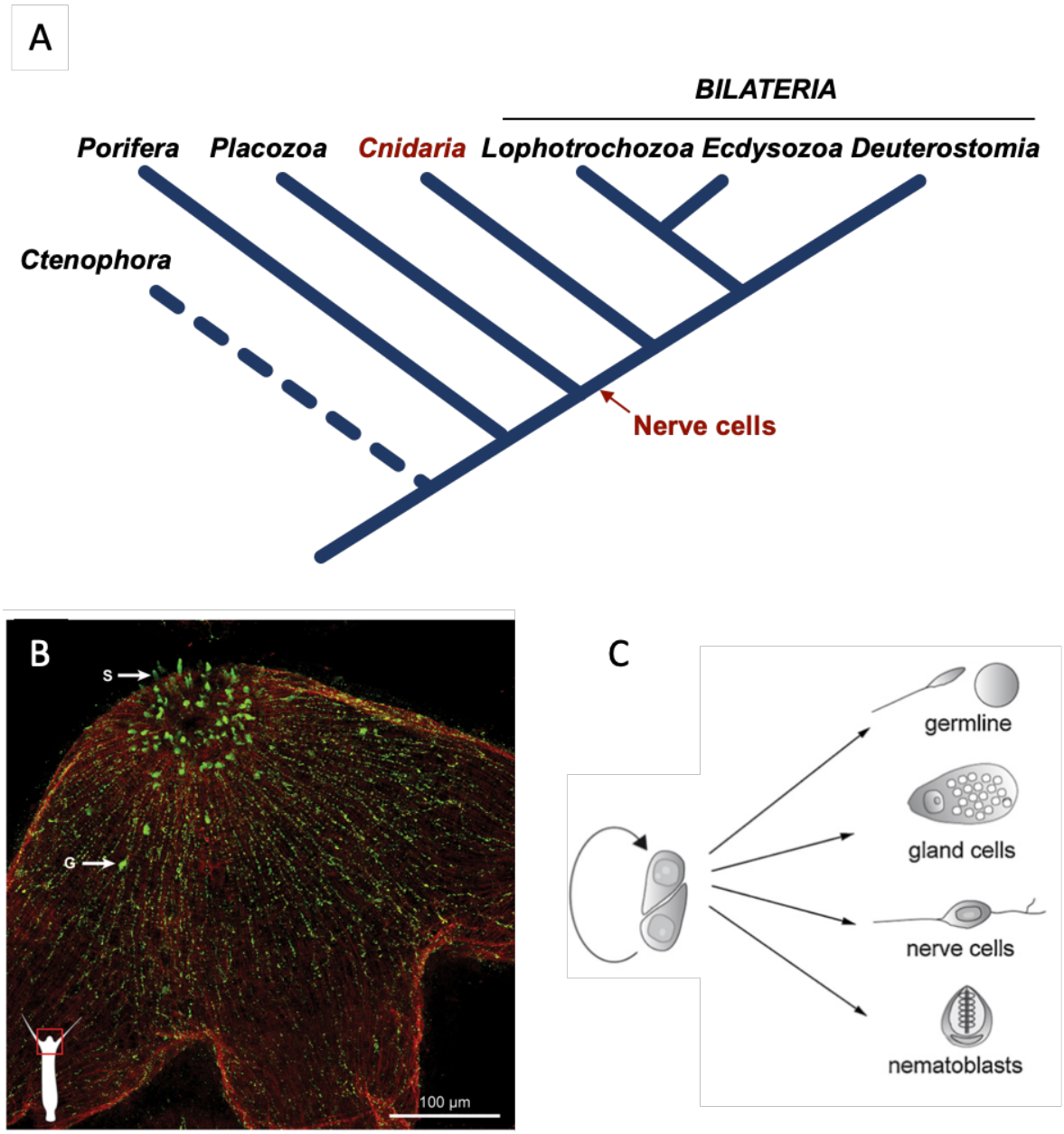

Figure 1. (A) Cnidarians have the oldest extant nervous system among the eukaryotes. Note that the position of Ctenophora, which possess a nervous system vastly different than the eumetazoans, is currently debated[44,45]. (B) The *Hydra* nerve net. Sensory (S) and ganglion (G) neurons are marked with arrows. (C) Interstitial cells continuously give rise to neurons and other cell types in adult polyps. A,B: Adapted from Klimovich and Bosch (2018)[43]. C: Adapted from Boehm and Bosch (2012)[46].

Microbiota-nervous system interactions within the cnidarian *Hydra vulgaris*

Within the phylum Cnidaria, the *Hydra vulgaris* AEP (hereafter *Hydra*) holobiont in particular has received a lot of attention. Despite the fact that *Hydra* has been cultured in the lab for over 40 years, its species-specific microbial community has remained surprisingly stable[47,48].

Recent work in mice has demonstrated that the ancestral microbiome of mice (the microbiota of wild caught mice) provides a stronger fitness advantage than the microbial community of lab mice[49]. Because of the stability of the *Hydra* microbial community in the lab environment, *Hydra* can provide nuanced information about the effect of an evolutionarily-relevant microbial community on the nervous system. In fact, *Hydra* microbiota have protective effects against fungal pathogens[3], and in the related species *Hydra oligactis* the microbiota have even been implicated in tumour formation[50]. The microbiota are also important mediators in feeding behaviour duration and contraction frequency of the polyps – both nerve cell-dependent behaviours[41,42]. The mechanisms through which the microbiota interact with the *Hydra* nervous system is currently unclear.

The nervous system of *Hydra*, like other cnidarians, is arranged in a nerve net (Figure 1B). Morphologically, there are two types of *Hydra* neurons, sensory and ganglion, and these were described over a century ago[51,52]. The sensory neurons are exposed to the environment (either the gastric environment or the external environment, where direct contact with the microbiota is theoretically possible), while the ganglion neurons form the nerve net that stretches throughout the body[53]. These cells are produced continuously in adult polyps from multipotent stem cells called interstitial cells[54] (Figure 1C).

However, the simplicity evident under the microscope does not reflect reality at the molecular level. Recent work using single cell transcriptomics has successfully identified unique transcriptional signatures of at least 7 neuronal populations, suggesting that *Hydra* neurons may be specialized to a degree not previously appreciated[55,56]. Indeed, researchers have recently taken advantage of *Hydra*'s transparency to visualize its entire nervous system as it underwent a variety of behaviours and found that within the nerve net, there are several non-overlapping networks that control different aspects of behaviour[53].

As mentioned above, the spontaneous contractions of *Hydra* (Figure 2A) are mediated by *Hydra* microbiota[41]. Germ-free *Hydra* contract at roughly 60% the rate of control (i.e. microbe-containing) polyps. Recolonization of germ-free polyps increases, but does not fully restore, the contraction frequency (Figure 2B). Importantly, the increase in contraction frequency was observed when the germ-free polyps were reconventionalized with only the

five main colonizing bacterial species of *Hydra*, which make up the majority its species-specific bacterial microbiome. Monocolonization of germ-free polyps with these five microbiota members was not enough to increase contractions to control levels (Figure 2C). However, one bacterial strain, *Pelomonas* sp. AEP2.2, was able to increase the contraction frequency relative to the germ-free polyps, suggesting that this strain may play a role in the mediation of contraction frequency. It is interesting to note that these experiments were performed on four-week starved animals and this could imply that there are structural changes to the nervous system that could not be repaired under nutrient limitation. Of course, it is also possible that the antibiotics used to render the animals germ-free was the damaging agent, or that the microbiome of the reconventionalized animals was not equivalent to the microbiome of control animals and this reconstituted microbiome was not as effective at controlling contractions than the microbiome of control animals.

Finally, a third line of evidence suggests that *Hydra* microbiota may affect nervous system function. Cultivation of *Hydra* microbiota in vitro, and extraction of the secreted metabolites at either 24 or 48 hours and application these extracts to germ-free polyps was also able to increase contraction frequency (Figure 2D). Because these polyps were incubated with the extracts for only around 16 hours, it seems unlikely that the underlying nervous system structure was affected, and that these extracts worked by directly or indirectly affecting nervous system function.

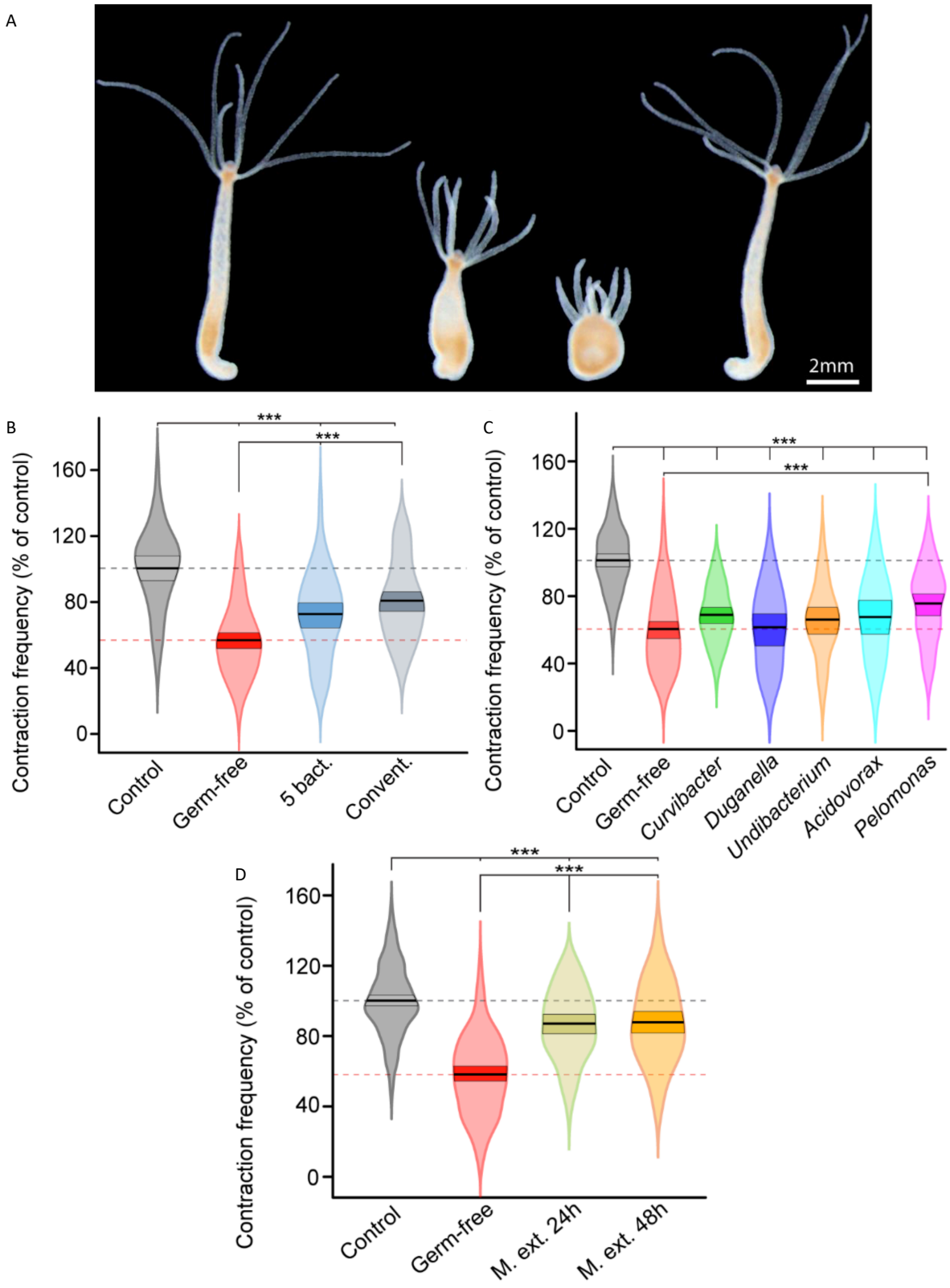

Figure 2. (A) Longitudinal contractions of the *Hydra* body column. Treatment-naïve polyps contract on average 10.86±0.53 times per hour. (B) Antibiotic treated, germ-free polyps contract roughly 60% as often as control polyps. Colonizing germ-free polyps with microbiota from conventionally-raised polyps (Convent.) increased their contraction frequency relative to control polyps. Using a synthetic community of only the five main colonizing bacterial species of *Hydra* (5 bact.) likewise increased contraction frequency, but

in neither case was contraction frequency fully restored. (C) Monocolonization of germ-free polyps with four of the five main colonizing bacterial strains of *Hydra* did not impact contraction frequency. The fifth strain tested, *Pelomonas*, was able to increase contractions relative to germ-free polyps. (D) Application of a microbe-conditioned medium increases contraction frequency of germ-free polyps. Two microbial extracts were created, with similar effects on contraction frequency: microbes were either cultured for 24 or 48 hours (M. ext. 24h and M. ext. 48h, respectively). Figure adapted from Murillo-Rincon et al.[41].

Molecular aspects of *Hydra* contraction frequency and feeding response regulation

The spontaneous contractions of the *Hydra* body column arise through the longitudinal contraction of the epithelial cells[57]. Thanks to a combination of single-cell transcriptomics, behavioural assays and in situ hybridization, we now know that the neuronal population controlling contraction behaviour sits just below the base of the tentacles. This population of nerve cells expresses nicotinic acetylcholine receptors, and three different ion channel-like transcripts (ANO1-, SCN-, and TRPM-like) that have been linked to gut motility or pacemaker cells in mammalian systems[55]. By interfering with these ion channels using inhibitors or activators of the channels, researchers were able to influence the contraction rate of the polyps.

Other research groups have investigated the role of various small molecules on the contraction rate of *Hydra* and found that the amino acid/inhibitory neurotransmitter glycine decreases contractions, as does the non-proteinaceous amino acid taurine[58]. In the same study, the authors demonstrate a negative effect of the plant metabolite and toxin strychnine[59] on contraction frequency, and conclude that these effects occur through the action of a strychnine-sensitive glycine receptor. It is worth noting that these chemicals also affect the duration of the feeding response in *Hydra*, another behaviour found to be influenced by *Hydra* microbiota. These chemicals increase the duration of the feeding response[60], as does the presence of microbes in *Hydra*[42]. In that study, the authors also test the amino acid D-serine, and this had the opposite effect on the feeding response, decreasing duration. D-serine was not tested in the contraction study, so its effects on contraction frequency remain unknown. Another small molecule that interacts with the feeding and contractions of *Hydra* is the neurotransmitter GABA. GABA decreases contraction rates, while increasing the duration of the feeding response[61].Taken together, these studies have an interesting implication. The small molecule studies suggest that the feeding response and

contractions are antagonistic, yet the microbiota of *Hydra* increase both feeding duration and contraction frequency. The implication, then, is that there are multiple neuroactive substances produced by *Hydra*'s microbial colonizers.

Metabolomics as a way to identify microbially-produced compounds within the metaorganism

Metabolomics seeks to identify all small molecules in an organism, tissue, or fluid. In practice, however, the picture is different: depending on the instrumentation and settings used, it is only possible to identify some fraction of the metabolites present in a given sample. Nevertheless, metabolomics has emerged as an important tool in biomarker discovery, and has been successfully applied to the study of host-microbe interactions[62,63]. It is possible, for example, to compare the metabolome of germ-free and conventionalized hosts and observe the effects of life without microbes on the metabolome[62]. Researchers have even induced mutations in microbial strains, allowed them to colonize a host, and were able to detect metabolic changes in the host[63]. Clearly, this can be a very powerful technique for determining the effect that resident microbiota have on their host species.

The *Hydra* metaorganism is particularly well-suited for metabolomics research

A major challenge in the field is pinpointing which metabolites are of microbial origin. Colonization of a host is likely to increase a whole suite of metabolites; some of these will be host-derived. Combining microbiome research with metabolomics in the *Hydra* metaorganism presents a unique opportunity in this regard: the main colonizers of *Hydra* are easily culturable, allowing for simultaneous investigation of main colonizer metabolomes and the metabolomes of microbe-containing and germ-free *Hydra*. The soft-bodied animals are easily homogenized, allowing for analysis of the entire organism's metabolome. Thus, one could identify compounds high in microbe-containing animals relative to germ-free animals and look for evidence of bacterial origin by examining individual microbial metabolomes. Further, we know that the microbes are able to produce contraction-regulating compounds in vitro as the application of a microbial extract produced from in vitro cultured microbes increased contraction frequency.

Aims

1. Develop a metabolomics pipeline for examination of the *Hydra* metabolome, and that of its resident microbes
2. To identify potential contraction-mediating compounds produced by *Hydra* microbiota
3. To search for evidence of microbial influence on nervous system function in *Hydra* by searching for microbially-produced neurotransmitters
4. To look for evidence of structural changes to the nervous system elicited by the microbiome

Methods

Generation and cultivation of germ-free and control polyps for BrdU labelling and behavioural assays

Germ-free polyps were generated by a two-week incubation in an antibiotic mixture containing 50 µg/mL ampicillin, neomycin, rifampicin, and streptomycin, and 60 µg/mL spectinomycin. The control animals were incubated in 0.1% dimethyl sulfoxide as the germ-free animals contain the same concentration owing to its addition in the rifampicin stock solutions[41,64]. Media were refreshed every other day. Polyps were allowed one-week recovery in sterile s-medium following antibiotic treatment. Routine checks for sterility followed the antibiotic treatment. This was accomplished by macerating a single polyp and plating the resultant liquid on R2A-agar (ROTH) and checking for signs of colony formation after 3 days incubation at room temperature. A final sterility check for non-culturable bacteria was done on the last day of treatment by isolating DNA from macerated polyps (DNeasy Blood & Tissue Kit, Qiagen) and confirming the absence of a 16S ribosomal RNA gene (hereafter 16S) PCR amplification product using the universal 16S eubacterial primer (F = 5'-CCTACGGGAGGCAGCAG-3' and R = 5'- ATTACCGCGGCTGCTGGC-3').

Sterile feeding of *Hydra*

Previous experiments comparing the contraction frequency of germ-free and control polyps were performed using *Hydra* that had been not fed for the entire 4-week duration of the antibiotic treatment and recovery period[41]. I reasoned that nutritional status may impact the extent of the differences observed between microbe-containing and microbe-free polyps. If the effect size was greater, then I could use less animals to detect differences between my treatments, increasing my capacity for extract testing. To test this, I used fed, long-term germ-free and control polyps that were kindly supplied by my colleague, Jinru He.

His protocol for feeding of these polyps using germ-free *Artemia salina* nauplii was as follows: commercial *Artemia* cysts (Ocean Nutrition) were *Hydra*ted with sterile Milli-Q water for one hour with aeration and decapsulated by a 10 minute incubation on ice with 1:1 (v/v) diluted 12% sodium hypochlorite solution (Roth)[65]. Cysts hatched overnight in 2.5% (w/v) antibiotic-

treated sterile artificial seawater (350 rpm at 30^{o}C). Following hatching, *Artemia* larvae were incubated in the antibiotic cocktail for four days with daily medium replacement, followed by a two-day incubation period in antibiotic-free sterile artificial seawater.

Hydra were fed every two days and maintained under sterile conditions in antibiotic-free media for a total of 30 weeks. Sterility of both *Hydra* and *Artemia* were confirmed by the absence of bacterial colonies on R2A-agar and a lack of 16S PCR amplification products, as described above.

Neurogenesis and neuronal density assessment

To look for changes in neurogenesis I used the thymidine analogue 5-bromo-2-deoxyuridine (BrdU), which labels dividing cells through incorporation of BrdU into growing DNA strands[66]. Neuronal density was assessed by counting the ratio of neurons to epithelial cells. I used starved animals (given one-week recovery following two-week antibiotic treatment) (n = 50 germ-free and 50 control polyps; 3 replicates) and well-fed animals from the long-term germ-free culture (n = 20 germ-free, 20 recolonized, and 20 control polyps; 2 replicates). I incubated polyps in sterile s-medium containing 2 mM bromodeoxyuridine (BrdU) and changed the medium every 12 hours, for a total of 72 hours incubation time. At 72 hours, I macerated the animals and mounted them on gelatine-covered slides for visualization of BrdU by immunohistochemical labelling[67]. To achieve sufficient cell densities, 8 starved polyps, or 1-2 fed polyps were macerated onto a single slide. Immunodetection of BrdU was performed as described previously[68]. To assess the differences in labelling and nerve cell density of starved germ-free and control polyps, I used Welch's *t*-test (GraphPad Prism 4). For fed control, recolonized, and germ-free animals, I used an analysis of variance (ANOVA) (GraphPad Prism 4). Data are expressed as means ± SEM (standard error of the mean).

Preparation of original bioactive extracts for solid phase metabolite extraction

A small amount of the original contraction-mediating extracts used in the Murillo-Rincon paper[41] were left over and were provided by Dr. Murillo-Rincon so that I could reveal their metabolic contents via mass spectrometry. The full methods are detailed in the paper, but briefly, these two extracts were prepared by inoculating an R2A-agar plate with three

homogenized *Hydra* polyps and grown for three days at 18°C before a final incubation for either 24- or 48 hours in s-medium. The microbially-conditioned media were concentrated through a solid phase extraction (SPE) using a C18 column. In the final step of the SPE, the metabolites were released from the column using methanol. This methanol was evaporated before they were resuspended in s-medium.

The overall concentration of salt in s-medium is low, but my preliminary experiments indicated that these salts may interfere with signal acquisition, so I desalted the samples using a standard C18 SPE (described below). To prepare the two extracts for the C18 extractions, the volume of samples available (approximately 500 μL) were acidified using 1 mL 0.12 N HCl in ultrapure water.

Preparation of germ-free and control *Hydra* for solid phase metabolite extraction

Germ-free and control *Hydra* were cultured according to the study by Murillo-Rincon[41] using two weeks antibiotic treatment and two weeks recovery time in sterile s-medium. Fifty total polyps were used per replicate, with a total of five replicates per treatment. During the routine sterility assessment (described above) one germ-free replicate was found to be contaminated and removed from further processing.

On the thirteenth day of recovery in sterile s-medium, the *Hydra* polyps were washed and checked for sterility a final time before resuspension in 25 mL sterile s-medium. One day later, the tubes were immersed in liquid nitrogen until completely frozen and lyophilized (CHRIST Alpha 2-4 LSC) for 48 hours to dryness. These dried samples were resuspended in 1 mL pure methanol (LiChrosolv® grade, Merck) sonicated for 20 seconds and homogenized by bead-beating in a pre-cooled Precellys homogenizer (5,800 RPM, 2x15 seconds, with 30 second pause). The resultant homogenate was centrifuged at 10,000 x *g* for 10 minutes at 20°C. The methanol was evaporated using a vacuum centrifuge at 8 mBar for one hour (40°C). Finally, the metabolites were resuspended in 1 mL acidified water (0.12 N HCl in ultrapure water).

16S PCR sequencing and analysis of control animals used for metabolomics analysis

DNA was isolated from each of the 5 control replicates for 16S sequence analysis. Sequencing was performed by the Institut für Klinische Molekularbiologie (IKMB) on the Illumina MiSeq platform. I annotated the sequences using QIIME 1.9.1[69], and used BioEdit 7.2[70] to search the resultant operational taxonomic units (OTUs) for the main colonizing species of *Hydra*, based on the reference 16S sequences found in the Compagen database[71].

In vitro cultivation and preparation of *Hydra* bacterial colonizers for solid phase metabolite extraction

R2A broth was inoculated with each of the five main colonizing bacterial strains of *Hydra* (*Undibacterium* sp. C1.1, *Pelomonas* sp. AEP2.2, *Duganella* sp. C1.2, *Curvibacter* sp. AEP1.3, *Acidovorax* sp. AEP1.4 – hereafter referred to by genus names only) and incubated for 2 days at 18°C (250 rpm). Each of these strains has a different growth rate in R2A, so I used the growth rate information supplied by Dr. Peter Deines to stagger the inoculation times such that all strains hit early stationary phase at the same time. By diluting the starter cultures to an OD_{600} of 0.1 and inoculating 10 mL of culture, I could assume that *Undibacterium*, *Pelomonas*, *Duganella*, *Curvibacter*, and *Acidovorax* would take 30, 27, 23, 33, and 25 hours to hit stationary phase, respectively.

R2A is a complex, chemically undefined medium and it needed to be removed lest it interfere with mass spectrometry data acquisition and analysis. To accomplish this, I centrifuged all cultures at 4,600 rpm for 25 minutes (4°C). I washed the remaining R2A away by resuspending the resultant pellet in sterile s-medium (a chemically defined medium used for standard culturing of *Hydra* with no carbon, nitrogen or phosphate source) and centrifuging a second time. I then discarded this s-medium and weighed the cell pellets in order to standardize the biomass in each culture. To create a co-culture of the main colonizers, I aliquoted 1.4 mL from each of these biomass-equilibrated cultures into a single test tube for a total of 7 mL cell suspension. For the individual strains, 7 mL of the biomass-adjusted cultures was used. All of these cultures were incubated for 24-hours at 18°C (250 rpm).

To quench the metabolism of the cultures quickly, I added 7 mL pure, cold (-80°C) methanol and froze the samples at -80°C until they could be transported on dry ice and further processed at the mass spectrometry lab in Munich.

Upon arrival in Munich, bacterial cells were immersed in an ultrasonic water bath for 30 minutes to release intracellular metabolites, and the cell fragments were removed by centrifugation at 10,000 x *g* for 10 minutes (4°C). 1 mL of this supernatant was removed, and the samples were dried for 5.25 hours at 8 mBar (40°C) in a vacuum centrifuge (Eppendorf Concentrator Plus). The metabolites were resuspended in 1 mL acidified water (0.12 N HCl in ultrapure water).

Solid phase extraction of metabolites from extracts, *Hydra* and bacteria

Ultimately, the *Hydra*, the in vitro bacterial samples, and the original bioactive extracts would be compared in their metabolite content. This required the same solid phase extraction protocol to ensure similar eluting conditions between experiments.

A fresh C18 column (50 mg sorbent, 1 mL capacity, Agilent Bond Elut) was loaded onto a vacuum manifold system (Standard 24-port, 57 250-U, Sigma-A) connected to a pump system (Vantage 3000 C S 10, Svenska Pump AB) at a flow rate of approximately 20 mL min^{-1}. The column was first washed with 1 mL 100% methanol (LiChrosolv® grade, Merck), and then conditioned with 1 mL acidified water (0.12 N HCl in MilliQ water), before the 1 – 1.5 mL acidified sample was loaded. The column was washed with 3 mL 0.12 N HCl before the samples were eluted in 1 mL pure methanol.

Mass spectrometric analysis of the *Hydra*, in vitro bacterial samples and original extracts

These samples were analysed on a Bruker SolariX 12 Tesla Fourier transform ion cyclotron resonance mass spectrometer (FTICR-MS). The samples did not require dilution prior to analysis. Spectra were acquired in negative ionization mode with a scanning range between a mass-to-charge ratio (m/z) of 147 to 1000.

Preprocessing of mass spectrometry data from *Hydra*, in vitro bacterial samples and original extracts

Preprocessing of metabolomics data is an important step that helps select true metabolites from among the noise that accompanies high-resolution mass spectrometry data and results in a table of aligned peak and intensity information[72]. This step is required for comparison of spectra across samples.

The first step in preprocessing is spectrum calibration. This step corrects for the small differences in mass traces from their expected values. Here, I used Bruker Compass DataAnalysis software for internal spectrum calibration. The calibration lists contain mass traces of various molecular weights across the scanning range, so that they can be identified within the mass spectra of the samples and the spectra can be shifted accordingly. The internal calibration file used for calibration was designed by Jenny Uhl (Helmholtz Munich) and contained *Hydra*-specific mass traces (Supplementary Table 1). This file was used to linearly calibrate the spectra with a maximum mass difference of 1 ppm (part per million). The mass lists are exported individually, and the peaks aligned with an error window of 1 ppm using Matrix Generator 0.4.

Statistical analysis of mass spectrometry data from *Hydra*, in vitro bacterial samples and original extracts

My preprocessing strategy produced a large matrix containing peak list information from the three experiments. The goal here was to find mass traces high in control polyps that were also present in the bioactive extracts and produced by *Pelomonas* and/or in the co-cultured bacterial samples. Structural differences in the datasets prevented further processing using the entire matrix file, so the experiments were separated.

Statistical analysis of metabolomics data from germ-free and control *Hydra*

To find mass traces high in control relative to germ-free samples, I applied the "modified 80% rule"[73] as a first step in addressing the missing values in the dataset. A standard 80% rule would require 80% or more of the intensity values for a given mass trace to be above zero.

The modified 80% rule includes class information as well – mass traces must be above zero in at least 80% of the replicates for at least one treatment.

Further processing was done using Metaboanalyst 4.0[74]. Remaining zeroes were replaced with half of the minimum positive value in the dataset, under the assumption that compounds corresponding to these mass traces were below the limit of detection. To ensure a Gaussian distribution, data were log normalized and auto-scaled (mean-centred and divided by the standard deviation of each variable). A *t*-test combined with fold-change analysis was used to determine which mass traces has significantly different intensity values (fold change > 1.5, $p_{raw} < 0.05$). Data were visualized using a principal component analysis (PCA) and a heatmap.

Statistical analysis of metabolomics data from liquid-cultured bacteria

For the bacterial dataset, the "modified 80% rule"[75] was applied before upload to Metaboanalyst 4.0[74], where remaining missing values were replaced by a half of the minimum positive value in the dataset. Similar to the *Hydra* dataset, the data were log transformed and auto-scaled. Statistical differences in mass traces were identified using ANOVA with a Fisher's least significant difference post hoc test (significance threshold $p > 0.05$). Data were visualized with a PCA and heatmap.

Searching for overlap between the datasets

I created a relational database to check for overlaps in the output of the three experiments using SQL (Structured Query Language) and looked for three types of overlap: (1) mass traces high in *Hydra*, and present in both the bioactive extracts and in at least one liquid bacterial culture, (2) mass traces high in *Hydra* and present in the extracts, and (3) mass traces common between the extracts and present in at least one liquid bacterial culture.

From mass trace to compound name: metabolite annotation

To putatively annotate the m/z list, I used the CEU Mass Mediator 3.0 tool[76] to simultaneously search the KEGG[77], LipidMaps[78], and Human Metabolome Database (HMDB)[79], and Metlin[80]

databases (using an error window of 1 ppm). To account for the possible formation of adducts, the compound annotations included the following possible adducts: M+H, M+Cl, M+FA+H, and M-H+H_2O. Peptides were also included in the annotation results.

Cultivation of bacteria for new extracts used in both behavioural assays and mass spectrometry analysis

My extraction methods were based on that developed by Dr. Murillo-Rincon[41]. I modified the basic protocol to create three different bacterial extracts for contraction testing (Figure 3A). The original method utilized three *Hydra* polyps, washed with sterile s-medium and homogenized in a microcentrifuge tube using a microcentrifuge pestle as the inoculum for bacterial culturing on R2A-agar plates. The bacteria were then cultured for 3 days at 18°C, and the colonies were gently removed using 3 mL sterile s-medium and water. This cell concentrate was then added to 400 mL sterile s-medium and allowed to incubate for 24 hours at 18°C (250 rpm).

I also created a vehicle control extract to test the effect of the low levels of R2A that might be carried over using this protocol. This extract was made in the same way as the microbial extract, except I washed an empty R2A-agar plate with 3 mL sterile s-medium and "inoculated" this into 400 mL s-medium (Figure 3B). After a 24-hour incubation, I plated 1 mL of the suspension on R2A-agar to check for contamination.

Finally, I created an extract that did not require microbes to be acquired directly from the host. Because previous extracts utilized the microbiota from three single polyps, I used three-fold the reported carrying capacity of a single *Hydra* polyp[3]. I cultured each of the five main colonizing species of *Hydra* independently in liquid R2A medium (LAB) at 18°C (250 rpm). These starter cultures were diluted to equal colony forming units per mL and inoculated onto R2A-agar using the same steps outlined above (Figure 3C).

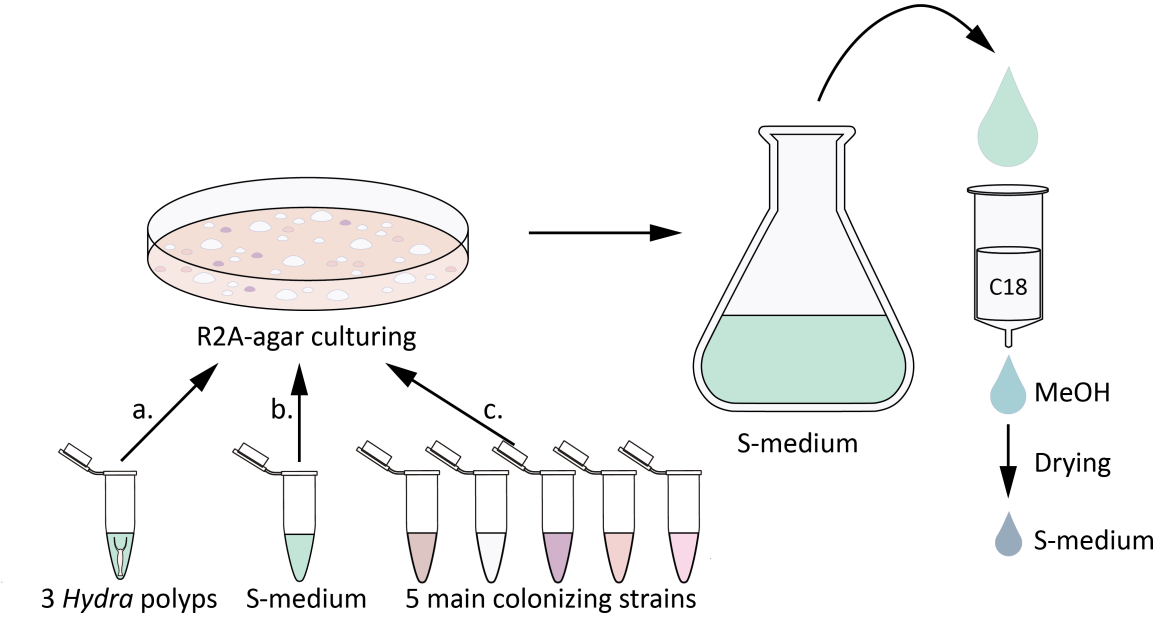

Figure 3. Three extraction protocols were utilized in this report. The first (a) was created according to Murillo-Rincon et al.[41]. The second was a microbe-free control (b), while the third (c) utilized the five main colonizing species, plated at equal colony forming units per millilitre to create a more reproducible assay. C18 = C18 SPE column; MeOH = Methanol.

Solid phase extraction of bacterial metabolites for behavioural assays

Following the 24-hour incubation in s-medium, the media need to be concentrated, and the cells removed. To accomplish this, I employed an SPE. I centrifuged the cells (4250 x *g* for 15 minutes at 4°C), reserving two 100 µL aliquots of the resultant pellet for 16S analysis, and filtered them using a 0.2 µm filter. Sequence acquisition and analysis was performed as stated above.

For the SPE, I used an C18 column (Supelco Supelclean 60 mL), prepared by washing the column in 50 mL methanol (UPLC-grade, Sigma), followed by column conditioning with 50 mL MilliQ water. I then add the bacterially-conditioned medium (400 mL), and washed the column using 150 mL MilliQ water. I used pure methanol (UPLC grade, Sigma) to elute the metabolites. I reserved 1 mL of the eluant and stored it at -80°C until mass spectrometry analysis. To test the extracts on *Hydra*, the methanol needs to be removed. I used lyophilization for this step. Because of methanol's extremely low freezing point, I needed to decrease the concentration of methanol to 40% before drying completely (ca. 24 hours) in a freeze dryer (CHRIST Alpha 2-4 LSC).

Behavioural assays

The protocol for behavioural assays was based on the original protocol described by Dr. Murillo-Rincon[41]. The germ-free and control animals were washed a final time in s-medium before being incubated overnight at 18°C in s-medium or s-medium plus bacterial extract (diluted 1:25). To ensure the animals were light-adapted, the light remained on during this incubation period. The following day, the polyps were arranged under a dissecting microscope (M3C Wild Heerbrugg) in a concave glass slide containing approximately 0.5 mL s-medium (and extract, when used). Each slide contained a single polyp, which was recorded using a digital camera (Breukhoven Microscopes Systems). The live images from the camera were captured using Chronolapse software set to take a screen capture every 3 seconds. Each polyp was recorded for a total of 80 minutes, with the first 20 minutes discarded as the acclimatization period. The series of jpeg screen shots were processed by ImageJ to produce a video, which was used to count the contractions during the hour-long recording window.

Statistical analysis and visualization of behavioural assays

Statistical analysis and graphics were created using R and the ggplot2 and yarrr packages[81–83]. The initial R script was kindly supplied by Dr. Murillo-Rincon and I made changes where appropriate for my own data structure. I converted the number of contractions per hour to the percentage of the mean control value, checked to make sure the data were normally distributed (packages Car and MASS)[84,85] and assessed the differences in contractions via a Welch's *t*-test. Each individual polyp was considered a single replicate.

Mass spectrometry analysis of the new five-microbe bacterial extracts

After observing that the five-microbe extract increased contraction frequency, I scaled this experiment up to include three microbe-containing extracts and three microbe-containing controls, which were all resuspended in MilliQ water rather than s-medium so I could avoid a second C18 extraction and concentrate the samples, if needed. With this amendment to the protocol I was able to run the six samples directly on the mass spectrometer.

The scanning range of m/z 147 – 1000 utilized in the above listed mass spectrometry experiment did not provide strong candidate molecules for behavioural testing. I reasoned this may be a result of the scanning window, as many bioactive molecules have molecular masses outside of this range. To address this, these samples were run on an FTICR-MS at Kiel University (7 Tesla, SolariXR) that offers greater flexibility in scanning range. Samples were run in both positive and negative ionization mode with a scanning range between m/z 65 - 950.

Preprocessing of the five-microbe bacterial extracts mass spectra

To calibrate the mass spectra, I used MetaboScape 4.0 (Bruker). The data were calibrated linearly using an internal mass list with a calibration tolerance of 1 mDa and an intensity threshold of 10^6. Mass traces were only included in downstream analyses if they were present in at least 2 of the 6 samples. Peak annotation was performed using an in-house mass list specific for neurotransmitters.

Statistical analysis of the five-microbe bacterial extracts mass spectra

For further processing, mass traces needed to be present in at least two of the three replicates in at least one treatment (microbe versus R2A control). The raw spectra were uploaded to Metaboscape 4.0. in MRMS single spectra mode. Linear calibration was used using internal calibration lists with a tolerance of 1.00 mDa and an intensity threshold of 10^6. Mass features were annotated using a neurotransmitter-specific annotation list. The mass lists were processed using Metaboanalyst with the same normalization techniques used previously (log normalization and auto-scaling). To identify significant differences, a *t*-test was combined with a fold-change analysis ($p < 0.05$, $FC > 1.5$) and these traces were visualized using GraphPad Prism.

Metabolic modelling of GABA metabolism in *Hydra*'s main colonizers

Metabolic models for GABA metabolism were generated by Georgios Marinos (Institute of Experimental Medicine, University Medical Center Schleswig-Holstein). Briefly, the metabolic models were created using the draft genomes of *Curvibacter, Undibacterium, Pelomonas, Duganella,* and *Acidovorax.* The nutritional environment used for modelling was based off of

the nutritional profile of R2A and included a small quantity of GABA (10^{-6} mM) because preliminary experiments detected a small amount of GABA in uninoculated medium and because it was important to ensure GABA was available for exchange reactions. The models were created using GapSeq (development version 3185ca1) and run using R and the package sybil[86].

Bacterial growth on putrescine as a sole carbon and nitrogen source

I grew each of the main colonizing species for two days in 3 g/L of the complex medium R2A at 18°C (250 RPM). Then, I washed these starter cultures twice in s-medium by centrifuging at 3,000 x *g* (10 min at 4°C), removing the supernatant, adding an equal volume of s-medium, vortexing 30 seconds and repeating. Next, I inoculated the clean cultures with a 1:50 dilution into s-medium with putrescine (Sigma) at final concentrations of 0, 1, and 10 mM, or into R2A as a positive growth control. Growth was assessed on a 96-well plate by recording the OD_{600} of each culture (Tecan Spark 10M) at intervals of 15 minutes for a total of 23 hours (18°C).

Data visualization and statistical analysis

I used an R script to visualize the bacterial growth curves based off of the one published by Brian Connolly[87]. This code uses the R core functions and the packages reshape2, dplyr, ggplot2 and gtable[81,82,88–90]. I used the package growthcurver[91] to obtain the maximum carrying capacity of the different media types so that I could perform statistical analysis using R core functions (analysis of variance with Holm-Bonferroni post-hoc analysis)[81]. Note that the cultures did not reach stationary phase, thus the carrying capacity in these cultures was not reached and the maximum density is simply used as a proxy for biomass accumulation.

Searching mass spectrometry data for bioactive compounds influencing bacterial chemotaxis

The data processing pipeline I developed to search for a bacterially-derived, contraction-regulating molecule could be modified to search for common compounds between *Hydra* and its bacterial colonizers. There are 67 mass traces that overlap between these two mass spectrometry datasets (these compounds were significantly increased or decreased in control

polyps relative to germ-fee polyps). New work from Dr. Peter Deines revealed increased chemotaxis-eliciting effects of germ-free *Hydra* relative to control *Hydra*[92]. I searched the list of compound annotations for known chemotaxis-eliciting compounds that might be responsible and found a compound (m/z 227.1401) that corresponded to a chemotaxis-eliciting dipeptide. The intensities of this mass trace were analysed and visualized using GraphPad Prism 5.0.

Prediction of secondary metabolites based on the genomes of the main colonizers

Having a list of the metabolic potential of the bacteria could be useful in compound identification. Therefore, I used antiSMASH[93] (Antibiotics and Secondary Metabolite Analysis Shell) to search the draft genomes of the main colonizing strains to search for potentially bioactive secondary metabolites.

MS/MS to confirm the identity of the dipeptide

To confirm the identity of m/z 227.1401, I cultured *Curvibacter, Duganella, Acidovorax, Undibacterium* and *Pelomonas* as previously described. I amended the metabolism quenching step to improve efficiency by simply centrifuging the samples following their 24-hour incubation in s-medium (3000 x *g*, 10 minutes, 4°C), and dropping them directly in liquid nitrogen. The samples were then loaded on the 7 Tesla SolariXR FTICR-MS in flow injection mode with an injection volume of 60 µL. Ionization was done in both positive and negative mode. To fragment the target ion, we chose the sample with the highest concentration of the target (*Undibacterium*) for MS/MS fragmentation.

To increase the total concentration of the 227.1401 target ion further, I grew the bacterial strain as before but did not dilute the culture before metabolic quenching. The sample was loaded with the four possible dipeptide isomers prolyl-leucine (Sigma), leucyl-proline (Sigma), isoleucyl-proline (Bachem), and prolyl-isoleucine (Bachem) at 1 nM concentrations. Using DataAnalysis (Bruker), I searched the spectra for the expected fragmentation patterns of the dipeptides that are published in the HMDB[94] and Metlin[80] databases.

Results

Microbiota do not influence neurogenesis or nerve cell density in adult polyps

To assess microbial influences on neurogenesis, fed and starved *Hydra* (with and without microbes) were incubated in BrdU-containing s-medium for 72 hours. The proportion of unlabelled:labelled cells was counted and is reported here as the labelling index (in percent). After 72-hours continuous labelling, no differences could be detected in either starved (control: 23.1 ± 2.5%, n = 9; germ-free: 22.3 ± 3.2%, n = 13; p = 0.79; Figure 4B,C), or fed polyps (control: 28.3 ± 4.8%, n = 7; germ-free: 29.3 ± 2.8%, n = 7; recolonized: 31.4 ± 3.4%, n = 7; p = 0.84) (Figure 5B,C).

In the absence of an altered rate of neurogenesis in germ-free animals, changes to the density of the nerve net, as measured by an increase of the nerve cell to epithelial cell ratio, were still possible. No such changes to neuronal density were observed in starved (control: 0.29 ± 0.035, n = 6; germ-free: 0.34 ± 0.02, n = 7; p = 0.23; Figure 4C) or fed polyps (control: 0.19 ± 0.012, n = 15; germ-free: 0.21 ± 0.011, n = 14; recolonized: 0.20 ± 0.014, n = 13; p = 0.72) (Figure 5C).

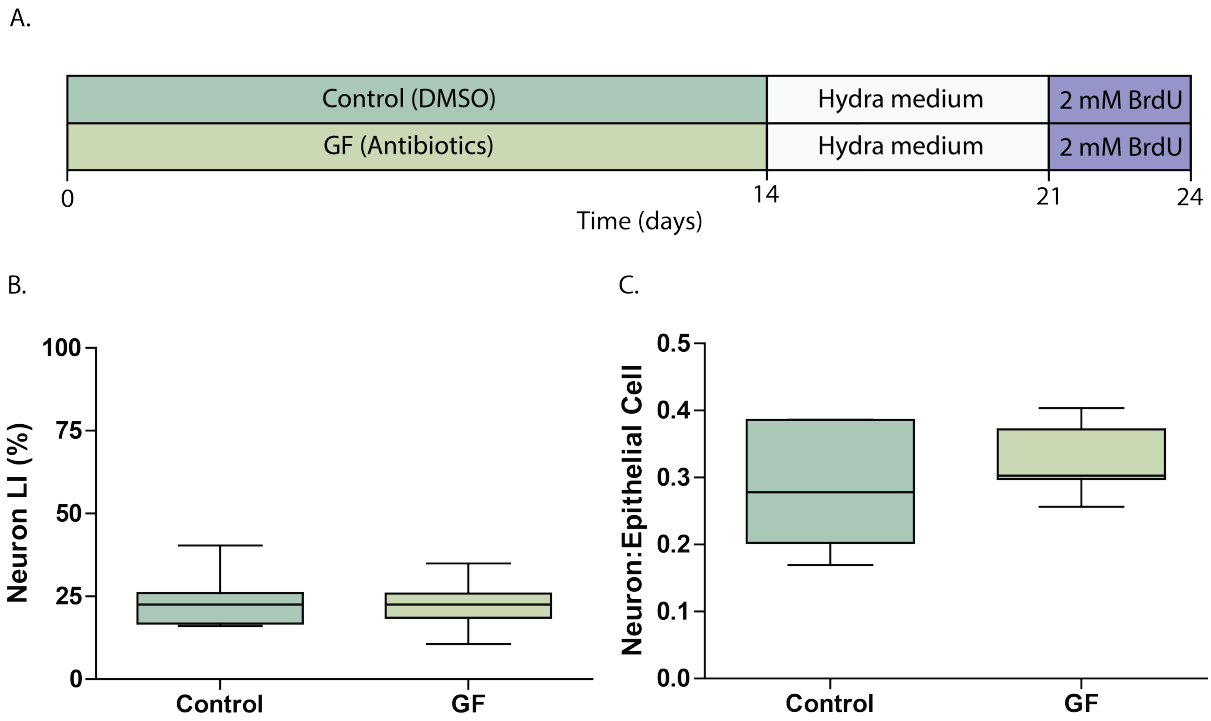

Figure 4. The BrdU labelling index of the neurons of starved control polyps and that of starved germ-free polyps did not vary significantly after 72 hours continuous labelling. (A) Culturing and antibiotic treatment scheme. (B) The labelling index of neurons from control and germ-free individuals was not different (C) The nerve cell density was similarly unaffected in starved animals.

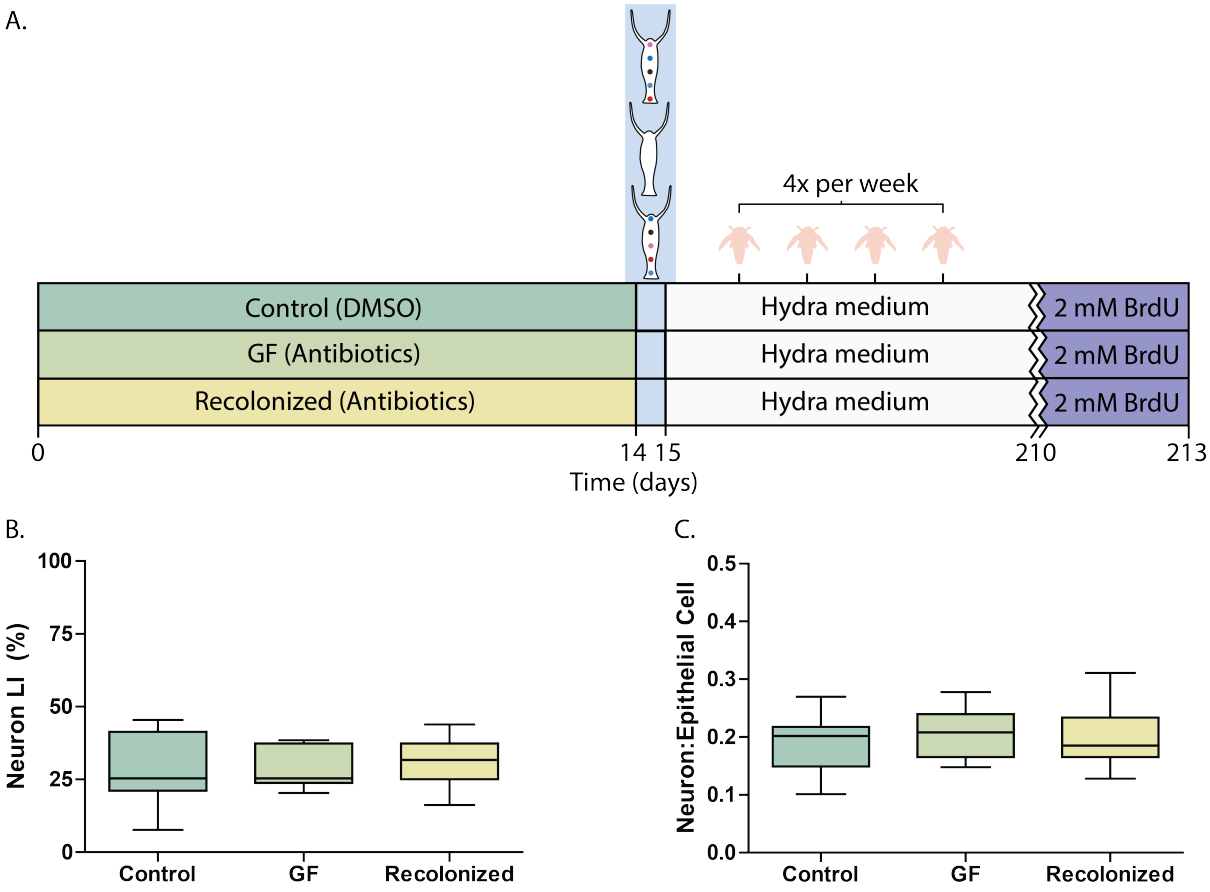

Figure 5. Nerve cell density and neurogenesis are not impacted by the *Hydra* microbiome in long-term, fed polyps. (A) Antibiotic treatment, culturing protocol and feeding schedule for the long-term germ-free polyps. (B) No difference in neurogenesis between control, recolonized, or germ-free polyps (p = 0.84) was observed. (C) The neuronal density in these animals was similarly unaffected (p = 0.72).

16S analysis of germ-free and control *Hydra* polyps used for metabolomics analysis

16S analysis of the native bacteria of *Hydra* indicated that one of the five control animals had a high relative abundance of the spirochaete *Turneriella* sp. The relative abundance of *Turneriella* sp. in this sample was 36.4%, while the other four samples had abundances between 0 and 0.1% (Supplementary Table 2). This sample did not contain any members of phylum Bacteroidetes, despite a total average abundance between 5.2 and 29.2% in the other four samples. The remaining four samples were much more homogeneous in their microbial composition (Figure 6), so the *Turneriella*-containing sample was excluded from metabolomics analysis. One germ-free sample was similarly excluded because, despite a lack

of colony growth on R2A-agar, there was successful amplification of 16S DNA in the polyp, indicating that the sample may have been contaminated.

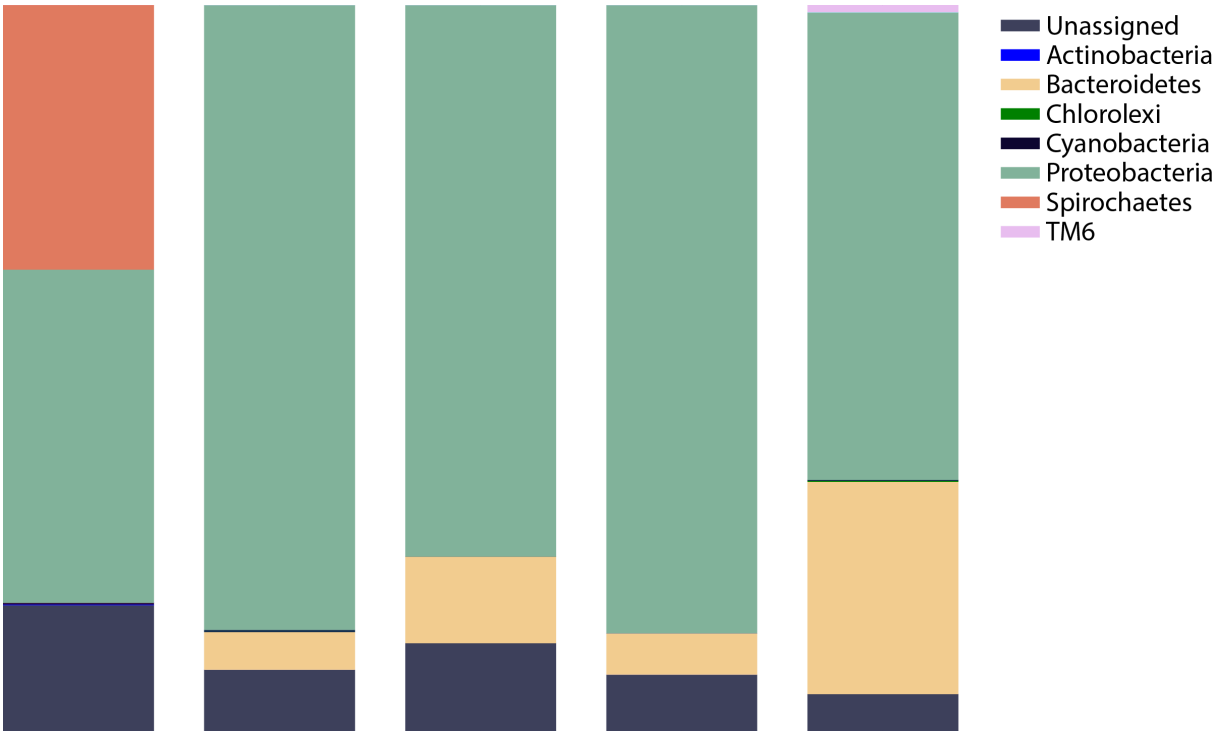

Figure 6.16S sequence analysis resolved at the level of phyla. Each bar represents a single sample. Replicate one (far left) contains a high abundance of Spirochaetes and is devoid of Bacteroidetes so it was excluded from further analysis.

Metabolomic analysis of germ-free and control *Hydra*

To understand what compound(s) were influencing contraction frequency in *Hydra*, I looked for mass traces that were common between microbe-containing *Hydra*, in vitro cultured *Hydra* colonizers, and the original bioactive extracts. This required three separate untargeted mass spectrometry experiments. In the first, I examined the metabolomes of germ-free and control *Hydra* to find mass traces that might represent bacterially-derived compounds. Compounds high in control *Hydra* (FC > 1.5, $p < 0.05$) were flagged as potentially microbially-derived and proceeded through my data processing pipeline.

The raw mass spectra of the *Hydra* samples contained 4619 unique mass traces. Many of these are artefacts and need to be removed before biological interpretation can be

accomplished. I used the modified 80% rule[73] (technically 75% since there were only four samples per replicate) to reduce *Hydra*-specific mass list to 3084 mass traces. Differences in the metabolite profiles between germ-free and control animals are visible in both the PCA plot and heatmaps (Figure 7Figure 8). There were 149 compounds high in control polyps relative to germ-free polyps and 196 low in controls relative to the germ-free polyps (FC > 1.5, $p < 0.05$).

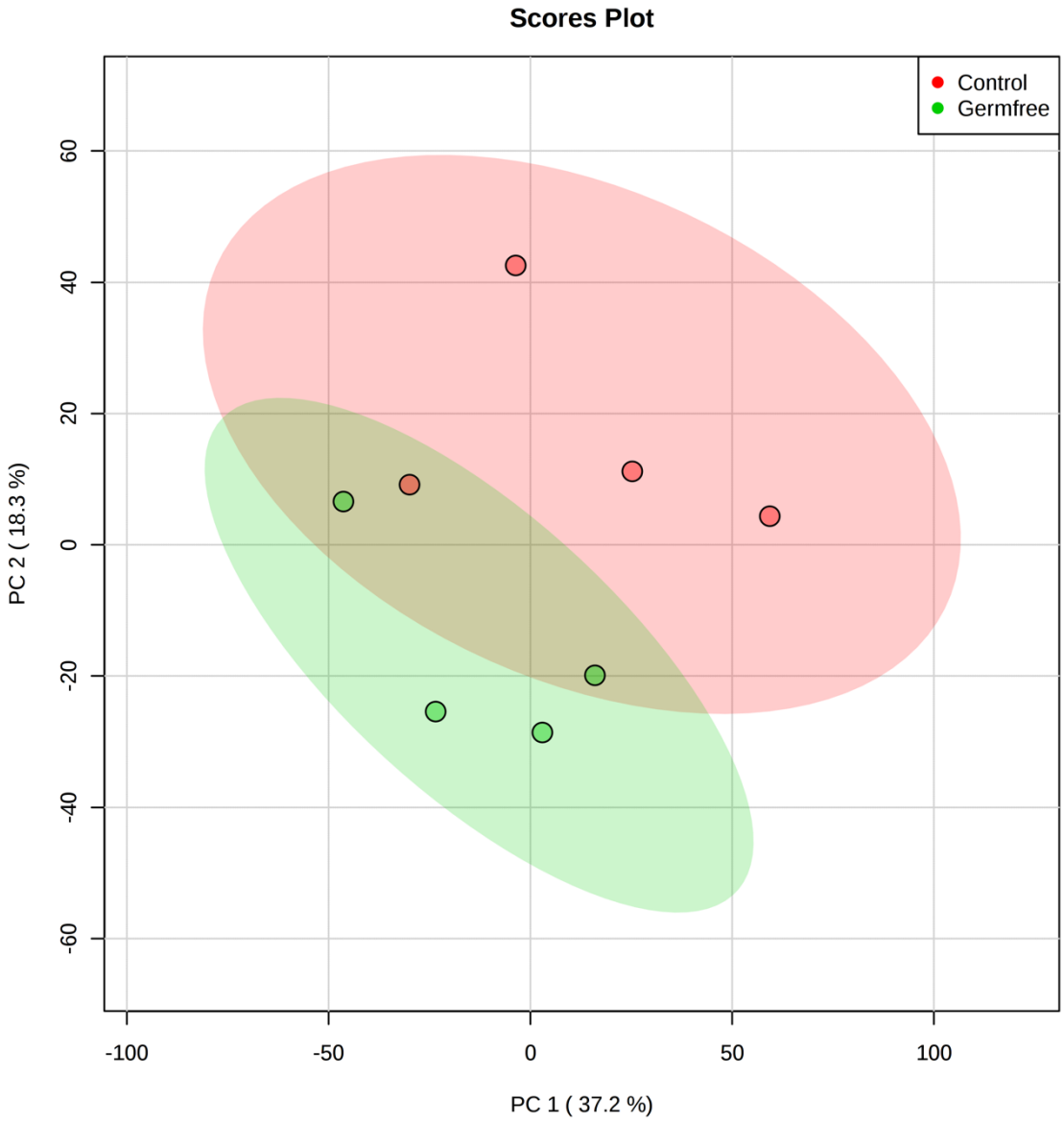

Figure 7. PCA plot of the germ-free and control *Hydra* metabolomics data. Each point represents a single replicate containing 50 polyps each.

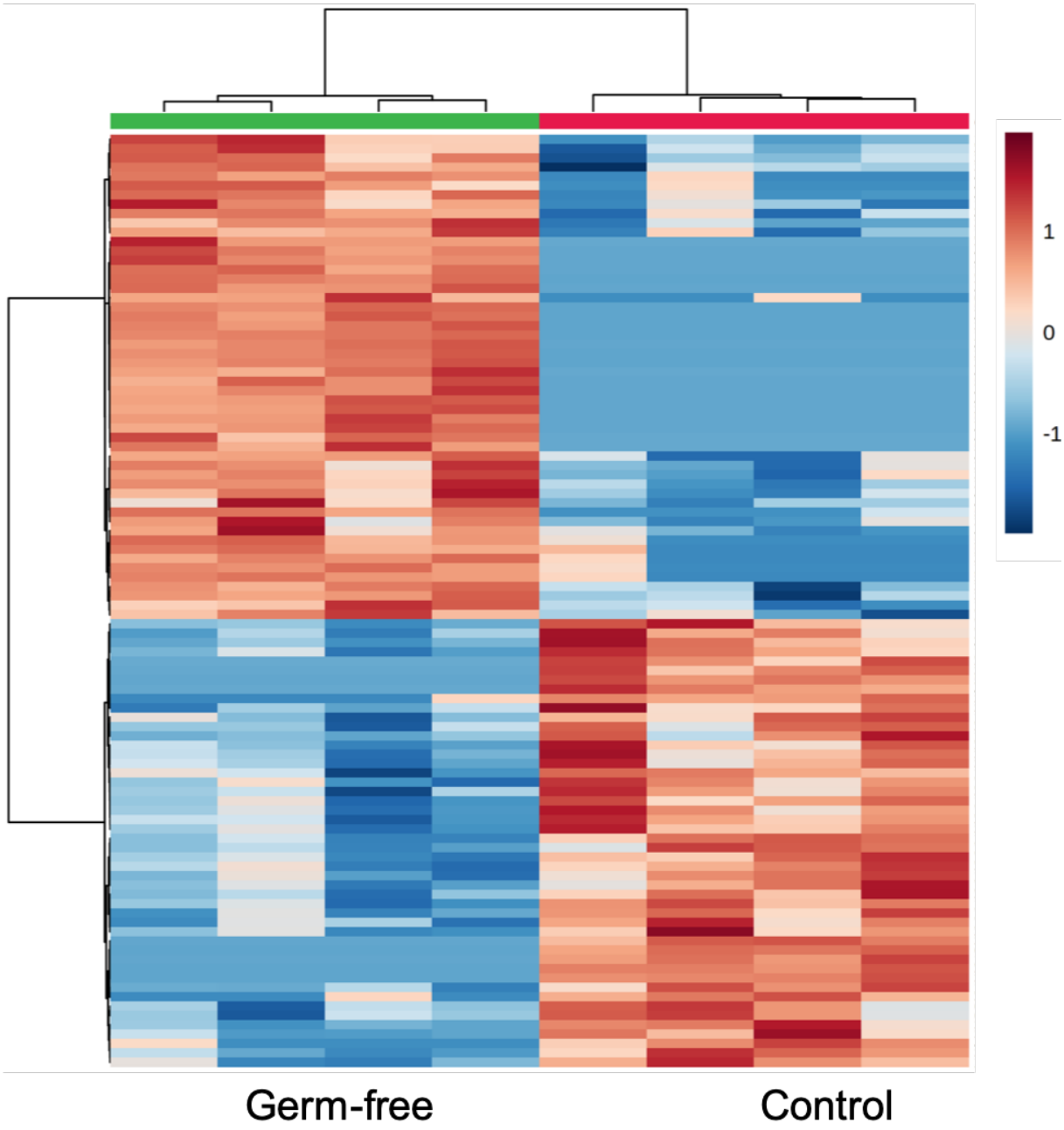

Figure 8. Heatmap showing the top 100 mass traces altered between germ-free and control polyps. The samples and mass traces were clustered hierarchically using a Ward's linkage algorithm with Euclidean distances. Each sample is represented as a single column, with germ-fee animals in green and control animals in red.

127 mass traces were significantly altered (FC > 1.5, $p < 0.05$; Figure 9) and I was able to annotate 88 of these with putative compound names, though many mass traces have hits to multiple compounds due to the presence of isomers or adducts, so there are a total of 1538 annotations for the 88 mass traces (Supplementary File 1).

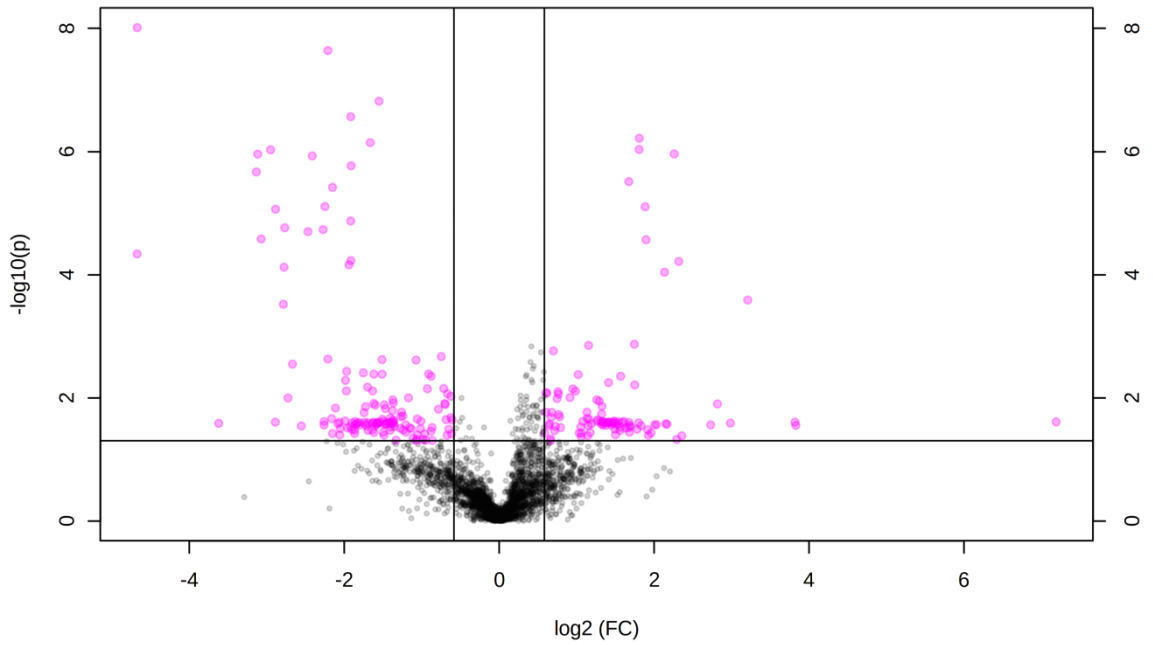

Figure 9. A volcano plot indicating significantly altered mass traces between germ-free and control polyps. Each point represents a single mass trace, with significantly altered traces in pink (FC > 1.5, $p < 0.05$). Mass traces high in control animals have positive fold change values (log2(FC)), while masses high in germ-free animals have negative fold change values.

Metabolomic analysis of in vitro bacterial samples

In the next mass spectrometry experiment, I examined the metabolomic profiles of the five main colonizers. Recolonization of germ-free *Hydra* with *Pelomonas* or all five main colonizers was enough to increase contraction frequency of control polyps[41]. Because the bioactive extracts were produced in vitro, I reasoned that *Pelomonas* and/or co-cultured main colonizers would produce contraction mediating compound(s) in vitro.

Following application of the modified 80% rule to remove problematic zero values from the bacterial mass spectra 1369 mass traces remained. Because I couldn't be sure that the mass trace(s) representing contraction-mediating compounds would be significantly different under my culturing conditions, the entire list of 1369 compounds was used to look for mass traces shared between this and the *Hydra* and original extracts datasets.

PCA plots indicate stark differences between the metabolite profiles of *Undibacterium* and *Curvibacter* relative to the other strains and the co-cultured strains (Figure 10). This is also evident in the heatmap, where one can see many *Curvibacter* and *Undibacterium*-specific mass traces (Figure 11). Fisher's Least Significant Difference post-hoc test identified 1039 mass traces as significantly altered across the strains (Supplementary File 2).

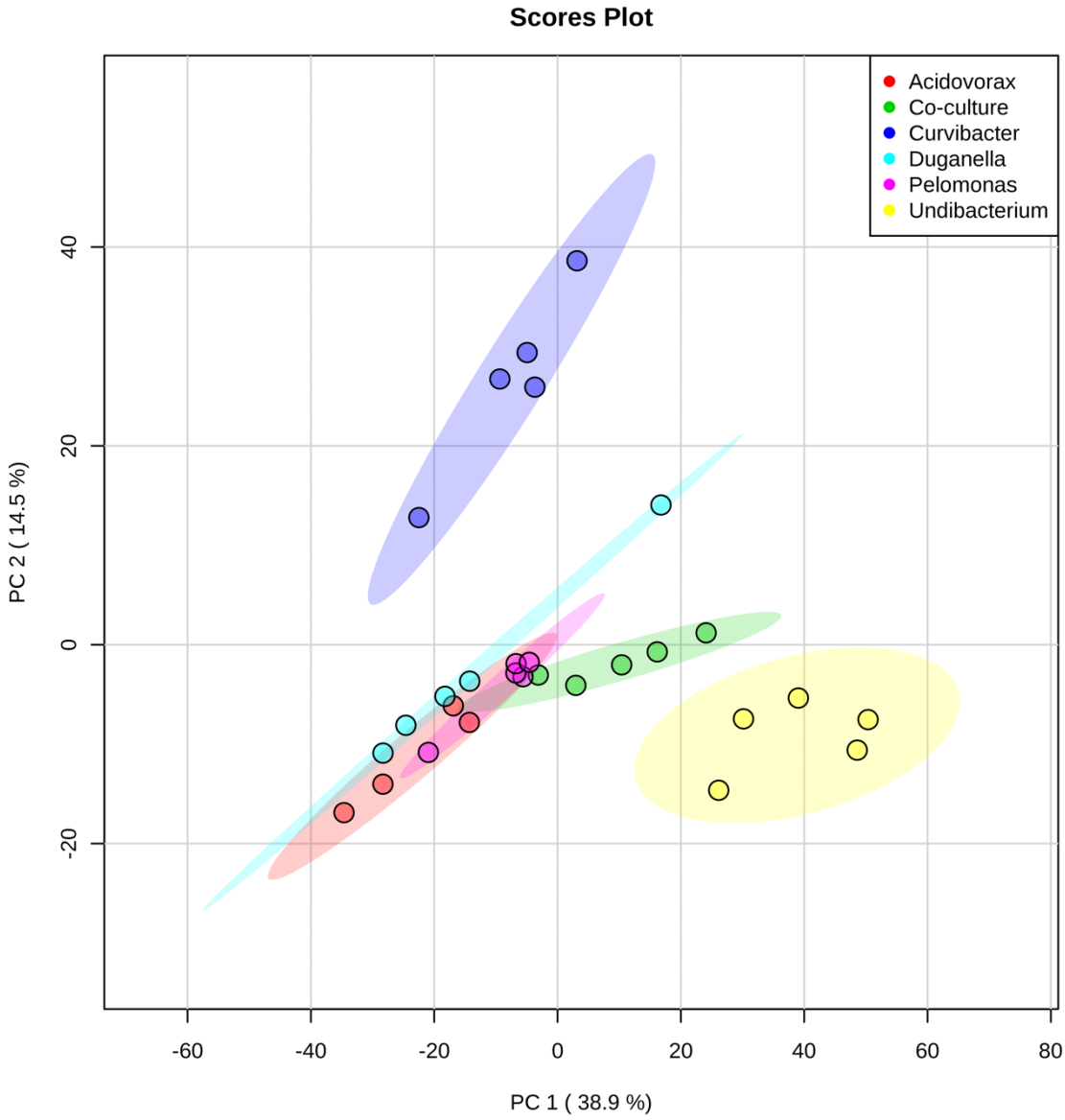

Figure 10. PCA plot of MS data from the main colonizers of *Hydra.* Each point represents an individual replicate, with the colours representing the strains and co-culture.

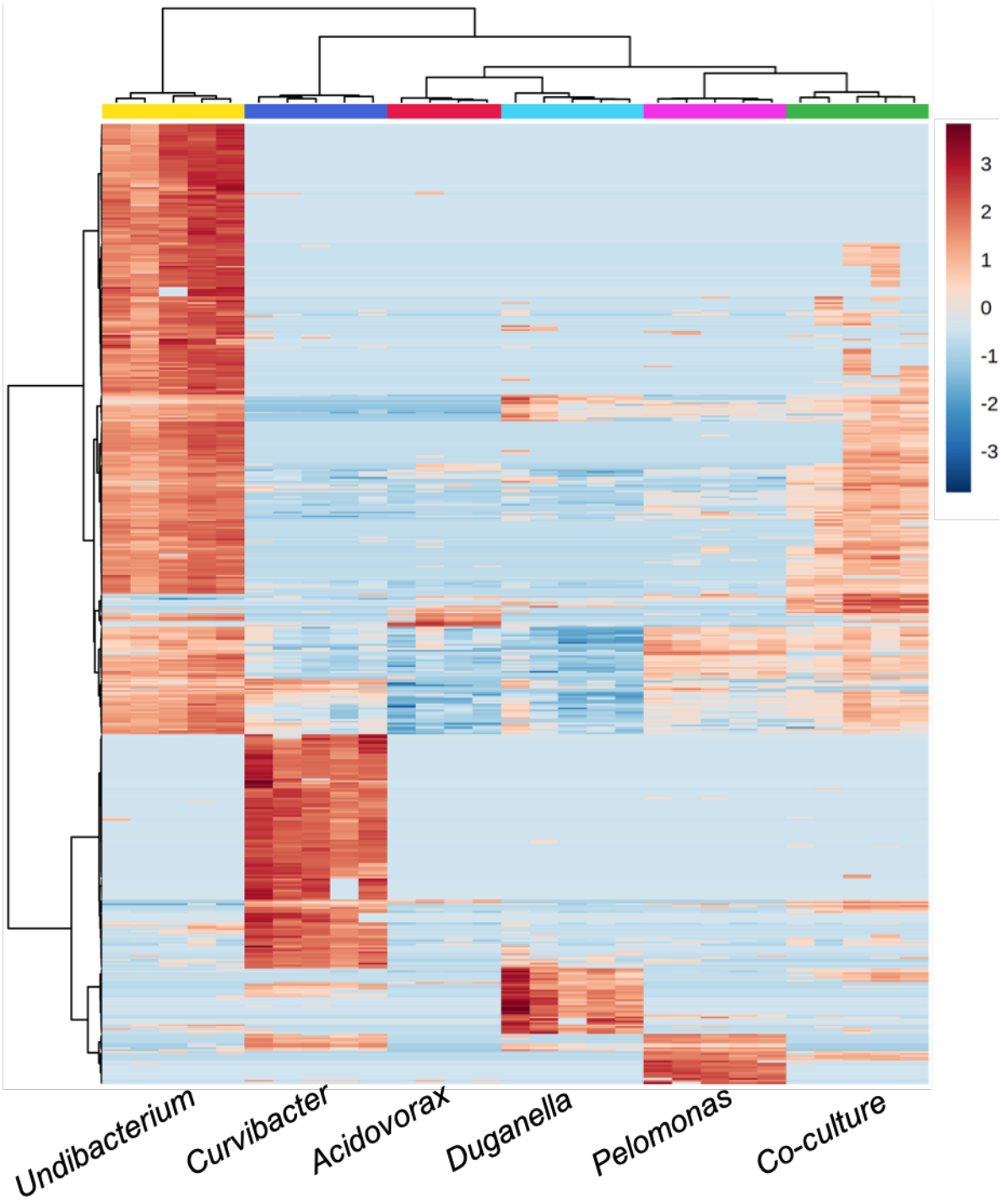

Figure 11. Heatmap depicting the relative intensities of the mass traces in the metabolic profiles of the five main colonizers of *Hydra* (alone and in co-culture).Each column represents a single sample, while the coloured bars represent the strains (*Undibacterium:* yellow, *Curvibacter:* dark blue, *Acidovorax:* red, *Duganella:* light blue, *Pelomonas:* purple, co-culture: green).

Metabolomic analysis of original extracts

Finally, in the third mass spectrometry experiment for the bioactive-compound-identification metabolomics pipeline, I examine the metabolomic profiles of the original bioactive extracts (these samples were used in the assays for the original report[41]). 16,063 mass traces were identified in the two original extracts, and 1188 of these were identified in both extracts. With only two replicates, this dataset did not lend itself well to statistical analysis, so all of the mass traces were included in the subsequent analyses in this pipeline.

Overlap between datasets

Finally, with these three experiments, I was able to create a data processing pipeline to look for compounds that might increase contraction frequency. I looked for mass traces common to control *Hydra*, the in vitro-cultivated microbes and the original extracts. Six mass traces meet these criteria (Supplementary Table 3) and I found annotations for 4 of the 6 mass traces. Due to the presence of isomers or adducts, these 4 mass traces match the expected m/z of 31 compounds (Supplementary Table 4, Supplementary File 3). One mass, 365.1373, matched with 17 compounds.

Of course, it is possible that the contraction-regulating compound(s) are quickly turned over in vivo or not produced at sufficient amounts to be detected by the mass spectrometer. To account for this, I also looked for compounds common between the extract and microbial datasets. 144 additional compounds were common between the datasets with annotations possible for 115 of the mass traces. The mass traces match the expected m/z of 1818 annotations (Supplementary Table 3, Supplementary File 4).

Further, I had to consider the possibility that the target compound(s) were not produced or not detected under the bacterial culturing conditions. In that case, compounds present in both the extracts and high in microbe-containing polyps are of interest. An additional 3 compounds that were high in control animals were also present in the extracts, but not in the microbial dataset (Supplementary Table 3, Supplementary File 5). Annotations were possible for all three of the mass traces, for a total of 13 annotations.

Germ-free *Hydra* polyps contract less frequently than control animals

The original behavioural assays that demonstrated the effect of *Hydra* microbiota on contraction frequency were performed on starved polyps[41]. I assessed the differences in contraction rate between germ-free and control *Hydra* that were well-fed because the nutritional status of polyps can affect contraction rate[95] and I reasoned that increased energy stocks might increase the differences in contraction rate between germ-free and control polyps. The hope was that an increase in effect size might allow for fewer animals to be used, speeding up the process of testing extracts or candidate molecules.

Germ-free animals starved for three weeks contracted at 87 ± 4.5% (mean ± standard error) the relative contraction frequency of control animals ($p = 0.11$; n = 32 control, 58 GF; Figure 12A). The decrease in contraction frequency was similar in the fed animals, with the average contraction frequency of germ-free polyps at 83.5 ± 5.6% relative to control animals ($p = 0.02$; n = 32 control, 31 GF; Figure 12B).

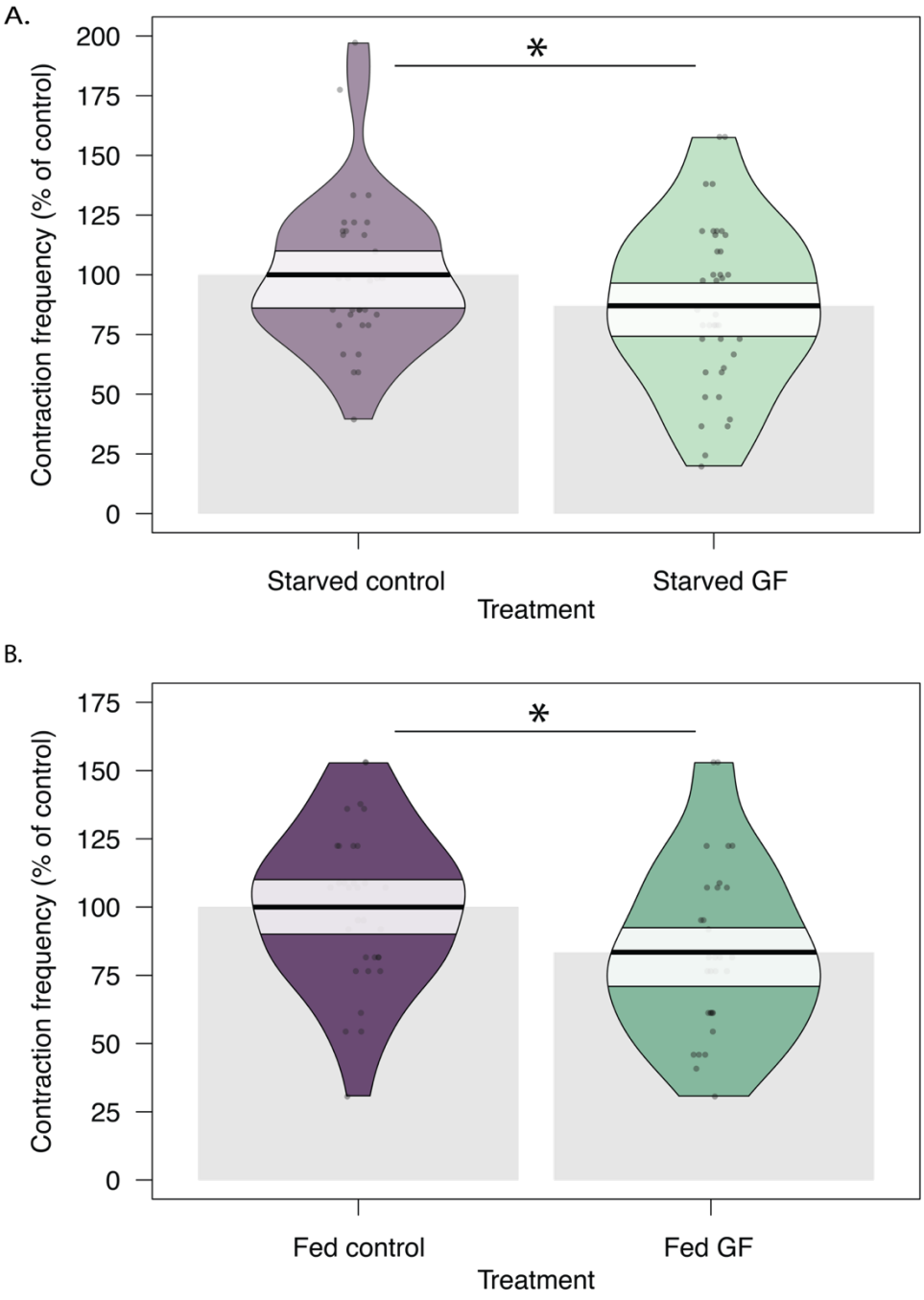

Figure 12. The contractions of germ-free animals are lower than the microbe-containing control animals. (A) Three week starved germ-free animals contracted at 87 ± 4.5% (mean ± standard error) the relative frequency of control animals (p = 0.11; n = 32 control, 58 GF). (B) Long-term, fed germ-free animals contracted at 83.5 ± 5.6% the relative frequency of the controls (p = 0.02; n = 32 control, 31 GF).

Effect of microbial extracts on contraction frequency

To begin to assess the effects of microbial extracts on the contraction frequency of *Hydra*, I tested a negative control. This was important because the original report did not include a microbe-free extract[41] and unpublished data from Dr. Murillo-Rincon indicated that the R2A medium used for microbial culturing has contraction-stimulating activity. If there was any R2A carried over into the microbe-free extract, it was not enough to elicit a measurable response of the germ-free polyps ($p = 0.58$; n = 41 GF, 35 vehicle control; Figure 13).

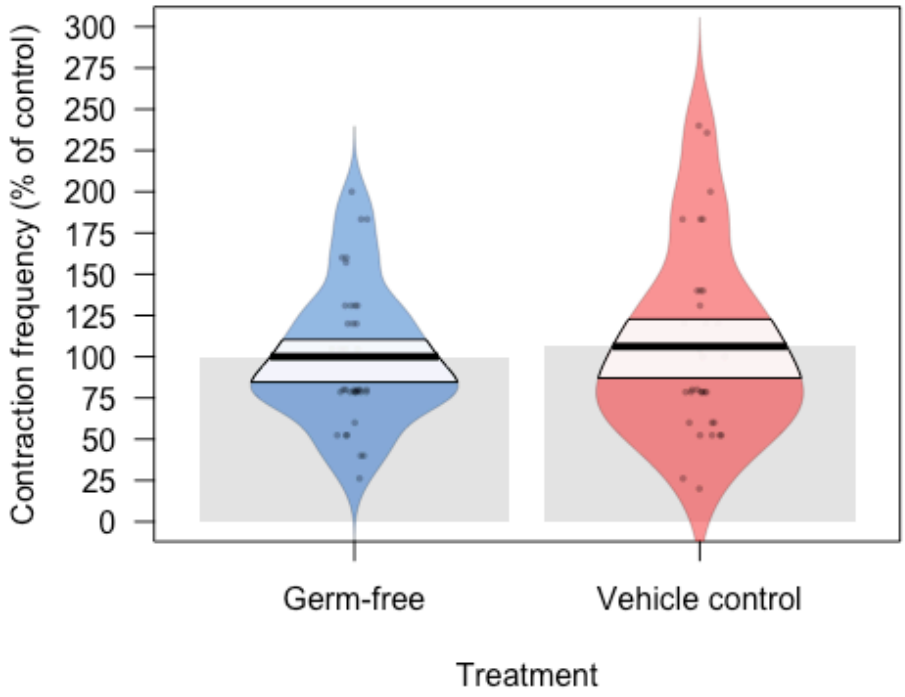

Figure 13. There was no effect of the vehicle control extract on contraction frequency ($p = 0.58$).

Next, I tested the extract that was prepared the same way as previous extracts, using the native microflora of *Hydra.* Addition of this extract to germ-free polyps reduced the contraction frequency to 64.2 ± 5.2% relative to germ-free polyps with no extract added ($p = 1.10 \times 10^{-5}$; n = 28 extract, 24 GF; Figure 14).

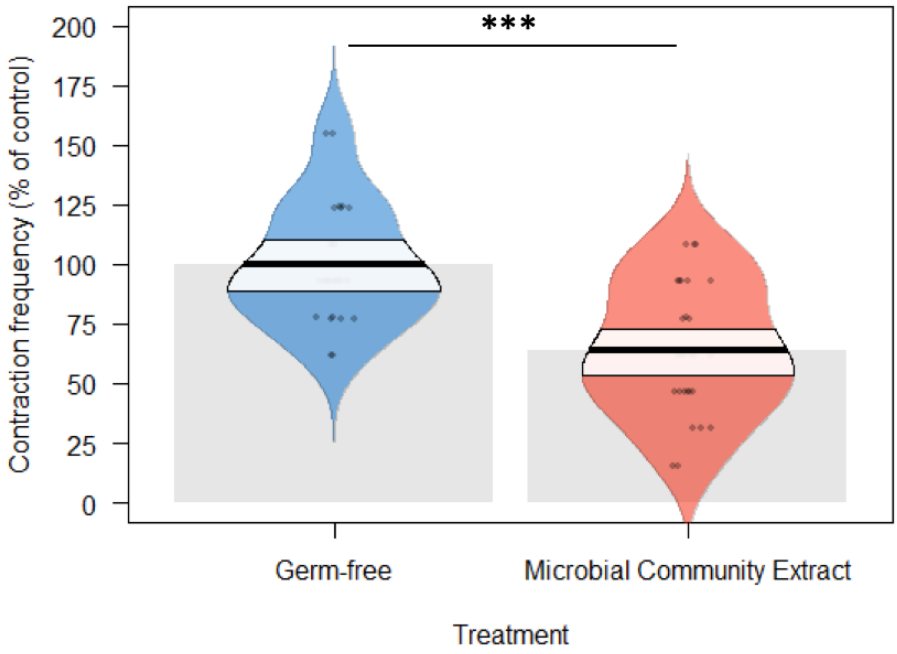

Figure 14. Addition of the extract containing the culturable microbial community of *Hydra* to germ-free polyps resulted in an unexpected decrease in contraction activity ($p = 1.1 \times 10^{-5}$; n = 28 extract, 24 GF polyps).

Finally, I used only the five main colonizers to produce an extract. Recolonization of germ-free polyps with these five colonizers increased contraction frequency[41], suggesting that a contraction-mediating molecule may be produced by co-culturing the five main colonizers. To test this, I created an extract using frozen glycerol stocks of these five strains and found that germ-free animals contracted 128 ± 7.3% more often when this extract was applied versus germ-free animals with no extract added (p = 0.25: n = 16 extract, 27 germ-free; Figure 15).

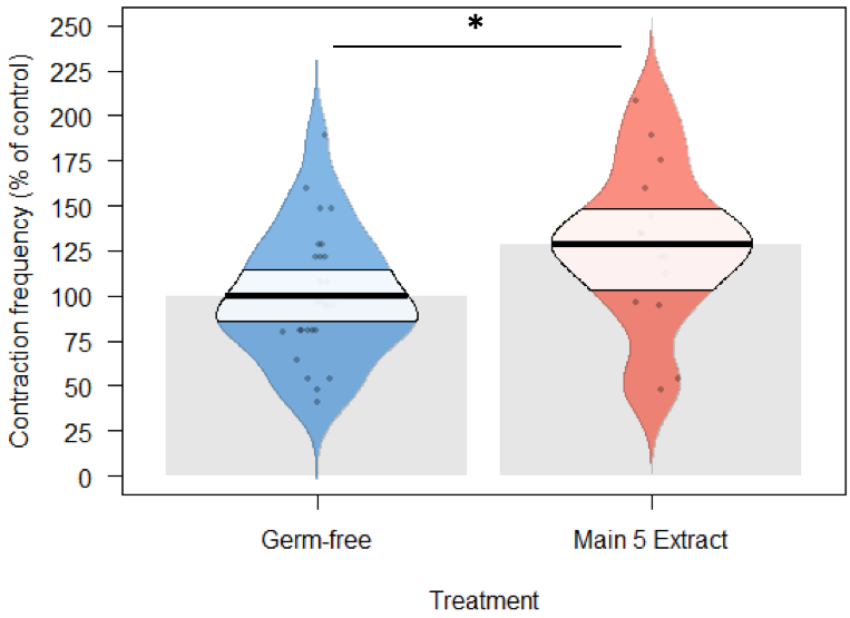

Figure 15. The new microbial extracts created with the five main colonizers increase contraction frequency by 28% relative to germ-free polyps (p = 0.035; n = 16 extract, 27 GF).

16S analysis of native microbiota extract

I was able to find four of the five main colonizing species of *Hydra* within the 16S sequences generated from the native microbiota extract. *Duganella* was not present, despite the fact that it is easily cultured on R2A agar[96]. Unfortunately, the 16S sequences of the original extracts was not tested[41], so it is not possible to compare the 16S sequences of the new and old extracts.

Metabolomic analysis of the five-microbe extract

In the previously described mass spectrometry experiments, the scanning range was between m/z 147 – 1000. Glutamate and GABA are too small to have been detected using this method and it was important to look for these compounds because they are modulators of the feeding response duration and contraction frequency[61], both of which are affected by microbes in *Hydra*[41,42]. Further, a new report found that the contraction frequency of *Hydra* is controlled by neurons that express acetylcholine receptors[55], and again acetylcholine has too low a molecular weight to have been detected in my previous mass spectrometry experiment. Since bacteria are reported to produce a number of neurotransmitters[97], I broadened my search criteria to include other neurotransmitters in my annotation results. Because the

scanning ranges of the two experiments overlapped, I was also able to look for the six mass traces common between the original extracts, in vitro-cultured microbes, and microbe-containing *Hydra*.

Of the 2740 compounds detected in the five-microbe extract, 197 were significantly different between the microbe-free and the five-microbe extracts. One or more of the 123 compounds higher in the microbe-containing extracts (Supplementary Table 5) could be responsible for the contraction-increasing behaviour attributed to these extracts, however, none of these mass traces matched with the six candidate molecules that overlapped between the three other mass spectrometry experiments.

In vitro GABA production by the main colonizing species of *Hydra*

Neither glutamate nor acetylcholine were increased in the microbe-containing extracts relative to the inactive microbe-free control. There was, however, an increase in GABA levels relative to the medium-only control (FC = 1.5, p = 0.018), suggesting that one or more of the main colonizing species of *Hydra* is able to produce GABA (Figure 16).

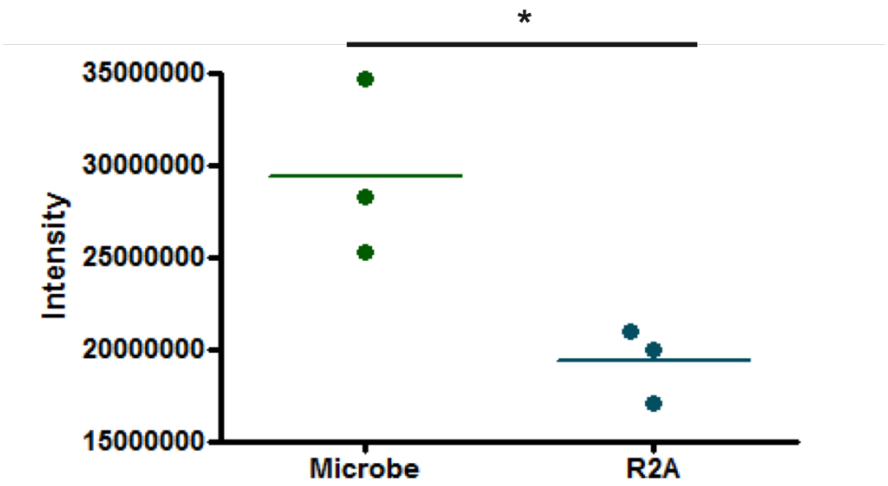

Figure 16. The levels of GABA increased in microbe-containing compared to microbe-free culture media (FC = 1.5, p = 0.018).

The genomes of all five bacterial strains suggest GABA-metabolizing capabilities

After obtaining the above results suggesting GABA production by *Hydra* microbiota, I set up a collaboration with Georgios Marinos (UKSH). Using his metabolic modelling approach, he found that the five main colonizing bacterial species of *Hydra* are able to produce GABA using putrescine as a precursor (Figure 17). However, only *Duganella* possess a GABA transporter, suggesting that the GABA present in mixed culture bacterial extracts may have originated from this strain (Supplementary File 6).

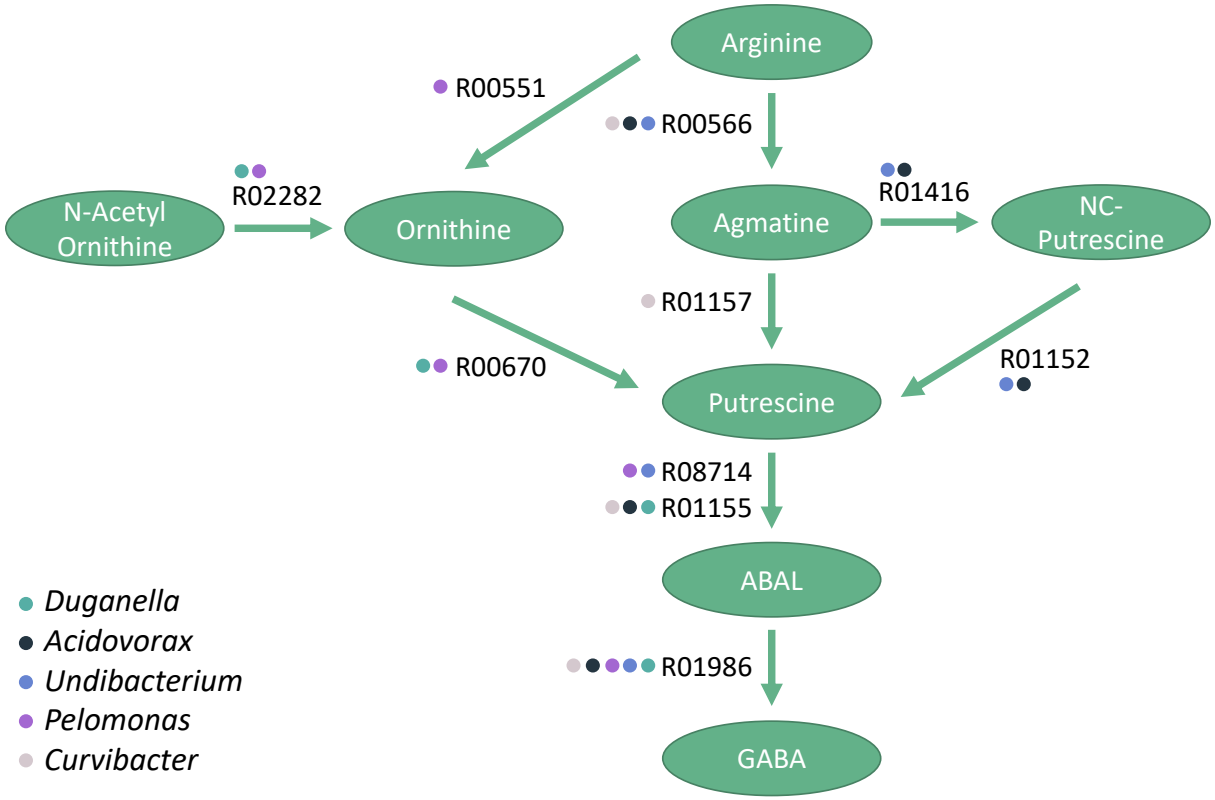

Figure 17. All five of the main colonizing bacterial strains of *Hydra* are predicted to produce GABA based off of metabolic modelling results. Although the enzymes and pathways differ, e.g. *Duganella* is not predicted to use arginine as a precursor, all of the strains use putrescine as an intermediate in GABA production. Kyoto Encyclopedia of Genes and Genomes (KEGG)[77] reaction identifiers are given in black.

Putrescine, a GABA precursor, has varied effects on the growth of *Hydra* colonizers

The modelling data predicts that all of the main colonizers of *Hydra* are able to metabolize putrescine to form GABA, which in turn can be used to produce the tricarboxylic acid (TCA)

cycle metabolite succinate[98]. Because of the link between putrescine, GABA and cellular respiration, I hypothesized that the bacteria may utilize putrescine as a growth substrate.

The results for *Curvibacter* were striking: it grew better in 10 mM putrescine than in the standard culturing medium R2A (Figure 18). The strain grew so well in putrescine that the carrying capacity (the maximum population size for each medium type, given in absorbance at $OD_{600;}$ k) in 1 mM putrescine was indistinguishable from the carrying capacity of R2A ($k_{1mM\ Put}$ = 0.049 ± 0.002, k_{R2A} = 0.045 ± 0.007, p = 0.64), and in 10 mM putrescine, the carrying capacity far exceeded that of R2A for this strain ($k_{10mM\ Put}$ = 0.40 ± 0.005, p = 7.2 x 10^{-11}). As stated in the methods section, stationary phase was not reached in the cultures, so carrying capacity here is used as a proxy for biomass accumulation.

Similarly, *Duganella* grew well in putrescine, but culture densities in R2A far exceeded those reached in either putrescine concentration (Figure 19). The carrying capacity of 1 mM putrescine ($k_{1mM\ Put}$ = 0.13 ± 0.002) was actually higher than that of 10 mM putrescine ($k_{10mM\ Put}$ = 0.056 ± 0.004; p = 0.00039), possibly owing to toxic effects at this concentration.

Acidovorax, in contrast, began to grow well in 1 mM putrescine, but the culture crashed around 2.5 hours post-inoculation (Figure 20). This behaviour was not observed in 10 mM putrescine (Figure 20), where the culture declined with time. *Pelomonas* exhibited similar growth dynamics in 1 mM putrescine, crashing at around 7 hours post-inoculation and its culture density decreased with time in 10 mM putrescine (Figure 21).

Perhaps the most surprising growth dynamics were exhibited by *Undibacterium*, where population densities began oscillating at about 10 hours post-inoculation (Figure 22).

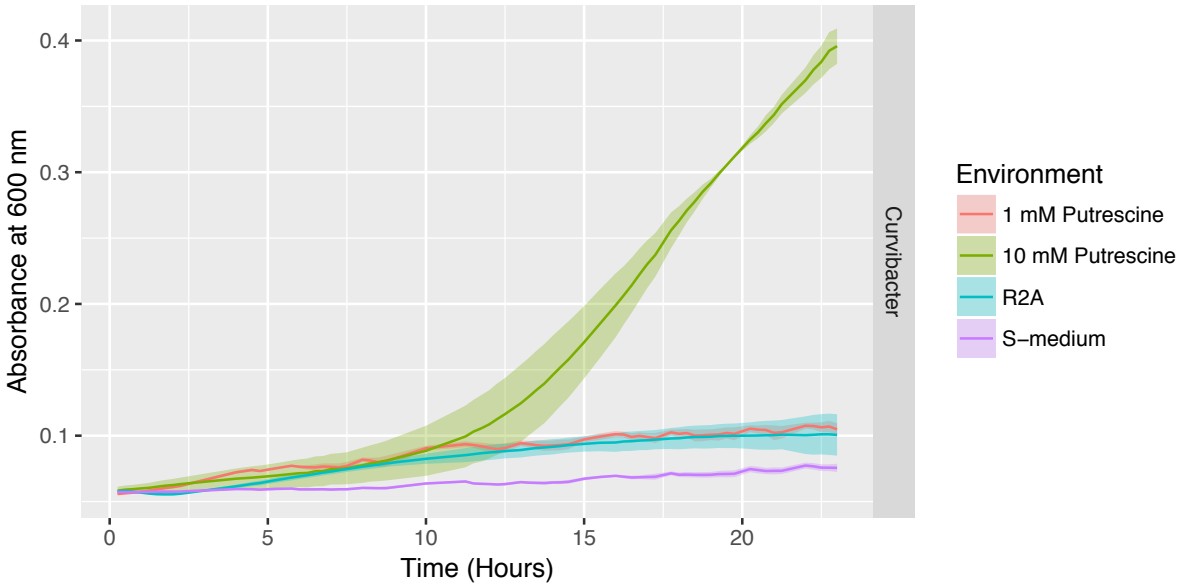

Figure 18. The growth curve of *Curvibacter* using putrescine as the only carbon and nitrogen source. The standard growing medium R2A is included on this graph to demonstrate the superiority of 10 mM putrescine to elicit growth in this strain. Transparent area around the curve shows standard deviation from the mean.

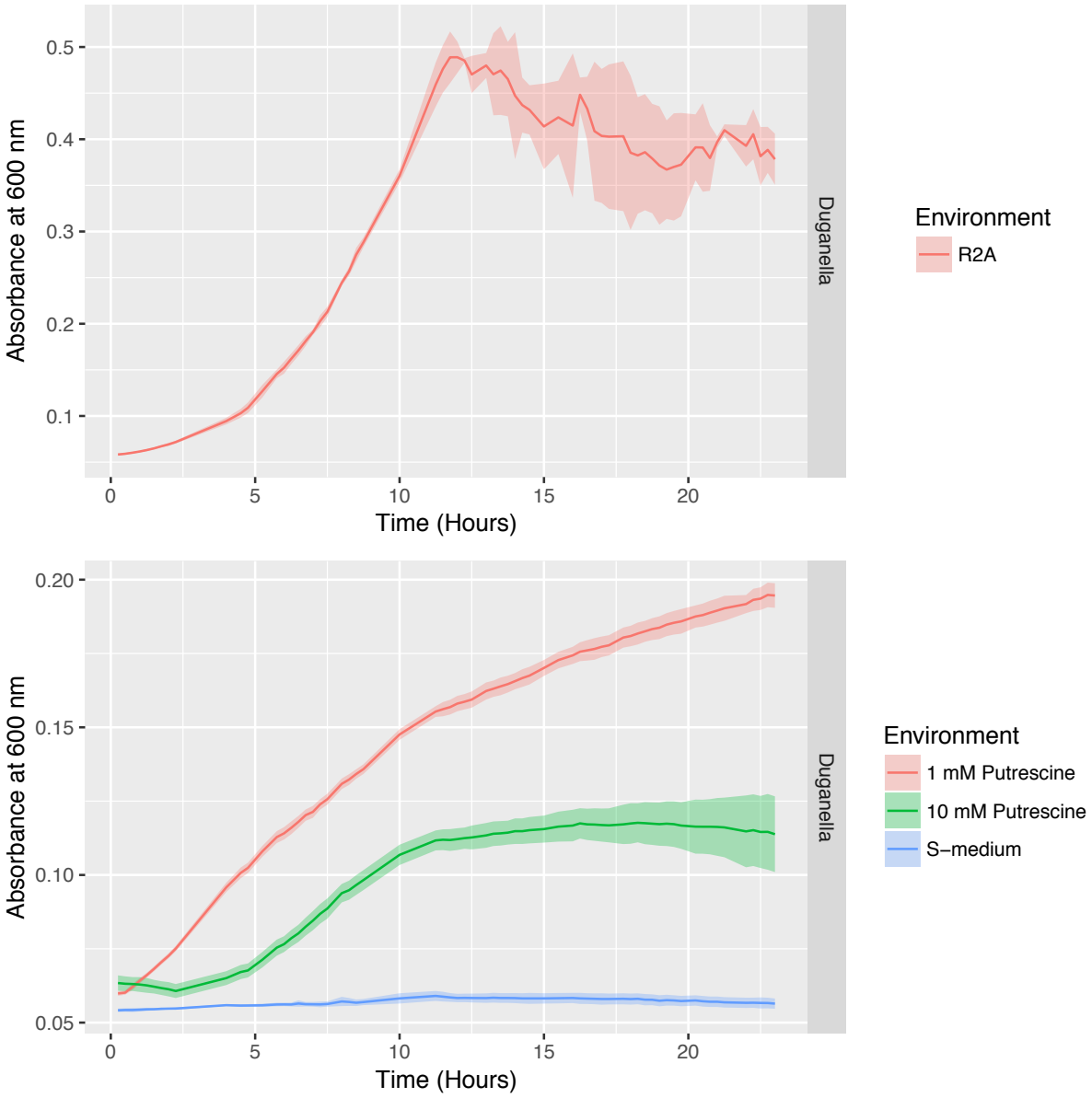

Figure 19. Growth of Duganella in s-medium supplemented with 1 or 10 mM putrescine. Growth in R2A was higher than in putrescine and was therefore separated to better observe the growth dynamics in putrescine-containing media. Transparent area around the curve shows standard deviation from the mean.

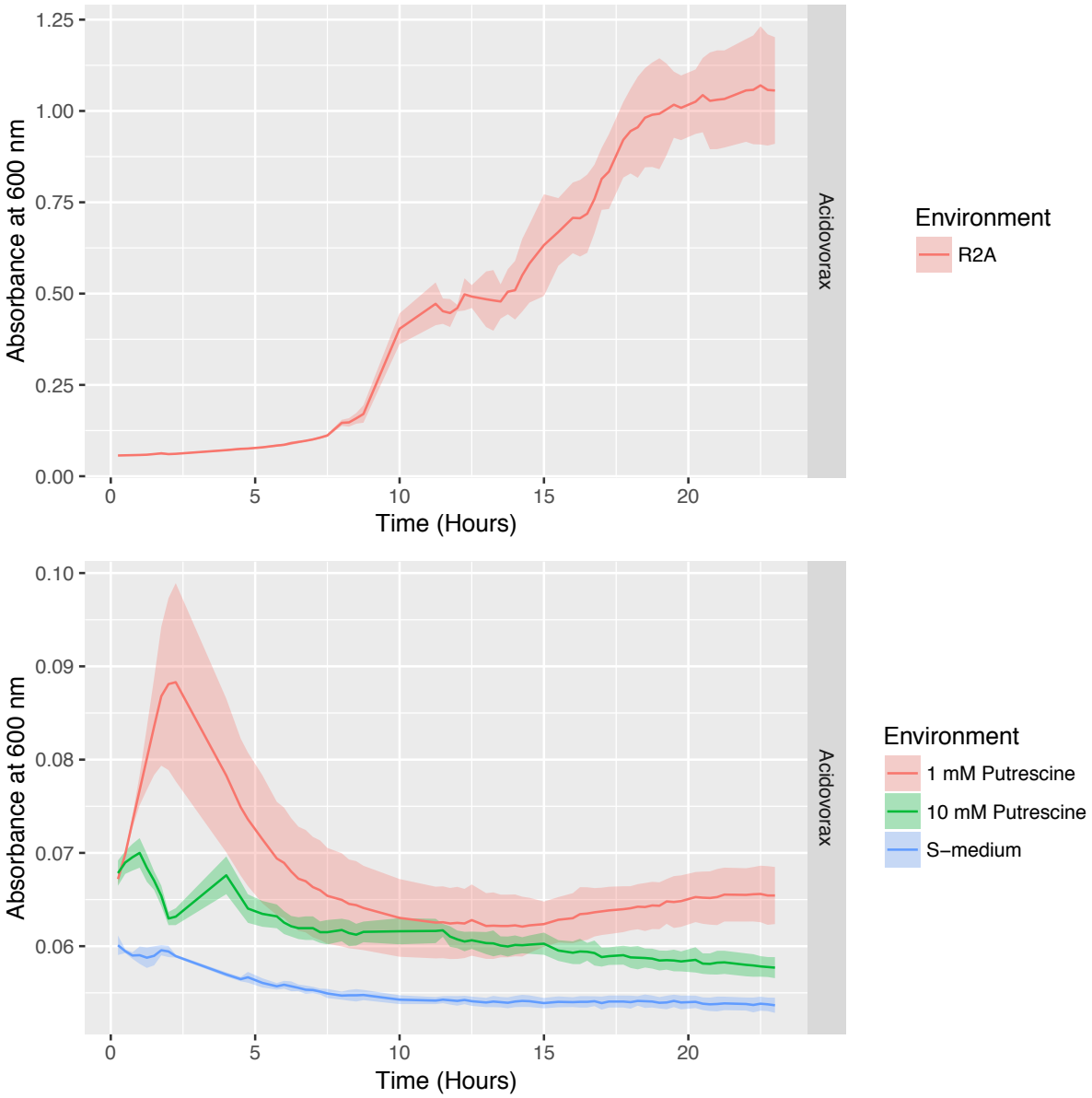

Figure 20. The growth of *Acidovorax* in 1 and 10 mM putrescine. The standard growth medium used for culturing *Acidovorax* is R2A and included here as a positive control. Transparent area around the curve shows standard deviation from the mean.

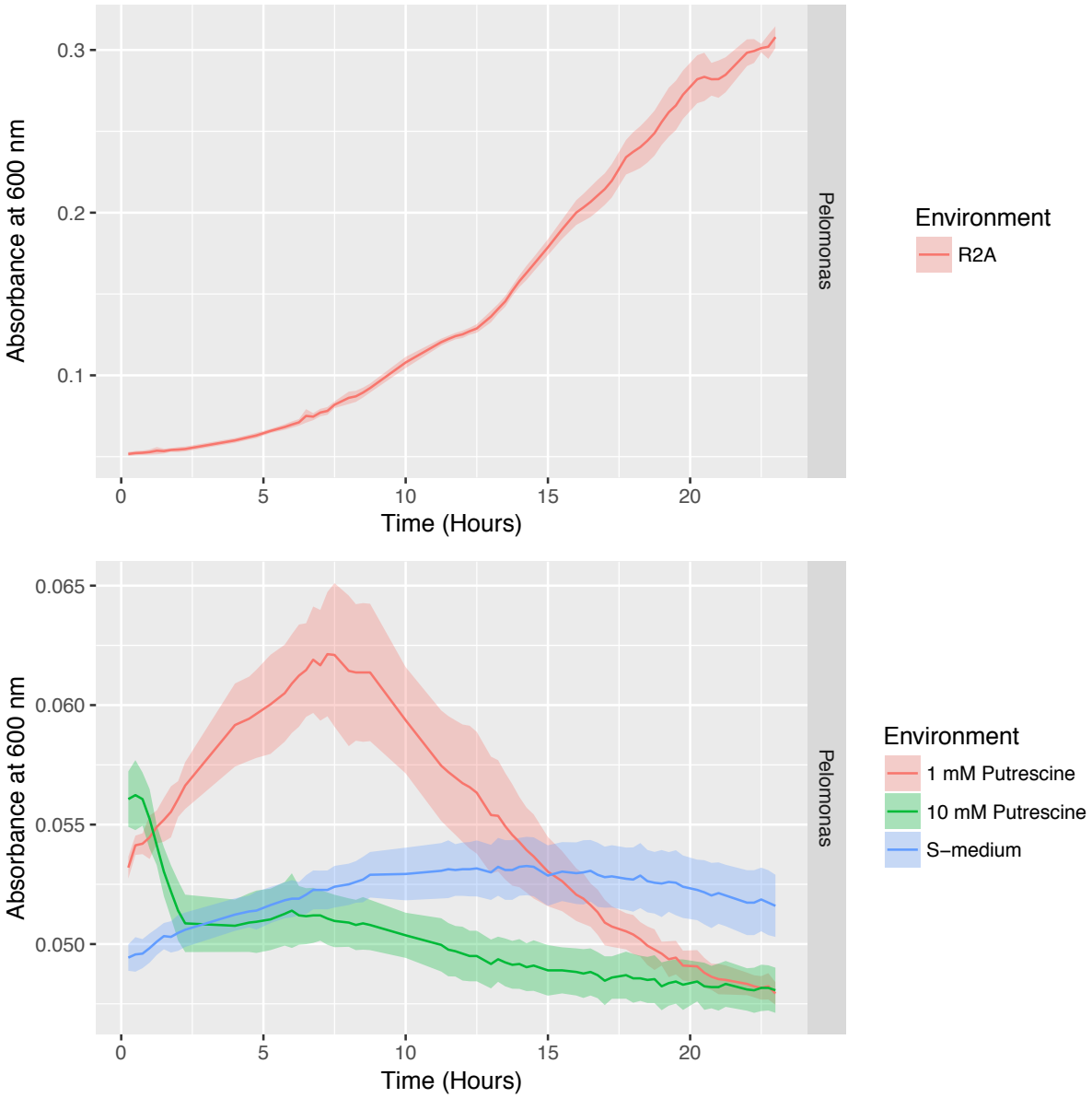

Figure 21. The growth curve of *Pelomonas* with only putrescine as a carbon and nitrogen source. S-medium contains no energy sources and thus provides a baseline for growth from existing cellular resources. Transparent area around the curve shows standard deviation from the mean.

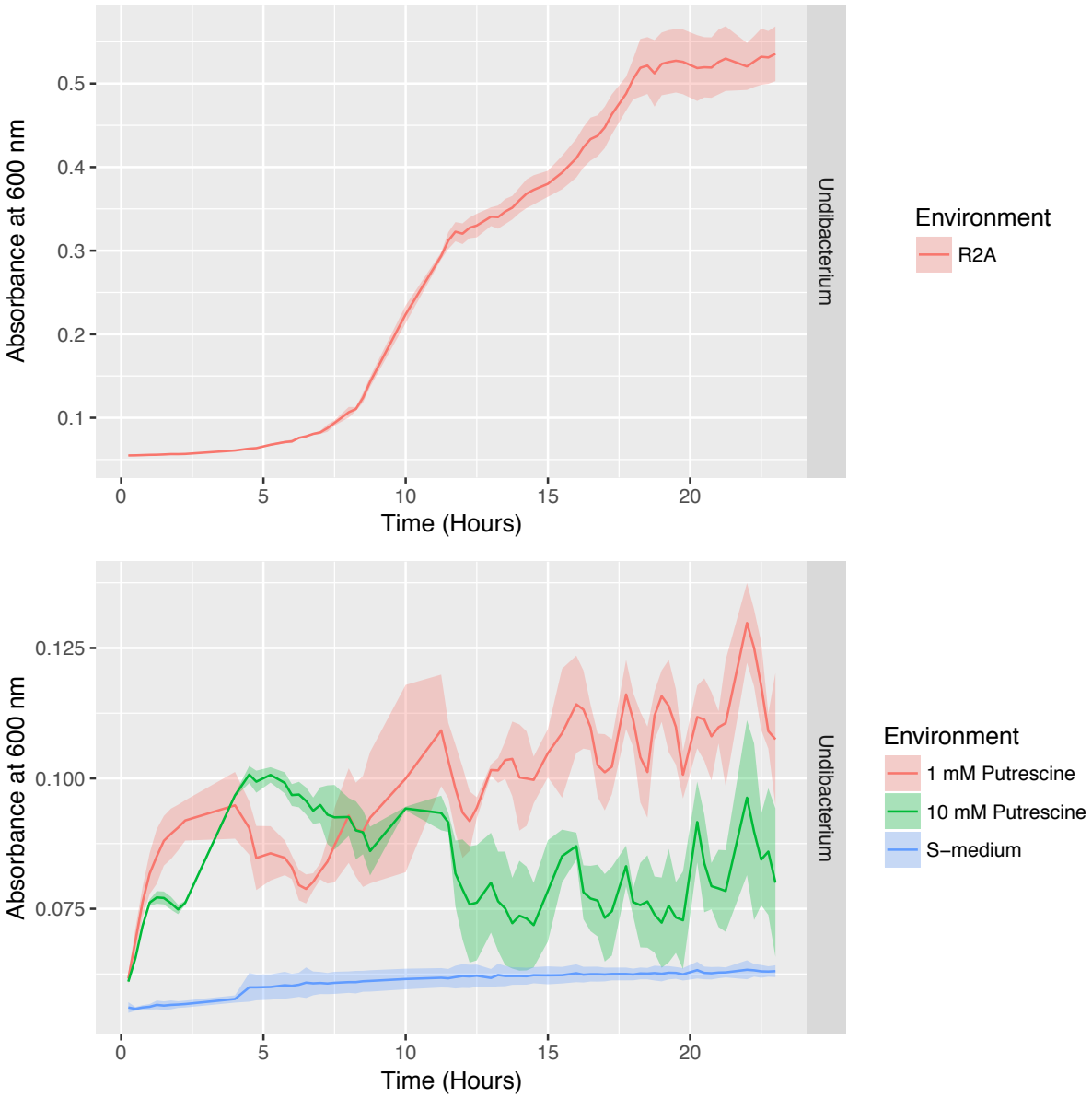

Figure 22. Growth of *Undibacterium* using only putrescine as a carbon and nitrogen source, with R2A and s-medium as positive and negative controls, respectively. Transparent area around the curve shows standard deviation from the mean.

The chemoeffector prolyl-leucine is produced by *Hydra* and members of its microbiome

One mass trace (m/z 227.1401), putatively annotated as prolyl-leucine, was chosen for follow up based on reports of the dipeptide acting as a chemoattractant in both eukaryotic and prokaryotic species[99,100]. This compound was 4-fold higher in germ-free polyps compared to control polyps ($p = 9.7 \times 10^{-8}$; Figure 23) and produced by *Undibacterium* and in co-culture (ANOVA $p > 0.0001$; Figure 24).

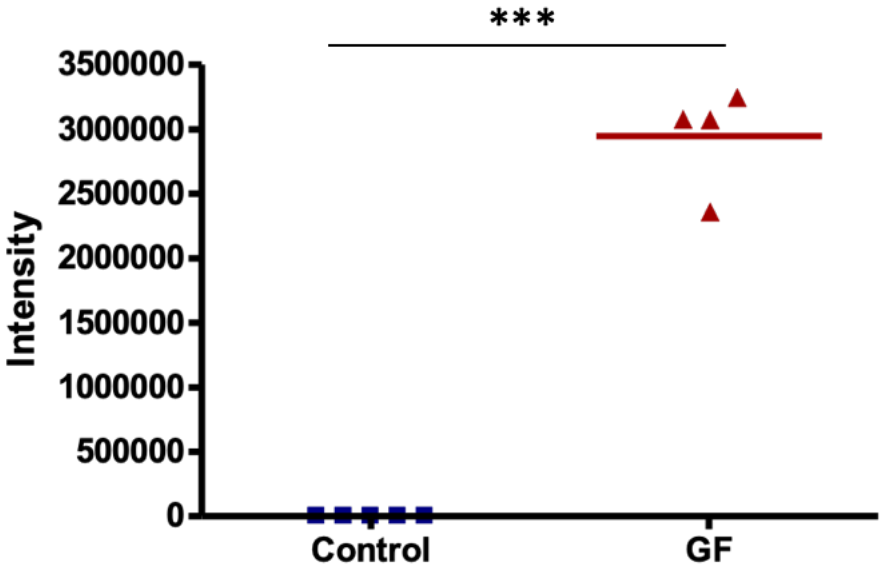

Figure 23. A mass trace matching the expected mass of the dipeptide prolyl-leucine is 4-fold higher in germ-free polyps relative to control polyps ($p = 9.7 \times 10^{-8}$).

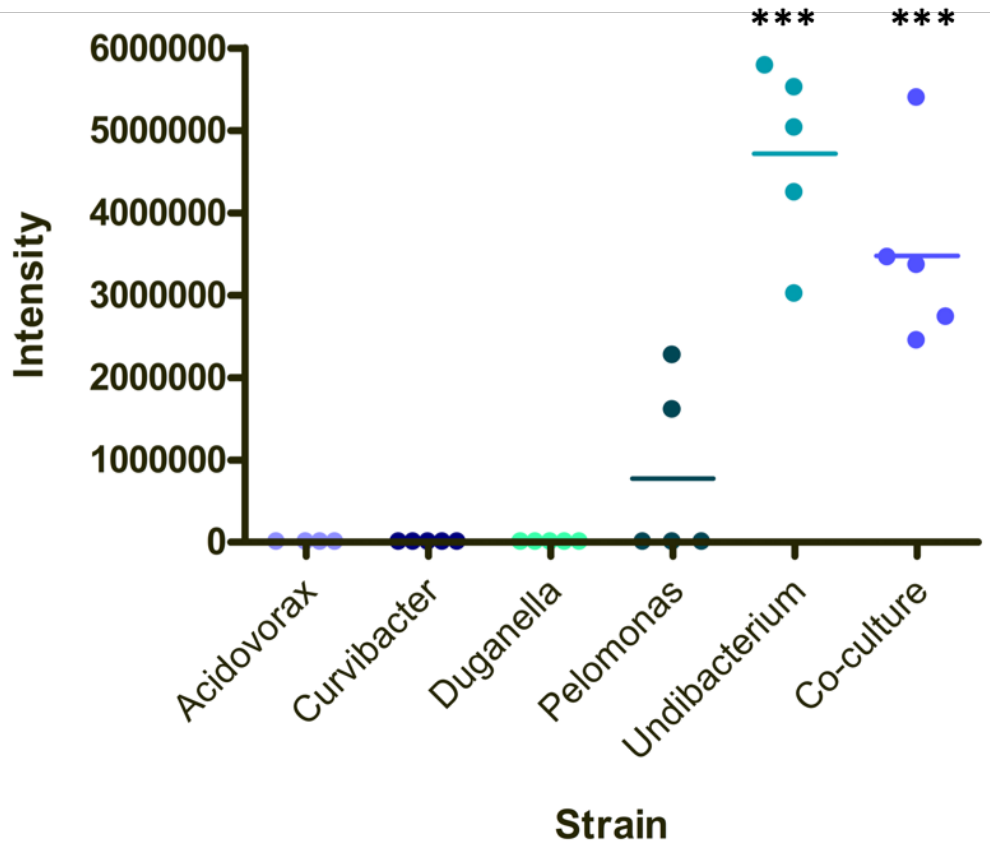

Figure 24. The putative dipeptide was also produced by *Undibacterium* and detected in co-culture, but not by the other main colonizers (ANOVA $p < 0.0001$).

MS/MS fragmentation is consistent with dipeptide annotation but unable to differentiate between the isomers

Fragmentation of the m/z 227.1401 mass trace was successful, but there were fragments matching all of the isomers present. This indicates that the mass trace may represent several chemical species, i.e. prolyl-leucine, leucyl-proline, isoleucyl-proline and prolyl-isoleucine may all be present in the sample.

Non-ribosomal peptide synthetases are predicted to be present in four of five main colonizers

I used antiSMASH to search the bacterial genomes for the metabolic potential to produce various secondary metabolites because having additional information about the metabolic potential of the bacterial strains could help with compound annotation. Putative non-

ribosomal peptide synthetases were identified in all of the genomes of the main colonizers except *Acidovorax* (Table 1), suggesting the bacteria may produce bioactive cyclic peptides or short peptide fragments.

Table 1. Secondary metabolite classes predicted to be produced by the main colonizers of *Hydra* based off of putative annotation from antiSMASH.

Secondary metabolite class	Pelo	Undi	Acido	Dug	Curvi
Acyl amino acids	4	0	1	2	0
Lanthipeptide	1	0	0	0	0
NRPS	1	1	0	2	1
Terpene	1	1	1	1	1
Bacteriocin	3	2	3	0	1
NRPS-like Homoserine lactone	1	0	0	0	1
NRPS, T1PKS	1	0	0	0	0
Homoserine lactone	0	1	0	0	1
Siderophore	0	1	0	0	0
Betalactone	0	0	1	0	2
NRPS-like	0	0	0	0	1

Discussion

Adult neurogenesis is not influenced by the microbiota of *Hydra*

There was no detectable influence of *Hydra* microbiota on neurogenesis or the nerve cell density of adult polyps (Figure 4Figure 5). Notably, we cannot rule out the possibility that the microbiota in *Hydra* play a role in early-life neurogenesis, as this study was performed on adult animals.

The influence of *Hydra* microbiota on feeding and contraction responses was observed in polyps that were allowed to develop to adults in the presence of their microbiota[41,42]. Clearly the microbes are interacting with the nervous system in some way, as contraction frequency and feeding duration are both nervous system-dependent behaviours[55]. As I mentioned in the introduction, microbiota can influence both nervous system anatomy and function. There is still the possibility that resident microbiota affect the anatomy of the *Hydra* nervous system at the cellular level, as I did not assess changes to neuron morphology. Alteration of dendritic branching has been observed in mouse and rat studies[101,102], and this could play a role in microbiota-nervous system interactions in *Hydra* as well.

For example, neuron morphology in rats is permanently altered through prenatal inhibition of the production of the kynurenine pathway, involved in tryptophan catabolism[102]. Microbial metabolism is hypothesized to alter the flux of metabolites through the kynurenine pathway, with these alterations playing a role in some microbiome-related pathologies[103]. In germ-free mice, hippocampal pyramidal neurons are shorter and less branched than those of conventionally-raised mice, effectively reducing the overall number of synaptic connections in that brain region[101]. Diaz et al. (2011) demonstrated altered behavioural activity of germ-free mice and found concurrent changes to the expression of synaptogenesis-related proteins, providing further evidence that changes to nerve cell structure can be mediated by the microbiota. It would be interesting to observe the finer structure of neurons in germ-free polyps to see if similar changes occur in *Hydra.*

A metabolomics pipeline for the identification of bacterially-derived compounds influencing host metabolite profiles

Another possibility is that contraction frequency and feeding duration are altered through modulation of nervous system function, be it direct or indirect. At least in the case of contraction modulation, we can assume alteration of the nervous system function rather/also plays a role because the addition of microbial extracts to germ-free polyps increased contraction frequency after an incubation period of only about 16 hours[41,42], and it seems unlikely that much rewiring can take place so quickly in 4-week starved polyps. One of the aims of this study was to identify which of the bacterially-derived molecules in the extracts were responsible for the observed increase in contraction frequency. By analysing these very extracts on a high-resolution mass spectrometer, I was able to find 1188 unique mass traces. To reduce the chemical complexity, I designed an approach based on where the contraction-mediating compound could be assumed to be present. I made the following assumptions: (1) microbe-containing animals should have higher concentrations of the active compound than germ-free animals and (2) the molecule can be produced in vitro based on the biological activity of the in vitro-produced extracts.

First, I subjected germ-free and control polyps to mass spectrometry analysis. The difference between the metabolomic profiles of germ-free and control is nicely reflected in both the PCA plots and heatmaps (Figure 7 Figure 8). To find the contraction-mediating compound, only mass traces high in control animals are important, so I used a volcano analysis (Figure 9) to find compounds high in control animals relative to germ-free animals ($FC > 1.5$, $p < 0.05$). I compared these 127 mass traces to the clearly unique (based off of PCA and heatmap results, (Figure 10Figure 11) metabolomic profiles of the individual colonizers and the metabolomic profiles of the two original extracts. It is important to note that I did not restrict the comparison of the bacterial dataset to compounds high in the co-cultured sample, as the activity of the in vitro monocultures was unknown. This comparison yielded 6 unique mass traces (Supplementary Table 3). Regrettably, none of the 31 annotations (Supplementary Table 4) for these mass traces had links to contraction activity of *Hydra*. I searched the literature for contraction-mediating effects of the compounds in any organism, evidence of interaction with acetylcholine receptors, and gap junction proteins (gap junction signalling is

an important influencer of contractions in *Hydra*[104]). I also used KEGG and HMDB to look for links to known metabolic pathways.

Many of the hits seemed potentially spurious. The 17 potential identities were often plant-associated metabolites for the mass trace measured at m/z 365.1373 (Supplementary Table 4). Picrocrocin, is a metabolite of saffron that inhibits the growth of cancer cells[105]. 8-epiiridodial glucoside is an intermediate in the production of plant iridoid glucosides[106]. Similarly, iridodial glucoside is a precursor for other iridoid glucosides found in plants[107]. The various glucoside derivatives were also mainly associated with plant production[108]. Portuloside A is likewise a monoterpene glucoside isolated from purslane (*Portulaca oleracea*)[109]. Epijasminoside A contains a glycoside bonded to a sugar compound (compound class: o-glycosyl compounds) and was isolated from jasmine (*Gardenia jasminoides*)[110]. The various isomers of schizonepetoside are monoterpene glucosides derived from Japanese catnip (*Schizonepeta tenuifolia*)[111–113]. Importantly, all of the main colonizers contain biosynthetic gene clusters for terpene production (Table 1). There is a huge variety of terpenes and glucosides in nature, and some of them do interact with the nervous system in various ways[114,115].

Tetranor-PGFM, on the other hand, is structurally quite different than the other isomers. It is a prostaglandin that has been found in urine and faeces of mammals and is an apparent marker for pregnancy in cats and pandas[116,117]. Unlike the other metabolites matching m/z 365.1373, prostaglandins as a metabolite class have been reported in cnidarians, where they seem to be important for defense[118].

The compounds matching the expected mass of m/z 349.1423 were, again, plant-associated. (-)-trans-carveol glucoside, (+)-trans-carveol glucoside, and perilloside A are monoterpene glycosides[108,119,120].

Moving on to hits matching m/z 363.1216, again there are glucosides and prostaglandins. Finally, m/z 363.158 has only one hit: (10S)-juvenile hormone III diol phosphate, an insect hormone[77]. The final two mass traces measured at 347.1267 and 361.1423 did not match any metabolites in the databases searched.

In the end, there was not a strong enough case to test any of the 31 compounds that could represent the six candidate mass traces – essentially, they all seem to have similar probabilities of being a bacterially-produced, contraction-regulating molecule. Applying each of the compounds here to germ-free *Hydra* is theoretically possible, of course, but it does not fit within the timeframe of a PhD project. It is possible that the answer lies within these six mass traces: bacteria do indeed produce compounds often recognized as plant metabolites, for example, and the molecules listed do generally belong to bioactive compound classes. The fact that these six compounds were not measured in the five-microbe extract does not necessarily mean they were not there since they were measured on a different mass spectrometer. It's possible that the true identity of the compounds was not found because it simply was never input into the databases searched, or even more intriguingly, has never been identified before.

Another possibility that would explain the lack of a suitable candidate using this approach is that the contraction-regulating compound(s) lie outside of the scanning range of the mass spectrometer or were not ionized and therefore were not detected. For example, neuropeptides are important relayers of information in the *Hydra* nervous system, and some even interact directly with the microbiome[121–123].These compounds are too large to have been detected with the mass spectrometer settings used. Smaller compounds, for example the amino acid neurotransmitters GABA, glycine and glutamate are too small for detection.

We must also consider the possibility that the assumptions made to make these comparisons were faulty. Perhaps the compound(s) were not produced at all in the in vitro assays, which were cultured in liquid R2A instead of R2A-agar. To get high enough levels of the compound(s), perhaps less abundant members of *Hydra* microbiota needed to be present. For these reasons, I also investigated the mass traces present in the extract and in *Hydra*, which adds a further 13 annotations, but as before, none of the compounds stood out as plausible contraction-mediating compounds. Lastly, I looked at the compounds present in the in vitro cultured microbes and the extracts, because if the compound(s) were not present in high enough levels in whole polyps, they would not have made it through the pipeline. There were 144 mass traces common between the two mass spectrometry experiments, with 1818

annotations. Obviously, the data need to be reduced significantly for a thorough investigation of these compounds.

Advances towards a fractionation-based approach for contraction-mediating molecule identification

Without a strong candidate for a contraction-mediating molecule, I adjusted my approach. A standard approach for bioactive molecule identification is to chemically fractionate bioactive extracts and test the fractions for biological activity. For example, one could use C18 solid-phase extraction with increasing concentrations of methanol. Some molecules will elute at low methanol concentrations and others at higher concentrations, and the fractions with elevated levels of a bioactive compound will have the most biological activity (assuming a dose-dependent effect). Importantly, this approach can help in the identification of so-called "unknown unknowns", which are metabolites that have never before been described[124].

To work towards this approach, I began by replicating the methods of the original study[41,42]. My results are congruent with that study; however, the magnitude of the effect was smaller (Figure 12A). Germ-free animals contracted at 87 ± 4.5% the relative frequency of control animals ($p = 0.11$), while in the previous study the germ-free animals contracted at roughly 60% the frequency of control animals[41]. The difference in the effect size could have arisen due to differences in our handling of the polyps, which become quite small and fragile in the absence of food. Another possibility is that the microbiota changed over time and that the microbiota of the polyps I worked with was less effective at increasing the contraction rate. When I extracted the metabolites of the resident microbiota using Dr. Murillo-Rincon's technique, the extract unexpectedly decreased contraction frequency (Figure 14), lending credence to the latter hypothesis. Further, the 16S sequences of the negative-acting extract did not contain *Duganella*, a strain easily cultured on R2A agar. Although it could have been outcompeted on the plate, when taken together, the evidence suggests a change to the microbiota that influenced the contraction rate.

The nutritional status of *Hydra* polyps influences its contraction frequency – contractions increase with increasing feeding frequency[95]. Hoping to see a greater effect size or less variability within treatments in well-fed animals, I also assessed the contraction frequency in

our long-term germ-free culture. This could have reduced the number of replicates required to see an effect, increasing my capacity to perform the assay. Unfortunately, the effects were quite similar to those of the starved polyps, with the contractions of germ-free animals occurring at 83.5 ± 5.6% the relative frequency of the controls ($p = 0.02$; Figure 12B).

I performed the rest of the behavioural assays on starved polyps, first addressing the issue of a missing negative control on contraction frequency. This extract had no effect on contraction of germ-free polyps (Figure 13). I concluded from this that the vehicle control does not have appreciable levels of contraction-mediating compounds. Next, I created an extract using only the main colonizers of *Hydra*, which were able to increase contraction frequency when they were used to recolonize germ-free *Hydra*[41] (Figure 2B). This extract increased contraction frequency of germ-free polyps to 128 ± 7.3% ($p = 0.035$; Figure 15). In Dr. Andrea Murillo-Rincon's experiments, her microbial extracts were created by homogenizing *Hydra* polyps and culturing the microbes in the homogenates. These extracts increased contractions to 148% relative to the germ-free polyps (averaged between the two extracts tested). The difference in the activities in the extracts could very well have arisen due to the presence of less abundant, but biologically important, members of the *Hydra* microbiota. Interindividual variation in contraction frequency is also quite high[61], and the assay does have some subjective aspects (it is not always clear whether or not a potential contraction should be counted). These may have played some role in the observed differences in effect size. In any event, the result was a bioactive extract whose microbial composition was known and easily reproduced.

This extraction method could be employed in future studies in a fractionation-based approach. However, I would recommend taking advantage of recent advances in the field to move towards a higher throughput bioassay. Researchers have developed a whole-body calcium imaging system that allows for simultaneous investigation of several polyps and it was successfully employed to measure contraction frequency under different biotic and abiotic conditions (osmolarity, temperature, nutrition, and body size)[125]. In this experiment, five animals were place together in a single well. It may be possible to do the same without resorting to changing the setup used in the present work (in this work, each well contained a single polyp). In another study, a machine learning algorithm was used to characterize and

quantify *Hydra* behaviour[126]. Automating behavioural quantification could improve throughput and allow for simultaneous investigation of the other five behaviours this algorithm recognizes (elongation, tentacle swaying, body swaying, elongation and silent).

Applying the metabolomics pipeline for identification of other bioactive molecules influencing host-microbe dynamics

As mentioned in the introduction, microbes do not only influence host behaviour, but many aspects of host physiology. From the perspective of the host then, it seems prudent to have some control over its microbial colonizers. Indeed, there is evidence that hosts can influence their microbial community's composition. The host immune system can manipulate the community composition of its microbiota through, for example, the production of antimicrobial peptides[127]. In *Hydra*, the nervous system can play a direct role in host-led microbial community composition alteration through secretion of neuropeptides that have antimicrobial effects[122].

Host-derived compounds that increase the abundance of particular bacterial strains, rather than acting through antimicrobial mechanisms, seem to be less reported in the literature. However, evidence suggests that these types of host-led microbial community changes occur as well. For instance, human breast milk contains oligosaccharides that may influence the microbial community composition of breast-fed infants[128]. Furthermore, recent, as yet unpublished work from Dr. Peter Deines revealed that germ-free *Hydra* polyps elicit microbial chemotaxis to a greater degree than microbe-containing polyps[92]. This could suggest that germ-free *Hydra* produce a chemotaxis-eliciting molecule that may even shape microbial community composition.

I searched the metabolome of germ-free *Hydra* for compounds that may be responsible and found that germ-free *Hydra* produce a dipeptide with known chemotaxis-eliciting activity (Figure 23). This dipeptide, tentatively labelled prolyl-leucine, elicits chemotaxis in *Escherichia coli* through the action of the Tap signal transducer and a dipeptide permease[99]. This annotation is considered tentative because of the possibility that proline is on the C- rather than the N- terminus (i.e. the mass trace could represent leucyl-proline). These compounds have the same molecular weight and therefore cannot be distinguished by m/z alone, but

both of them elicit chemotaxis in bacteria[99]. Similarly, leucine has a structural isomer, isoleucine, further complicating the analysis.

To confirm the identity of the dipeptide, we used MS/MS to obtain its fragmentation pattern. This was performed on a sample from *Undibacterium*, which also produces a compound measured at m/z 227.1401 (Figure 24). *Undibacterium* was used because MS/MS is less sensitive than mass spectrometry alone and it is possible to grow significant quantities of bacterial culture. The fragmentation pattern contained fragments associated with all four potential dipeptide identities, and this could indicate that multiple isomers are present in the sample. Further, I cannot rule out the possibility that a D-enantiomer is present. It may be possible to use a fractionation-based approach to further isolate the compound(s) and perhaps identify the mass trace with higher confidence.

Dipeptides can be formed through a few mechanisms, including nonribosomal peptide synthetases (NRPS)[129]. These enzymes can also accept D-amino acids[130] and could be responsible for the formation of the dipeptide measured at m/z 227.1401. Using the bacterial genomes of *Curvibacter, Acidovorax, Duganella, Undibacterium* and *Pelomonas*, I searched for evidence of secondary metabolite biosynthesis gene clusters. *Undibacterium* contained one NRPS cluster, which could potentially be involved in dipeptide production (Table 1). Moreover, the analysis predicted the presence of NRPS gene clusters in *Curvibacter, Duganella* and *Pelomonas.* Considering the importance of peptide signalling in the nervous system of *Hydra*, these gene clusters deserve more attention. Further, the *Pelomonas* genome encodes 12 distinct secondary metabolite synthesis gene clusters. Bearing in mind the capabilities of this strain to increase contraction frequency of *Hydra*, one might examine these results in further detail.

Mass spectrometry analysis of in vitro cultured *Hydra* microbiota and metabolic modelling reveals in vitro production of the neurotransmitter GABA

With the influence of *Hydra* microbiota on two nervous system dependent behaviours[41,42], and in the absence of obvious changes to nervous system anatomy, I turned to the microbial extracts to look for bacterially-derived molecules that influence nervous system function. Neural excitability can be influenced directly through the action of bacterial metabolites, for

example, the short chain fatty acid butyrate increases excitability of enteric neurons in a dose-dependent manner[131]. Bacterial production of neuroactive compounds, including GABA, dopamine, acetylcholine, and 5-hydroxytrytamine, may also impact nervous system function[132].

In the five-microbe extract, the neurotransmitter GABA was present in higher amounts than in the medium-only control (Supplementary Table 5, Figure 16). A second line of evidence that *Hydra* colonizers produce GABA comes from the modelling work of Georgios Marinos (Figure 17). These results suggested the presence of putrescine-dependent GABA production in all five main colonizers, though a transporter for secretion of GABA was only present in *Duganella*. Much of the GABA in the five-microbe extract therefore likely arose from this strain.

As mentioned in the introduction, GABA increases the duration of the feeding response in *Hydra*[61], and an unknown interaction between *Hydra* and its microbiota also increases the feeding response. Could GABA be one of the microbially-derived compounds influencing feeding duration in *Hydra*? This is possible, but more evidence is needed. Examining the levels of GABA in germ-free, control and recolonized polyps would be a good first step at understanding the role of microbially-produced GABA on *Hydra*. Bearing in mind that of the five main colonizing bacterial species, only *Duganella* has a high likelihood of influencing host levels through GABA secretion, it would be wise to confirm the modelling results by looking for GABA production by *Duganella* in vitro. This would link nicely to a series of monocolonization experiments with the five colonizers. The expectation would be that *Duganella* would be the most effective at prolonging feeding duration. The in vivo assay is important here because *Duganella* may reduce host levels of GABA by using the antiporter to uptake GABA for use in the TCA cycle, rather than producing GABA.

Importantly, microbiota often affect behaviours through several mechanisms, and other mechanisms may play a role when it comes to microbial effects on the feeding response of *Hydra*. Reduced glutathione is used to elicit the feeding response in *Hydra*. This compound was initially isolated from food extracts and is sensitive to oxidation by hydrogen peroxide[133]. It is noteworthy that recent work from our lab uncovered aberrant peroxidase activity in

germ-free polyps[134]. This hydrogen peroxide-reducing enzyme, usually restricted in its expression to the foot region, was expressed in seemingly random hot spots along the body of germ-free polyps. We might expect an increase in peroxidase expression in the presence of increased hydrogen peroxide, as this has been demonstrated for other peroxidase enzymes[135]. Could this imply an increase in hydrogen peroxide concentrations in germ-free polyps? If increased levels of hydrogen peroxide are also present externally, we might expect a faster rate of glutathione oxidation in germ-free polyps, terminating the feeding response earlier than in control polyps. Additionally, other recent work from the Bosch lab revealed that germ-free *Hydra* have higher concentrations of reactive oxygen species (ROS) than control animals (the assay measured the ROS in the surrounding medium) which further supports the hypothesis that oxidation of reduced glutathione may contribute to the shortened feeding response duration in germ-free polyps[136]. This hypothesis could be tested by assessing the levels of oxidized, reduced and total glutathione after incubation with germ-free, conventionalized and control polyps; a colorimetric assay for this is readily available.

GABA links to core metabolic pathways in *Hydra* colonizers

The microbial production of GABA may influence *Hydra*, but why is it that the bacteria produce the compound at all? The lack of a secretory mechanism for GABA in four of the five bacterial strains searched (Figure 17) suggests that GABA is used for some intracellular processes. Indeed, GABA can be degraded to succinate, which feeds directly into the TCA cycle. Of course, the TCA cycle is a central metabolic pathway that provides energy to cells. This implies that GABA production could be an intermediate in a core metabolic pathway where putrescine supplies energy to resident microbiota. Putrescine has been detected in *Hydra* via high-performance liquid chromatography (HPLC)[137], so putrescine could theoretically be host-supplied. Any GABA release may simply be a by-product of the use of putrescine in central bacterial metabolism. In fact, it has been hypothesized that bacteria elicit behavioural changes in their hosts as a result of their core metabolic processes, rather than production for outright host behaviour manipulation[138].

To investigate the role of putrescine in core bacterial metabolism, I cultured *Cuvibacter*, *Undibacterium*, *Duganella*, *Pelomonas* and *Acidovorax* in a medium containing only putrescine as a carbon, nitrogen, and energy source. All the strains achieved higher densities

in s-medium (*Hydra* growth medium containing only salts) supplemented with putrescine than they did in s-medium alone, suggesting that all strains were able to uptake and utilize putrescine to some degree (Figure 18-22). This preliminary experiment needs to be repeated with a higher initial inoculum density because the cultures did not reach stationary phase, but the data nevertheless look promising. Additionally, the results are corroborated by a substrate utilization assay which demonstrated that all five strains are able to use putrescine as a carbon source[139].

Perhaps most strikingly, *Curvibacter* grew to higher densities in 10 mM putrescine than it did in the standard growth medium, R2A (Figure 18). In the other strains, 10 mM putrescine seemed somewhat inhibitory relative to 1 mM putrescine, likely owing to putrescine's toxic effects[140]. *Undibacterium* also had curious growth dynamics, with an oscillating pattern in the presence of putrescine that was not observed in R2A or s-medium (Figure 22). These kind of growth dynamics have been reported before for bacteria grown in the presence of bacteriophages[141]. Indeed, *Undibacterium* does harbour a temperate phage[142] so this is a plausible hypothesis, and could be confirmed by examining putrescine-supplemented *Undibacterium* cultures for phages.

Thus, it appears that GABA production via putrescine is part of core bacterial metabolism, and is not produced to manipulate host behaviour, just as Johnson and Foster predicted[138]. Why *Duganella* secretes GABA is still an open question. In *Pseudomonas fluorescens*, exposure to GABA reduces biofilm formation and alters cell envelope structure (specifically the lipopolysaccharide component lipid A)[143]. In *Agrobacterium tumefaciens*, exposure to GABA reduced the levels of the quorum sensing molecule N-(3-oxooctanoyl)homoserine lactone (OC8-HSL)[144]. *Duganella* appears to produce OC8-HSL as well[145], but it is unclear what effect the quorum sensing molecule has on *Duganella*. Considering that GABA can apparently be used for growth in *Duganella*, I would predict GABA secretion primarily in high nutrient environments. This could mean that the OC8-HSL is produced preferentially in low nutrient environments. If GABA and OC8-HSL are negatively correlated as they are in *A. tumefaciens*, I would predict that OC8-HSL may elicit changes in *Duganella* that are important for survival under nutrient-limited conditions (e.g. reduction of biofilm formation[146]).

Challenges and future directions

This is the first untargeted study of the *Hydra* metabolome, and the first to find that there is a demonstratable effect of microbes on the metabolism of *Hydra*. Similarly, studies in mammals have demonstrated the strong effect microbes have on host metabolomes by comparing the metabolomes of blood and tissue samples from germ-free and microbiota-containing hosts[147,148]. Understanding what metabolites in these perturbed profiles are microbially-derived and what microbiota members are capable of producing the compounds continues to be an area of difficulty in metaorganism metabolomics studies[63]. One strategy is to compare the metabolomic profiles of germ-free and microbe-containing hosts with the metabolomic profiles of the bacterial colonizers.

The data generated in the current study provide the means to do just that: 30 mass traces are common between the microbial dataset and high in control polyps. Although outside of the scope of the current study, some of these mass traces could represent important compounds in host-microbe co-metabolism or dynamics. This could represent a novel way to identify bacterially-derived metabolites in vivo. A similar approach has been employed using the HuMiX system (human-microbial cross-talk), where human cell lines are grown in co-culture with bacteria found in the human gut microbiome and the metabolomics profiles can be compared to those of monocultured cells[149]. Using only a cell line is unlikely to recapitulate the complexities of the whole system, however. In another study, researchers were able to identify compounds produced by *Clostridium sporogenes* in monocolonized mice after screening in vitro cultures for bioactive compounds[63].

In contrast, here I suggest a way to probe the entire metabolome of a metaorganism with concurrent investigation of the metabolomes of the majority of its bacterial colonizers, allowing for tracing of microbially-derived metabolites. This unique situation arises as a result of the utility of the model *Hydra* in metaorganism research: specifically, *Hydra*'s clonal nature, soft body and small, species-specific microbiome.

One of the major challenges in this study was compound annotation: identifying the compound that is represented by a particular mass trace. This is a major bottleneck in any metabolomics study[150]. In the current work, I use databases to search for putative mass trace

identities and often found a single mass trace could represent one of any number of compounds. Options for annotation based off of metabolic models is possible (e.g. using Mummichog[151]) but mostly restricted to humans or well-established model systems. This approach naturally restricts the compound annotations to compounds predicted to be present based on genomic information. This means that some of the mass traces will remain unannotated, and the compounds representing these mass traces may play an important role in the system. For example, enzymes often catalyze reactions with multiple substrates: some of the reactions may not be identified. There is also the problem of genes of unknown function (from both host and microbiota) which contribute to metabolism in unaccounted for ways. Specific to metaorganism metabolomics, the hologenome is not considered in the creation of the models and therefore microbially-derived metabolites could easily remain unannotated.

One option for improved compound annotation is to use gas chromatography-mass spectrometry (GC-MS). The retention time of metabolites in the column is highly reproducible and by combining the retention time with an accurate mass, more reliable compound annotation can be accomplished. Tandem mass spectrometry (e.g. MS/MS) can also be used for compound identification thanks to the reproducible nature of the chemical fragmentations induced by MS/MS. In any event, an annotated compound list can be used for chemical similarity enrichment analysis (ChemRICH)[152]. This tool uses chemical similarities rather than metabolic models to understand the data structure in a way that is genome-independent, which is an important consideration in metaorganism metabolomics.

By comparing the metabolomes of microbe-containing *Hydra*, its microbial colonizers and contraction frequency-increasing extracts, I was able to identify six candidate masses that may influence contraction frequency. Here the problem with mass spectrometry annotation was obvious: none of the annotations for the six mass traces seemed likely to be of microbial origin, with most of the annotations being specific to plants. Had the six traces corresponded to six compounds, the molecules could have been tested directly for contraction-regulating activity. To get a high-confidence identity on these mass traces, MS/MS could be performed, but more samples would be needed. To move forward with the identification of bacterially-derived, contraction-mediating molecules, I would recommend focusing on using the five-

microbe extraction method to fractionate the extracts and test each fraction for bioactivity. Using this approach, one should be able to scale up the production of the samples which could allow for compound identification using, for example, GC-MS or MS/MS. To accomplish this, an increase in the throughput of the behavioural assay is recommended.

Another challenge of the present study was the apparent changes to the resident microbiota of *Hydra* between this study and the previous study that demonstrated the effect of microbiota on the contraction frequency of *Hydra*. There seems to have been a reduction in the size of the contraction-mediating effects of microbiota between the two studies. In addition, the microbial extract I created using the established method had unexpected contraction-reducing activity (Figure 14). By using only the main colonizers, which had already been demonstrated to partially restore contraction frequency[122], I was able to create an extract that increased contraction frequency. Synthetic microbial communities are an important tool for metaorganism research because it allows reproduction of results over time or between labs. This is demonstrated nicely here, as I relied on the results of the contraction assay using animals colonized with the five-member minimal consortia to inform my own experimental design. As more labs catch on to the utility of *Hydra* as a model metaorganism, synthetic communities like the five-member minimal consortia will become very useful, allowing easy discourse between labs.

Hydra biology has been studied for over a hundred years[52] and our knowledge of the biology of the individual colonizing strains is nowhere near as advanced. Here, this was demonstrated most clearly in the growth curves for *Curvibacter* and *Undibacterium* in putrescine-containing media. *Curvibacter* is the most abundant colonizer of *Hydra*, yet performs the worst of the main colonizers when grown on the standard medium (R2A)[153]. Could putrescine uptake and utilization give *Curvibacter* a competitive edge in vivo? One could approach this question by setting up a series of competition experiments between *Curvibacter* and the other colonizers. The growth curve of *Undibacterium* hints at the intriguing possibility that a host metabolite can cause prophage induction. This possibility should be examined further as bacteriophages can be an important regulator of microbiome composition[154].

Just how important is putrescine for host-bacteria interactions? Putrescine and other polyamines have a wide variety of effects on micro- and macro-organisms. They are called polyamines because they contain multiple positively charged amino groups ($-NH_3^+$) and these positively charged groups allow them to interact with negatively-charged molecules like DNA, RNA and proteins[155]. Polyamines can act as antioxidants, increase cell proliferation, influence bacterial swarming behaviours, affect DNA and protein synthesis, and influence apoptosis[156,157]. The concentration of polyamines decreases with age, and supplementation can improve lifespan, but too much of a good thing may be detrimental: polyamine concentrations also increase in tumors[155]. *Hydra* polyps contain putrescine[137], but its physiological effects are unclear. The existence of putrescine-degradation pathways in all five main colonizers of *Hydra* suggests that these bacterial strains may impact putrescine levels in vitro. Understanding the impact of putrescine on *Hydra* physiology and the effects that its microbiota have on putrescine levels could prove an interesting avenue for future studies.

Summary

Hydra's resident microbiota are able to interact with its nervous system, manipulating its contraction frequency and feeding response[41,42]. In this report, I investigate the possible role of microbially-dependent alterations to nervous system structure and function. Nervous system structure in adult polyps, in terms of neurogenesis and nerve-cell density was not impacted by microbes in *Hydra*, suggesting the alteration of nervous system function is the more likely mechanism through which this occurs. To understand what bacterial metabolites might play a role in altering nervous system function, I developed a metabolomics pipeline to identify metabolites of bacterial origin in vivo. This pipeline can be used to determine what colonizers produce a particular compound, provided that compound is produced in vitro. Although I was not able to identify the molecule responsible for bacterially-dependent contraction modulation in *Hydra*, this pipeline has utility beyond the function it was initially developed for. For example, as recent results from the lab suggested the production of a chemotaxis-eliciting compound in germ-free *Hydra*[92], I used the pipeline to search the metabolome of germ-free *Hydra*, and identified a candidate chemotaxis-eliciting dipeptide.

Finally, to look for evidence of functional manipulation of the *Hydra* nervous system by its bacterial colonizers, I checked for the in vitro production of neurotransmitters by *Hydra*

microbiota and found that the colonizing bacteria produced GABA in co-culture. Metabolic modelling results suggest that all five main colonizers can metabolize GABA, but only *Duganella* possessed the transporter required for GABA secretion. As the feeding response can be prolonged through exogenous application of GABA[61], bacterial production of GABA may be one way that bacteria increase feeding response duration.

Erklärung

Hiermit erkläre ich, dass ich die vorliegende Dissertation, nach Regeln guter wissenschaftlicher Praxis, eigenständig verfasst und keine anderen als die angegebenen Hilfsmittel und Quellen benutzt habe. Dabei habe ich keine Hilfe, außer der wissenschaftlichen Beratung durch meinen Doktorvater Prof. Dr. Dr. h.c. Thomas C. G. Bosch in Anspruch genommen. Des Weiteren erkläre ich, dass ich noch keinen Promotionsversuch unternommen habe, diese Arbeit noch nicht im Rahmen eines Prüfungsverfahren vorgelegt wurde und keine Teile dieser Arbeit zur Publikation eingereicht wurden. Darüber hinaus wurde mir wurde noch kein akademischer Grad entzogen.

Kiel, den

_____

Danielle M. M. Harris

Acknowledgements

First off, I'd like to thank my supervisor Prof. Dr. Thomas Bosch for the opportunity to work in his lab, his advice through the years and his patience as I got this project off the ground. Thank you to Dr. Andrea Murillo-Rincon for helping me find my footing in the lab and for sharing your results and technical expertise with me. Thanks to Dr. Alexander Klimovich for the many impromptu in-depth discussions and critical analysis of my work. I'm grateful to Drs. Peter Deines and Tim Lachnit who also provided much appreciated advice and good discussions. Dr. Janina Lange, Jinru He, Dr. Kai Rathje and Jay Bathia were always willing to lend an ear – this was indispensable for my thinking on the project and made my experience in the lab more enjoyable (the significance of the latter cannot be overstated). Christoph Giez and Gabriele Crupi, thank you for sharing and discussing your results with me, helping to provide a greater context to my work. Doris Willoweit-Ohl, Eva-Maria Herbst, Maria Franck and Jörg Wittlie, thank you for providing excellent technical assistance and being a pleasure to work with. Anika Hintz and Dr. Cleo Pietschke thank you for all the work you do to keep things running behind the scenes.

To my thesis committee members, Prof. Dr. John Baines and Prof. Dr. Thomas Röder, thank you for your guidance on my project and for the critical evaluation of my work.

I had excellent help with mass spectrometry from both the labs of Prof. Dr. Philippe Schmitt-Kopplin and Prof. Dr. Karin Schwarz. I really enjoyed the time I spent in both labs and my work here would have been impossible without your support and guidance. Dr. Basem Kanawati, Jenny Uhl and Dr. Tobias Demetrowitsch thank you for taking hours out of your day to help me understand the nitty gritty of mass spectrometry data analysis and somehow even making the process enjoyable.

Prof. Dr. Christoph Kaleta and Georgios Marinos, thank you for taking the time to contribute to the work presented here. It has been made stronger thanks to your contributions.

Mr. Science and Mrs. Show, Ulf Evert and Katharine Simmons, you both taught me so much about the importance of story in science. This manuscript would have been a much harder read if our paths had never crossed. Thank you.

Nancy Obeng and Shauni Doms, thank you for your feedback on parts of this manuscript, but more importantly, thank you for being my friend. Daniel Dieckwisch, you helped me find my motivation in hard times and I will always be grateful.

To my parents and sisters for their love and support through the years – I wouldn't have made it this far without you. Thank you is not enough. I love you!

References

1. Donohoe, D. *et al.* The microbiome and butyrate regulate energy metabolism and autophagy in the mammalian colon. *Cell Metab.* **13**, 517–526 (2011).
2. Silva, M. S. B. & Giacobini, P. Don't Trust Your Gut: When Gut Microbiota Disrupt Fertility. *Cell Metabolism* **30**, 616–618 (2019).
3. Fraune, S. *et al.* Bacteria-bacteria interactions within the microbiota of the ancestral metazoan Hydra contribute to fungal resistance. *ISME J.* **9**, 1543–1556 (2015).
4. Ogbonnaya, E. S. *et al.* Adult Hippocampal Neurogenesis Is Regulated by the Microbiome. *Biol. Psychiatry* **78**, e7–e9 (2015).
5. Rees, T., Bosch, T. & Douglas, A. E. How the microbiome challenges our concept of self. *PLOS Biol.* **16**, e2005358 (2018).
6. Bosch, T. C. G. & McFall-Ngai, M. J. Metaorganisms as the new frontier. *Zoology* **114**, 185–190 (2011).
7. Sudo, N. *et al.* Postnatal microbial colonization programs the hypothalamic–pituitary–adrenal system for stress response in mice. *J. Physiol.* **558**, 263–275 (2004).
8. Ait-Belgnaoui, A. *et al.* Probiotic gut effect prevents the chronic psychological stress-induced brain activity abnormality in mice. *Neurogastroenterol. Motil.* **26**, 510–520 (2014).
9. Möhle, L. *et al.* Ly6Chi monocytes provide a link between antibiotic-induced changes in gut microbiota and adult hippocampal neurogenesis. *Cell Rep.* **15**, 1945–1956 (2016).
10. Breit, S., Kupferberg, A., Rogler, G. & Hasler, G. Vagus nerve as modulator of the brain-gut axis in psychiatric and inflammatory disorders. *Frontiers in Psychiatry* **9**, 44 (2018).
11. O'Leary, O. F. *et al.* The vagus nerve modulates BDNF expression and neurogenesis in the hippocampus. *Eur. Neuropsychopharmacol.* **28**, 307–316 (2018).
12. Ronchi, G., Ryu, V., Fornaro, M. & Czaja, K. Hippocampal plasticity after a vagus nerve injury in the rat. *Neural Regen. Res.* **7**, 1055–1063 (2012).
13. Schumann, C. M. & Amaral, D. G. Stereological analysis of amygdala neuron number in autism. *J. Neurosci.* **26**, 7674–7679 (2006).
14. Rajkowska, G., Miguel-Hidalgo, J. J., Dubey, P., Stockmeier, C. A. & Krishnan, K. R. R. Prominent reduction in pyramidal neurons density in the orbitofrontal cortex of elderly depressed patients. *Biol. Psychiatry* **258**, 297–306 (2005).
15. Perez-Burgos, A. *et al.* Psychoactive bacteria Lactobacillus rhamnosus (JB-1) elicits rapid

frequency facilitation in vagal afferents. *J Physiol Gastrointest Liver Physiol* **304**, 211–220 (2013).

16. Barrett, E., Ross, R. P., O'Toole, P. W., Fitzgerald, G. F. & Stanton, C. γ-Aminobutyric acid production by culturable bacteria from the human intestine. *J. Appl. Microbiol.* **113**, 411–417 (2012).
17. Shishov, V. A., Kirovskaya, T. A., Kudrin, V. S. & Oleskin, A. V. Amine neuromediators, their precursors, and oxidation products in the culture of Escherichia coli k-12. *Appl. Biochem. Microbiol.* **45**, 494–497 (2009).
18. Reigstad, C. S. *et al.* Gut microbes promote colonic serotonin production through an effect of short-chain fatty acids on enterochromaffin cells. *FASEB J.* **29**, 1395–1403 (2015).
19. Mcvey Neufeld, K. A., Mao, Y. K., Bienenstock, J., Foster, J. A. & Kunze, W. A. The microbiome is essential for normal gut intrinsic primary afferent neuron excitability in the mouse. *Neurogastroenterol. Motil.* **25**, 1830-e88 (2013).
20. Yano, J. M. *et al.* Indigenous bacteria from the gut microbiota regulate host serotonin biosynthesis. *Cell* **161**, 264–276 (2015).
21. Jadhav, K. S. *et al.* Gut microbiome correlates with altered striatal dopamine receptor expression in a model of compulsive alcohol seeking. *Neuropharmacology* **141**, 249–259 (2018).
22. Bravo, J. A. *et al.* Ingestion of Lactobacillus strain regulates emotional behaviour and central GABA receptor expression in a mouse via the vagus nerve. *Proc. Natl. Acad. Sci. U. S. A.* **108**, 16050–16055 (2011).
23. Vogt, N. M. *et al.* Gut microbiome alterations in Alzheimer's disease. *Sci. Rep.* **7**, 13537 (2017).
24. Sampson, T. R. *et al.* Gut microbiota regulate motor deficits and neuroinflammation in a model of Parkinson's disease. *Cell* **167**, 1469-1480.e12 (2016).
25. Lach, G., Schellekens, H., Dinan, T. G. & Cryan, J. F. Anxiety, depression, and the microbiome: a role for gut peptides. *Neurotherapeutics* **15**, 36–59 (2018).
26. Casén, C. *et al.* Deviations in human gut microbiota: A novel diagnostic test for determining dysbiosis in patients with IBS or IBD. *Aliment. Pharmacol. Ther.* **42**, 71–83 (2015).
27. Manichanh, C., Borruel, N., Casellas, F. & Guarner, F. The gut microbiota in IBD. *Nat.*

Rev. Gastroenterol. Hepatol. **9**, 599–608 (2012).

28. Sokol, H. *et al.* Fungal microbiota dysbiosis in IBD. *Gut* (2017). doi:10.1136/gutjnl-2015-310746
29. Lewis, G. *et al.* Dietary fiber-induced microbial short chain fatty acids suppress ILC2-dependent airway inflammation. *Front. Immunol.* **10**, 2051 (2019).
30. Hurst, N. R., Kendig, D. M., Murthy, K. S. & Grider, J. R. The short chain fatty acids, butyrate and propionate, have differential effects on the motility of the guinea pig colon. *Neurogastroenterol. Motil.* (2014). doi:10.1111/nmo.12425
31. Bhattarai, Y. *et al.* Gut microbiota-produced tryptamine activates an epithelial g-protein-coupled receptor to increase colonic secretion. *Cell Host Microbe* **23**, 775–785 (2018).
32. Sagan, L. On the origin of mitosing cells. *J. Theor. Biol.* **14**, 225–274 (1967).
33. Gray, M. W. Lynn Margulis and the endosymbiont hypothesis: 50 years later. *Mol. Biol. Cell* **28**, 1285–1287 (2017).
34. Zilber-Rosenberg, I. & Rosenberg, E. Role of microorganisms in the evolution of animals and plants: the hologenome theory of evolution. *FEMS Microbiol. Rev.* **32**, 723–735 (2008).
35. Douglas, A. E. & Werren, J. H. Holes in the hologenome: Why host-microbe symbioses are not holobionts. *MBio* **7**, e02099-15 (2016).
36. Doms, S., Hermes, B. M. & Baines, J. F. Evolutionary perspectives on the human gut microbiome. in *The Gut Microbiome in Health and Disease* 65–78 (Springer International Publishing, 2018). doi:10.1007/978-3-319-90545-7_5
37. Bordenstein, S. R. & Theis, K. R. Host biology in light of the microbiome: ten principles of holobionts and hologenomes. *PLOS Biol.* **13**, e1002226 (2015).
38. Leys, S. P. Elements of a 'nervous system' in sponges. *Journal of Experimental Biology* (2015). doi:10.1242/jeb.110817
39. Francis, W. R. *et al.* The genome of the contractile demosponge Tethya wilhelma and the evolution of metazoan neural signalling pathways. *bioRxiv* (2017). doi:10.1101/120998
40. Bosch, T. C. G. *et al.* Back to the basics: cnidarians start to fire. *Trends Neurosci.* **40**, 92–105 (2017).
41. Murillo-Rincon, A. P. *et al.* Spontaneous body contractions are modulated by the

microbiome of Hydra. *Sci. Rep.* **7**, 15937 (2017).

42. Murillo-Rincon, A. Modulation of neuronal activity by symbiotic bacteria in the early-branching metazoan Hydra. (Kiel University, 2017).
43. Klimovich, A. V. & Bosch, T. C. G. Rethinking the role of the nervous system: lessons from the hydra holobiont. *BioEssays* **40**, 1800060 (2018).
44. Moroz, L. L. Convergent evolution of neural systems in ctenophores. *Journal of Experimental Biology* (2015). doi:10.1242/jeb.110692
45. Telford, M. J., Moroz, L. L. & Halanych, K. M. Evolution: A sisterly dispute. *Nature* **529**, 286–287 (2016).
46. Boehm, A. M. & Bosch, T. C. G. Migration of multipotent interstitial stem cells in Hydra. *Zoology* **115**, 275–82 (2012).
47. Fraune, S. & Bosch, T. C. G. Long-term maintenance of species-specific bacterial microbiota in the basal metazoan Hydra. *Proc. Natl. Acad. Sci. U. S. A.* **104**, 13146–13151 (2007).
48. Franzenburg, S. *et al.* Distinct antimicrobial peptide expression determines host species-specific bacterial associations. *Proc. Natl. Acad. Sci. U. S. A.* **110**, E3730–E3738 (2013).
49. Rosshart, S. P. *et al.* Wild mouse gut microbiota promotes host fitness and improves disease resistance. *Cell* **171**, 1015-1028.e13 (2017).
50. Rathje, K. *et al.* Dynamic interactions within the host-associated microbiota cause tumor formation in the basal metazoan Hydra. *PLOS Pathog.* **16**, e1008375 (2020).
51. Karl, Y., Schneider, C., Hierzu, T. & Xvii, X. Histologie von Hydra fusca mit besonderer Beriick-sichtigung des Nervensystems der Hydropolypen. *Arch. für mikroskopische Anat.* **35**, 321–379 (1890).
52. Hadzi, J. *Über das Nervensystem von Hydra*. (1909).
53. Dupre, C. & Yuste, R. Non-overlapping neural networks in Hydra vulgaris. *Curr. Biol.* **27**, 1085–1097 (2017).
54. Heimfeld, S. & Bode, H. R. Growth regulation of the interstitial cell population in hydra. I. Evidence for global control by nerve cells in the head. *Dev. Biol.* **110**, 297–307 (1985).
55. Klimovich, A. *et al.* Prototypical pacemaker neurons are immunocompetent cells. *bioRxiv* 750026 (2019). doi:10.1101/750026
56. Siebert, S. *et al.* Stem cell differentiation trajectories in Hydra resolved at single-cell

resolution. *Science (80-.).* **365**, eaav9314 (2019).

57. Passano, L. M. & McCullough, C. B. The light response and the rhythmic potentials of Hydra. *Proc. Natl. Acad. Sci.* **48**, 1376–1382 (1962).
58. Ruggieri, R. D., Pierobon, P. & Kass-Simon, G. Pacemaker activity in hydra is modulated by glycine receptor ligands. *Comp. Biochem. Physiol. - A Mol. Integr. Physiol.* **138**, 193–202 (2004).
59. Heimberger, S. I. & Scott, A. I. Biosynthesis of strychnine. *J. Chem. Soc. Chem. Commun.* 217–218 (1973). doi:10.1039/C39730000217
60. Pierobon, P. *et al.* Putative glycine receptors in Hydra : a biochemical and behavioural study. *Eur. J. Neurosci.* **14**, 1659–1666 (2001).
61. Kass-Simon, G., Pannaccione, A. & Pierobon, P. GABA and glutamate receptors are involved in modulating pacemaker activity in hydra. *Comp. Biochem. Physiol. - A Mol. Integr. Physiol.* **136**, 329–342 (2003).
62. Wikoff, W. R. *et al.* Metabolomics analysis reveals large effects of gut microflora on mammalian blood metabolites. *Proc. Natl. Acad. Sci.* **106**, 3698–3703 (2009).
63. Guo, C.-J. *et al.* Depletion of microbiome-derived molecules in the host using Clostridium genetics. *Science (80-.).* **366**, eaav1282 (2019).
64. Franzenburg, S. *et al.* MyD88-deficient Hydra reveal an ancient function of TLR signaling in sensing bacterial colonizers. *Proc. Natl. Acad. Sci. U. S. A.* **109**, 19374–19379 (2012).
65. Rahat, M. & Dimentman, C. Cultivation of bacteria-free Hydra viridis: Missing budding factor in nonsymbiotic Hydra. *Science (80-.).* **216**, 67–68 (1982).
66. Kee, N., Sivalingam, S., Boonstra, R. & Wojtowicz, J. . The utility of Ki-67 and BrdU as proliferative markers of adult neurogenesis. *J. Neurosci. Methods* **115**, 97–105 (2002).
67. David, C. N. A quantitative method for maceration of hydra tissue. *Wilhelm Roux Arch. für Entwicklungsmechanik der Org.* **171**, 259–268 (1973).
68. Holstein, T. W., Hobmayer, E. & David, C. N. Pattern of epithelial cell cycling in hydra. *Dev. Biol.* **148**, 602–611 (1991).
69. Caporaso, J. G. *et al.* QIIME allows analysis of high-throughput community sequencing data. *Nat. Methods* **7**, 335–336 (2010).
70. Hall, T. A. BIOEDIT: a user-friendly biological sequence alignment editor and analysis program for Windows 95/98/ NT. *Nucleic Acids Symp. Ser.* (1999).

71. Hemmrich, G. & Bosch, T. C. G. Compagen, a comparative genomics platform for early branching metazoan animals, reveals early origins of genes regulating stem-cell differentiation. *BioEssays* **30**, 1010–1018 (2008).
72. Karaman, I. Preprocessing and pretreatment of metabolomics data for statistical analysis. in *Advances in Experimental Medicine and Biology* (ed. Sussulini, A.) **965**, 145–161 (Springer New York LLC, 2017).
73. Wei, R. *et al.* Missing Value Imputation Approach for Mass Spectrometry-based Metabolomics Data. *Sci. Rep.* **8**, (2018).
74. Chong, J. *et al.* MetaboAnalyst 4.0: towards more transparent and integrative metabolomics analysis. *Web Serv. issue Publ. online* **46**, (2018).
75. Yang, J., Zhao, X., Lu, X., Lin, X. & Xu, G. A data preprocessing strategy for metabolomics to reduce the mask effect in data analysis. **2**, 1–9 (2015).
76. Gil-De-La-Fuente, A. *et al.* CEU Mass Mediator 3.0: A Metabolite Annotation Tool. *J. Proteome Res.* **18**, 797–802 (2019).
77. Kanehisa, M. KEGG: Kyoto Encyclopedia of Genes and Genomes. *Nucleic Acids Res.* **28**, 27–30 (2000).
78. Fahy, E., Sud, M., Cotter, D. & Subramaniam, S. LIPID MAPS online tools for lipid research. *Nucleic Acids Research* **35**, W606-12 (2007).
79. Wishart, D. S. *et al.* HMDB: the Human Metabolome Database. *Nucleic Acids Res.* **35**, D521-6 (2007).
80. Smith, C. A. *et al.* METLIN: A metabolite mass spectral database. *Ther. Drug Monit.* **27**, 747–751 (2005).
81. Team R Core. R: A Language and Environment for Statistical Computing. *Vienna, Austria* (2018).
82. Wickham, H. *ggplot2*. *ggplot2* (Springer New York, 2009). doi:10.1007/978-0-387-98141-3
83. Phillips, N. yarrr: A Companion to the e-Book 'YaRrr!: The Pirate's Guide to R'. R package version 0.1.5. (2017).
84. Fox, J. & Weisberg, S. An R Companion to Applied Regression, Third Edition. (2019).
85. Venables, W. N. & Ripley, B. D. *Modern Applied Statistics with S. World* (2002). doi:10.2307/2685660
86. Gelius-Dietrich, G., Desouki, A. A., Fritzemeier, C. J. & Lercher, M. J. sybil – Efficient

constraint-based modelling in R. *BMC Syst. Biol.* **7**, 125 (2013).

87. Brian Connelly | Analyzing Microbial Growth with R. Available at: https://bconnelly.net/posts/analyzing_microbial_growth_with_r/. (Accessed: 5th March 2020)
88. Wickham, H. Reshaping Data with the reshape Package. *J. Stat. Softw.* **21**, (2007).
89. Wickham, H. & Francois, R. dplyr: A Grammar of Data Manipulation. *R package version 0.4.2.* (2015).
90. Wickham, H. gtable: Arrange 'Grobs' in Tables. R package version 0.2.0. (2016).
91. Sprouffske, K. & Wagner, A. Growthcurver: An R package for obtaining interpretable metrics from microbial growth curves. *BMC Bioinformatics* **17**, (2016).
92. Deines, P. Personal communication. (2020).
93. Blin, K. *et al.* antiSMASH 5.0: updates to the secondary metabolite genome mining pipeline. *Nucleic Acids Res.* **47**, 81–87 (2019).
94. Wishart, D. S. *et al.* HMDB 4.0: The human metabolome database for 2018. *Nucleic Acids Res.* **46**, D608–D617 (2018).
95. Passano, L. M. & McCullough, C. B. Co-ordinating systems and behaviour in Hydra: I. Pacemaker system of the periodic contractions. *J. Exp. Biol.* **41**, 643–664 (1964).
96. Li, X.-Y. *et al.* Which games are growing bacterial populations playing? *J. R. Soc. Interface* **12**, 20150121 (2015).
97. Wall, R. *et al.* Bacterial Neuroactive Compounds Produced by Psychobiotics. in *Microbial Endocrinology: The Microbiota-Gut-Brain Axis in Health and Disease* (eds. Lyte, M. & Cryan, J. F.) 221–239 (Springer New York, 2014). doi:10.1007/978-1-4939-0897-4_10
98. Wu, Q., Tun, H. M., Law, Y.-S., Khafipour, E. & Shah, N. P. Common distribution of gad operon in Lactobacillus brevis and its GadA contributes to efficient GABA synthesis toward cytosolic Near-neutral pH. *Front. Microbiol.* **8**, 206 (2017).
99. Manson, M. D., Blank, V., Brade, G. & Higgins, C. F. Peptide chemotaxis in E. coli involves the Tap signal transducer and the dipeptide permease. *Nature* (1986). doi:10.1038/321253a0
100. Köhidai, L., Soós, P. & Csaba, G. Effects of dipeptides containing the amino acid, proline on the chemotaxis of Tetrahymena pyriformis. Evolutionary conclusions on the formation of hormone receptors and hormones. *Cell Biol. Int.* **21**, 341–345 (1997).

101. Luczynski, P. *et al.* Adult microbiota-deficient mice have distinct dendritic morphological changes: differential effects in the amygdala and hippocampus. *Eur. J. Neurosci.* **44**, 2654–2666 (2016).

102. Khalil, O. S. *et al.* Prenatal inhibition of the kynurenine pathway leads to structural changes in the hippocampus of adult rat offspring. *Eur. J. Neurosci.* **39**, 1558–1571 (2014).

103. Kennedy, P. J., Cryan, J. F., Dinan, T. G. & Clarke, G. Kynurenine pathway metabolism and the microbiota-gut-brain axis. *Neuropharmacology* **112**, 399–412 (2017).

104. Takaku, Y. *et al.* Innexin gap junctions in nerve cells coordinate spontaneous contractile behaviour in Hydra polyps. doi:10.1038/srep03573

105. Escribano, J., Alonso, G. L., Coca-Prados, M. & Fernández, J. A. Crocin, safranal and picrocrocin from saffron (Crocus sativus L.) inhibit the growth of human cancer cells in vitro. *Cancer Lett.* (1996). doi:10.1016/0304-3835(95)04067-6

106. Uesato, S. *et al.* Intermediacy of 8-epiiridodial in the biosynthesis of iridoid glucosides by Gardenia jasminoides cell cultures. *Phytochemistry* **25**, 309–2314 (1986).

107. Uesato, S., Miyauchi, M., Itoh, H. & Inouye, H. Biosynthesis of iridoid glucosides in Galium mollugo, G. spurium var. Echinospermon and Deutzia crenata. Intermediacy of deoxyloganic acid, loganin and iridodial glucoside. *Phytochemistry* **25**, 2515–2521 (1986).

108. Wishart, D. S. *et al.* HMDB 3.0 - The Human Metabolome Database in 2013. *Nucleic Acids Res.* **41**, D801-7 (2013).

109. Sakai, N., Inada, K., Okamoto, M., Shizuri, Y. & Fukuyama, Y. Portuloside A, a monoterpene glucoside, from Portulaca oleracea. *Phytochemistry* **42**, 1625–1628 (1996).

110. Zhang, Z. L. *et al.* Study on the chemical components of Gardenia jasminoides (II). *J. Chinese Med. Mater.* **36**, 401–403 (2013).

111. Oshima, Y., Takata, S. & Hikino, H. Schizonodiol, Schizonol, and Schizonepetosides D and E, Monoterpenoids of Schizonepeta tenuifolia Spikes. *Planta Med.* **55**, 179–180 (1989).

112. Kubo, M., Sasaki, H., Endo, T., Taguchi, H. & Yosioka, I. The Constituents of Schizonepeta tenuifolia BRIQ. II: Structure of a New Monoterpene Glucoside, Schizonepetoside C. *Chem. Pharm. Bull.* **34**, 3097–3101 (1986).

113. Sasaki, H., Taguchi, H., Endo, T., Yosioka, I. & Iitaka, Y. The Constituents of Schizonepeta tenuifolia Briq. I. Structures of Two New Monoterpene Glucosides, Schizonepetosides A and B. *Chem. Pharm. Bull.* **29**, 1636–1643 (1981).
114. Kehr, J. *et al.* Ginkgo biloba leaf extract (EGb 761®) and its specific acylated flavonol constituents increase dopamine and acetylcholine levels in the rat medial prefrontal cortex: Possible implications for the cognitive enhancing properties of EGb 761®. *Int. Psychogeriatrics* (2012). doi:10.1017/S1041610212000567
115. Mannelli, L. D. C. *et al.* Anti-neuropathic effects of Rosmarinus officinalis L. terpenoid fraction: Relevance of nicotinic receptors. *Sci. Rep.* (2016). doi:10.1038/srep34832
116. Dehnhard, M. & Jewgenow, K. Measurement of faecal prostaglandins in felids and three ursid species. *Wien. Tierarztl. Monatsschr.* **100**, (2013).
117. Roberts, B. M. *et al.* Use of urinary 13,14, dihydro-15-keto-prostaglandin F2α (PGFM) concentrations to diagnose pregnancy and predict parturition in the giant panda (Ailuropoda melanolecua). *PLoS One* **99**, 79–86 (2018).
118. Gerhart, D. J. Emesis, learned aversion, and chemical defense in octocorals: a central role for prostaglandins? *Am. J. Physiol. Integr. Comp. Physiol.* **260**, R839–R843 (1991).
119. Schwab, W., Fischer, T. & Wüst, M. Terpene glucoside production: Improved biocatalytic processes using glycosyltransferases. *Eng. Life Sci.* **15**, 376–386 (2015).
120. Fujita, T. & Nakayama, M. Perilloside a, a monoterpene glucoside from Perilla frutescens. *Phytochemistry* **31**, 3265–3267 (1992).
121. Darmer, D. *et al.* Three different prohormones yield a variety of Hydra-RFamide (Arg-Phe-NH2) neuropeptides in Hydra magnipapillata. *Biochem. J.* **332**, 403–412 (1998).
122. Augustin, R. *et al.* A secreted antibacterial neuropeptide shapes the microbiome of Hydra. *Nat. Commun.* **8**, 1–8 (2017).
123. Takahashi, T. *et al.* A novel neuropeptide, Hym-355, positively regulates neuron differentiation in Hydra. *Development* **127**, 997 LP – 1005 (2000).
124. Wishart, D. S. Computational strategies for metabolite identification in metabolomics. *Bioanalysis* **1**, 1579–1596 (2009).
125. Yamamoto, W. & Yuste, R. Whole-body imaging of neural and muscle activity during behaviour in Hydra: bidirectional effects of osmolarity on contraction bursts. *bioRxiv* 2019.12.20.883835 (2019). doi:10.1101/2019.12.20.883835
126. Han, S., Taralova, E., Dupre, C. & Yuste, R. Comprehensive machine learning analysis of

Hydra behaviour reveals a stable basal behavioural repertoire. *Elife* **7**, e32605 (2018).

127. Royet, J., Gupta, D. & Dziarski, R. Peptidoglycan recognition proteins: modulators of the microbiome and inflammation. *Nat. Rev. Immunol.* **11**, 837–851 (2011).
128. Barile, D. & Rastall, R. A. Human milk and related oligosaccharides as prebiotics. *Curr. Opin. Biotechnol.* **24**, 214–219 (2013).
129. Yagasaki, M. & Hashimoto, S. Synthesis and application of dipeptides; current status and perspectives. *Appl. Microbiol. Biotechnol.* **81**, 13–22 (2008).
130. von Dohren, H., Dieckmann, R. & Pavela-Vrancic, M. The nonribosomal code. *Chem. Biol.* **6**, R273-9 (1999).
131. Neunlist, M., Dobreva, G. & Schemann, M. Characteristics of mucosally projecting myenteric neurones in the guinea-pig proximal colon. *J. Physiol.* **517**, 533–546 (1999).
132. Cox, L. M. & Weiner, H. L. Microbiota signaling pathways that influence neurologic disease. *Neurotherapeutics* **15**, 135–145 (2018).
133. Lenhoff, H. M. Behaviour, Hormones, and Hydra. *Science (80-.).* **161**, 434–442 (1968).
134. He, J. Personal communication. (2020).
135. Javier Ruiz-duen, F. *et al. Regulation of Peroxidase Transcript Levels in Liquid Cultures of the Ligninolytic Fungus Pleurotus eryngii*. *Applied and Environmental Microbiolgy* **65**, (1999).
136. Minten-Lange, T. Personal communication. (2020).
137. Hamana, K., Sakamoto, A., Nishina, M. & Niitsu, M. Polyamine distribution profiles within the Phyla Nematoda, Platyhelminthes, Annelida and Cnidaria. *Acad. Knowl. Arch. Gunma Institutes* **27**, 17–25 (2006).
138. Johnson, K. V. A. & Foster, K. R. Why does the microbiome affect behaviour? *Nat. Rev. Microbiol.* **16**, 647–655 (2018).
139. Deines, P., Hammerschmidt, K. & Bosch, T. C. G. Exploring the niche concept in a simple metaorganism. *bioRxiv* 814798 (2020). doi:10.1101/814798
140. Guarino, L. A. & Cohen, S. S. Mechanism of toxicity of putrescine in Anacystis nidulans. *Proc. Natl. Acad. Sci. U. S. A.* **76**, 3660–4 (1979).
141. Pantastico-Caldas, M., Duncan, K. E., Istock, C. A. & Bell, J. A. Population Dynamics of Bacteriophage and Bacillus Subtilis in Soil. *Ecology* **73**, 1888–1902 (1992).
142. Lachnit, T. Personal communication. (2020).
143. Dagorn, A. *et al.* Effect of GABA, a Bacterial Metabolite, on Pseudomonas fluorescens

Surface Properties and Cytotoxicity. *Int. J. Mol. Sci.* **14**, 12186–12204 (2013).

144. Chevrot, R. *et al.* GABA controls the level of quorum-sensing signal in Agrobacterium tumefaciens. *Proc. Natl. Acad. Sci.* **103**, 7460–7464 (2006).
145. Pietschke, C. *et al.* Host modification of a bacterial quorum-sensing signal induces a phenotypic switch in bacterial symbionts. *Proc. Natl. Acad. Sci.* **114**, E8488–E8497 (2017).
146. Allan, V. J. M., Callow, M. E., Macaskie, L. E. & Paterson-Beedle, M. Effect of nutrient limitation on biofilm formation and phosphatase activity of a Citrobacter sp. *Microbiology* **148**, 277–288 (2002).
147. Chuang, H.-L. *et al.* Metabolomics characterization of energy metabolism reveals glycogen accumulation in gut-microbiota-lacking mice. *J. Nutr. Biochem.* **23**, 752–758 (2012).
148. Wikoff, W. R. *et al.* Metabolomics analysis reveals large effects of gut microflora on mammalian blood metabolites. *Proc. Natl. Acad. Sci. U. S. A.* (2009). doi:10.1073/pnas.0812874106
149. Peisl, B. Y. L., Schymanski, E. L. & Wilmes, P. Dark matter in host-microbiome metabolomics: Tackling the unknowns–A review. *Anal. Chim. Acta* **1037**, 13–27 (2018).
150. Domingo-Almenara, X., Montenegro-Burke, J. R., Benton, H. P. & Siuzdak, G. Annotation: a computational solution for streamlining metabolomics analysis. *Anal. Chem.* **90**, 480–489 (2018).
151. Li, S. *et al.* Predicting network activity from high throughput metabolomics. *PLOS Comput. Biol.* **9**, e1003123 (2013).
152. Barupal, D. K. & Fiehn, O. Chemical Similarity Enrichment Analysis (ChemRICH) as alternative to biochemical pathway mapping for metabolomic datasets. *Sci. Rep.* **7**, 14567 (2017).
153. Li, X.-Y. *et al.* Temperate phages as self-replicating weapons in bacterial competition. *J. R. Soc. Interface* **14**, 20170563 (2017).
154. Lange, J., Fraune, S., Bosch, T. C. G. & Lachnit, T. The neglected part of the microbiome: Prophage TJ1 regulates the bacterial community of the metaorganism Hydra. *bioRxiv* 607325 (2019). doi:10.1101/607325
155. Minois, N., Carmona-Gutierrez, D. & Madeo, F. Polyamines in aging and disease. *Aging (Albany. NY).* **3**, 716–732 (2011).

156. Lenis, Y. Y., Elmetwally, M. A., Maldonado-Estrada, J. G. & Bazer, F. W. Physiological importance of polyamines. *Zygote* **25**, 244–255 (2017).

157. Sturgill, G. & Rather, P. N. Evidence that putrescine acts as an extracellular signal required for swarming in Proteus mirabilis. *Mol. Microbiol.* **51**, 437–446 (2004).

Supplementary Information

Supplementary Table 1. The internal calibration list used to calibrate the raw mass spectrometry data.

Formulae	m/z	z
C11H20O4	215.128884	1-
C12H21NO4	242.139783	1-
C13H20O5	255.123799	1-
C11H20N2O7	291.119777	1-
C17H28O3S	311.168641	1-
C19H32O3S	339.199941	1-
C18H32N2O5	355.223847	1-
C19H36N2O5	371.255147	1-
C20H36N2O6	399.250062	1-
C23H36O8	439.233744	1-
C21H37N3O7	442.255876	1-
C18H30O12S	469.138526	1-
C25H45N3O7	498.318476	1-
C27H49N3O7	526.349776	1-
C29H53N3O7	554.381076	1-

Supplementary Table 2. Relative abundances of the OTUs detected in the control *Hydra* used for metabolomics analysis.

OTU ID	% Abdundance					Taxa				
	C1	C2	C3	C4	C5	Phylum	Class	Order	Family	Genus
545507 (Acidovorax)	8.52	22.37	6.85	24.76	6.11	Proteobact.	β-proteobact.	Burkholderiales	Comamonad.	Acidovorax
750018	1.46	18.59	0.11	14.37	2.11	Proteobact.	γ-proteobact.	Pseudomonadales	Pseudomonad.	Pseudomonas
586766	2.03	14.18	11.12	10.87	2.45	Proteobact.	γ-proteobact.	Alteromonadales	Chromatiaceae	Rheinheimera
OTU1073	19.23	7.69	26.84	2.31	0.05	Proteobact.	β-proteobact.	Burkholderiales	Comamonad.	
4391034 (Pelomonas)	0.31	7.52	0.64	1.53	0.44	Proteobact.	β-proteobact.	Burkholderiales	Comamonad.	
OTU914	0.09	5.10	11.39	5.51	0.70	Bacteroidetes	Flavobacteria	Flavobacteriales	Flavobacteriaceae	Flavobacterium
OTU1107	13.81	3.57	5.75	2.86	0.25	Unassigned				
OTU657	2.27	2.80	3.94	2.96	2.18	Unassigned				
538007	7.05	2.38	7.04	4.10	0.06	Proteobact.	γ-proteobact.	Legionellales	Legionellaceae	
750411 (Cuvibacter)	0.82	2.23	0.14	0.05	0.01	Proteobact.	β-proteobact.	Burkholderiales	Comamonad.	
OTU718	1.18	1.92	2.23	1.86	1.07	Unassigned				
564678	0.43	1.78	0.63	3.31	0.01	Proteobact.	γ-proteobact.	Pseudomonadales	Pseudomonad.	Pseudomonas
141316	0.13	0.66	0.27	0.64	0.30	Proteobact.	β-proteobact.	Burkholderiales		
578551	0.59	0.65	0.25	3.28	5.29	Proteobact.	α-proteobact.	Sphingomonadales		
OTU706	0.08	0.57	0.24	0.00	0.03	Proteobact.	α-proteobact.	Rickettsiales		
336824	0.01	0.44	0.04	0.10	0.07	Proteobact.	β-proteobact.	Burkholderiales	Comamonad.	
4426763	1.60	0.42	0.36	11.24	19.03	Proteobact.	β-proteobact.	Burkholderiales	Comamonad.	
4316205	0.02	0.37	0.17	0.33	0.15	Proteobact.	γ-proteobact.	Alteromonadales	Chromatiaceae	Rheinheimera
OTU1176	0.03	0.35	0.31	0.32	0.29	Proteobact.	β-proteobact.	Burkholderiales	Comamonad.	Acidovorax
1136511	0.11	0.34	0.44	0.14	0.01	Proteobact.	β-proteobact.	Burkholderiales	Comamonad.	
OTU1229	0.00	0.33	0.12	0.18	0.02	Proteobact.	γ-proteobact.	Pseudomonadales	Pseudomonad.	Pseudomonas

256215	2.32	0.33	0.00	2.44	0.43	Proteobact.	γ-proteobact.	Pseudomonadales	Pseudomonad.	Pseudomonas
1787644	0.00	0.31	0.00	0.01	0.14	Cyanobacteria	Chloroplast	Streptophyta		
OTU471	0.01	0.29	0.06	0.19	0.03	Proteobact.	γ-proteobact.	Pseudomonadales	Pseudomonad.	Pseudomonas
OTU308	0.02	0.27	0.18	0.08	0.00	Proteobact.	β-proteobact.	Burkholderiales	Comamonad.	
309900	0.00	0.25	0.03	0.14	0.01	Proteobact.	β-proteobact.	Burkholderiales		
541859	0.02	0.24	0.00	0.18	0.04	Proteobact.	γ-proteobact.	Pseudomonadales	Pseudomonad.	Pseudomonas
833853	0.19	0.23	0.12	0.32	0.18	Proteobact.	β-proteobact.	Burkholderiales	Comamonad.	
336069	0.16	0.23	0.01	0.26	0.49	Proteobact.	γ-proteobact.	Legionellales		
679178	0.00	0.21	0.08	0.11	0.80	Proteobact.	δ-proteobact.	Myxococcales		
OTU111	0.00	0.18	0.04	0.03	0.02	Proteobact.	β-proteobact.	Burkholderiales	Comamonad.	
731749	0.02	0.18	0.14	0.06	0.00	Proteobact.	β-proteobact.	Burkholderiales	Comamonad.	
OTU1152	0.00	0.17	0.01	0.03	0.00	Proteobact.	β-proteobact.	Burkholderiales	Comamonad.	
OTU760	0.00	0.16	0.01	0.02	0.02	Proteobact.	β-proteobact.	Burkholderiales	Comamonad.	
OTU23	0.01	0.15	0.10	0.03	0.00	Proteobact.	β-proteobact.	Burkholderiales	Comamonad.	
549837	0.00	0.15	0.00	0.07	0.04	Proteobact.	γ-proteobact.	Pseudomonadales	Pseudomonad.	Pseudomonas
719367	0.00	0.12	0.02	0.01	0.00	Proteobact.	β-proteobact.	Burkholderiales	Comamonad.	
631674	0.05	0.12	1.09	1.76	1.02	Proteobact.	β-proteobact.			
OTU323	0.00	0.11	0.00	0.01	0.00	Proteobact.	β-proteobact.	Burkholderiales	Comamonad.	
320572	0.01	0.11	0.01	0.08	0.11	Proteobact.	β-proteobact.	Burkholderiales		
4408559	0.01	0.11	0.02	0.01	0.00	Proteobact.	β-proteobact.	Burkholderiales	Comamonad.	
254127	0.05	0.10	0.03	0.13	0.19	Proteobact.	α-proteobact.	Rickettsiales	Rickettsiaceae	
OTU980	0.00	0.10	0.06	0.05	0.01	Proteobact.	γ-proteobact.	Alteromonadales	Chromatiaceae	Rheinheimera
OTU754	0.03	0.10	0.09	0.06	0.02	Unassigned				
674057	0.03	0.10	0.03	0.10	0.03	Proteobact.	β-proteobact.	Burkholderiales	Comamonad.	Acidovorax
OTU655	0.01	0.09	0.10	0.03	0.04	Proteobact.	β-proteobact.	Burkholderiales	Comamonad.	Acidovorax
OTU1056	0.07	0.09	0.13	0.12	0.01	Proteobact.	α-proteobact.	Rhodobacterales	Rhodobacteraceae	Rhodobacter
33411	0.03	0.08	0.05	0.00	0.01	Proteobact.	β-proteobact.	Burkholderiales	Comamonad.	

OTU582	0.00	0.08	0.03	0.00	0.00	Proteobact.	α-proteobact.	Rickettsiales		
342084	0.00	0.08	0.01	0.00	0.00	Proteobact.	β-proteobact.	Burkholderiales	Comamonad.	
141042	0.01	0.07	0.04	0.01	0.00	Proteobact.	β-proteobact.	Burkholderiales	Comamonad.	
1106617	0.03	0.07	0.02	0.07	0.01	Proteobact.	β-proteobact.	Burkholderiales		
764682	0.01	0.06	16.82	0.05	0.00	Proteobact.	γ-proteobact.	Pseudomonadales	Pseudomonad.	Pseudomonas
OTU1177	0.00	0.06	0.02	0.06	0.04	Proteobact.	γ-proteobact.	Alteromonadales	Chromatiaceae	Rheinheimera
587805	0.05	0.06	0.10	0.01	0.00	Proteobact.	β-proteobact.	Burkholderiales	Comamonad.	
OTU1101	0.00	0.06	0.02	0.04	0.00	Proteobact.	γ-proteobact.	Pseudomonadales	Pseudomonad.	
60734	0.00	0.05	0.36	0.07	0.04	Bacteroidetes	Flavobacteriia	Flavobacteriales	Flavobacteriaceae	Flavobacterium
OTU1292	0.00	0.04	0.04	0.01	0.02	Proteobact.	γ-proteobact.	Pseudomonadales	Pseudomonad.	Pseudomonas
574722	0.01	0.04	0.08	0.04	0.00	Proteobact.	β-proteobact.	Burkholderiales	Comamonad.	
OTU983	0.03	0.04	0.01	0.01	0.01	Proteobact.	α-proteobact.			
580078	0.01	0.03	0.10	0.02	0.00	Proteobact.	γ-proteobact.	Alteromonadales	Chromatiaceae	Rheinheimera
OTU948	0.03	0.03	0.09	0.01	0.00	Unassigned				
OTU555	0.00	0.03	0.06	0.01	0.00	Proteobact.	γ-proteobact.	Pseudomonadales	Pseudomonad.	Pseudomonas
OTU916	0.00	0.03	0.04	0.03	0.00	Bacteroidetes	Flavobacteriia	Flavobacteriales	Flavobacteriaceae	Flavobacterium
OTU1052	0.01	0.03	0.01	0.11	0.45	Proteobact.	β-proteobact.	Burkholderiales	Comamonad.	
4017244	35.99	0.03	0.02	0.03	0.05	Spirochaetes	[Leptospirae]	[Leptospirales]	Leptospiraceae	Turneriella
578606	0.01	0.02	0.12	0.01	0.00	Proteobact.	γ-proteobact.	Pseudomonadales	Pseudomonad.	
616184	0.00	0.02	0.09	0.00	0.00	Proteobact.	α-proteobact.	Sphingomonadales	Sphingomonadaceae	Sphingomonas
OTU487	0.00	0.02	0.00	0.34	0.36	Proteobact.	β-proteobact.	Burkholderiales	Comamonad.	
OTU77	0.00	0.02	0.01	0.08	0.03	Proteobact.	γ-proteobact.			
OTU1091	0.00	0.02	0.00	0.13	0.11	Proteobact.	β-proteobact.	Burkholderiales		
OTU483	0.01	0.01	0.13	0.03	0.00	Proteobact.	γ-proteobact.	Legionellales	Legionellaceae	
40352	0.00	0.01	0.07	0.05	0.02	Bacteroidetes	Sphingobacteriia	Sphingobacteriales		
OTU863	0.00	0.01	0.01	0.22	0.22	Proteobact.	β-proteobact.	Burkholderiales	Comamonad.	Acidovorax

OTU78	0.15	0.01	0.00	0.01	0.00	Bacteroidetes	Flavobacteriia	Flavobacteriales	Flavobacteriaceae	Flavobacterium
143253	0.00	0.01	0.12	0.03	0.00	Proteobact.	β-proteobact.	Rhodocyclales	Rhodocyclaceae	
OTU418	0.01	0.01	0.01	0.03	0.41	Proteobact.	β-proteobact.	Burkholderiales	Comamonad.	
OTU339	0.00	0.00	0.04	0.10	0.24	Proteobact.	α-proteobact.	Rickettsiales		
1145471	0.00	0.00	0.04	0.91	13.08	Proteobact.	β-proteobact.	Burkholderiales	Comamonad.	
OTU674	0.45	0.00	0.00	0.00	0.01	Spirochaetes	Leptospirae	Leptospirales	Leptospiraceae	Turneriella
1108726	0.00	0.00	0.08	0.33	0.34	Proteobact.	β-proteobact.	Burkholderiales	Comamonad.	Rubrivivax
538346	0.00	0.00	0.06	0.01	28.12	Bacteroidetes	Saprospirae	Saprospirales	Saprospiraceae	
1116384	0.18	0.00	0.02	0.02	0.01	Proteobact.	β-proteobact.	Burkholderiales	Comamonad.	
OTU481	0.00	0.00	0.00	0.00	2.27	Proteobact.	γ-proteobact.	Legionellales	Legionellaceae	
581640	0.00	0.00	0.01	0.01	0.13	Proteobact.	β-proteobact.	Burkholderiales	Comamonad.	
OTU150	0.00	0.00	0.00	0.00	1.45	Proteobact.	α-proteobact.	Rhizobiales		
OTU1132	0.00	0.00	0.00	0.00	1.17	Unassigned				
4306966	0.00	0.00	0.00	0.00	1.15	Proteobact.	α-proteobact.	Rhizobiales	Hyphomicrobiaceae	Hyphomicrobium
366100	0.00	0.00	0.00	0.00	0.99	TM6	SJA-4			
590266	0.00	0.00	0.00	0.00	0.77	Proteobact.	α-proteobact.	Rhodobacterales	Hyphomonadaceae	
511723	0.00	0.00	0.00	0.00	0.74	Proteobact.	β-proteobact.	Rhodocyclales	Rhodocyclaceae	
812595	0.00	0.00	0.00	0.00	0.55	Proteobact.	δ-proteobact.	Myxococcales		
OTU875	0.00	0.00	0.00	0.00	0.39	Unassigned				
22253	0.00	0.00	0.00	0.00	0.35	Proteobact.	γ-proteobact.	Legionellales	Coxiellaceae	
566212	0.00	0.00	0.00	0.00	0.29	Proteobact.	α-proteobact.	Rhizobiales	Hyphomicrobiaceae	Hyphomicrobium
4333746	0.00	0.00	0.00	0.00	0.22	Proteobact.	α-proteobact.	Rhodobacterales	Rhodobacteraceae	Rhodobacter
702015	0.00	0.00	0.00	0.00	0.18	Bacteroidetes	Sphingobacteriia	Sphingobacteriales		

679997	0.00	0.00	0.00	0.00	0.18	Proteobact.	α-proteobact.	Rhodospirillales	Rhodospirillaceae	
665228	0.00	0.00	0.00	0.00	0.17	Bacteroidetes	Saprospirae	Saprospirales	Chitinophagaceae	
822806	0.00	0.00	0.00	0.00	0.13	Chloroflexi	Anaerolineae	SBR1031	A4b	
3995177	0.00	0.00	0.00	0.00	0.06	Proteobact.	α-proteobact.	Rhizobiales	Hyphomicrobiaceae	Hyphomicrobium
719608	0.00	0.00	0.00	0.00	0.05	Proteobact.	α-proteobact.	Rhizobiales	Rhizobiaceae	
735795	0.04	0.00	0.00	0.00	0.03	Proteobact.	α-proteobact.	Rhizobiales		
4385991	0.00	0.00	0.00	0.00	0.02	Proteobact.	α-proteobact.	Rhizobiales		
OTU230	0.00	0.00	0.00	0.00	0.02	Proteobact.	δ-proteobact.	Bdellovibrionales	Bdellovibrionaceae	Bdellovibrio
4312803	0.00	0.00	0.00	0.00	0.01	Proteobact.	α-proteobact.	Rhizobiales	Hyphomicrobiaceae	Devosia
OTU343	0.00	0.00	0.00	0.00	0.01	Proteobact.	α-proteobact.	Rhizobiales	Hyphomicrobiaceae	Hyphomicrobium
4323379	0.00	0.00	0.00	0.00	0.22	Proteobact.	β-proteobact.	Burkholderiales	Comamonad.	
672144	0.00	0.00	0.00	0.00	0.04	Proteobact.	β-proteobact.	Burkholderiales	Comamonad.	
1088305	0.11	0.00	0.00	0.00	0.00	Actinobacteria	Actinobacteria	Actinomycetales	Corynebacteriaceae	Corynebacterium
OTU420	0.00	0.00	0.00	0.01	0.29	Proteobact.	β-proteobact.	Burkholderiales	Comamonad.	
494367	0.00	0.00	0.00	0.01	0.00	Proteobact.	α-proteobact.	Rhizobiales	Rhizobiaceae	Agrobacterium
553551	0.00	0.00	0.00	0.03	0.25	Proteobact.	β-proteobact.	Burkholderiales	Comamonad.	

Supplementary Table 3. Overview of annotation results. The significantly increased mass traces from the microbe-containing versus germ-free polyps (FC > 1.5, p < 0.05) were searched for across the mass spectra of the microbial species and the active extracts. Six of these mass traces were present in all three datasets, and four could be annotated.

mz	Datasets	Adducts	Formulae	Cmpds
349.1423	All datasets	M+Cl	C16H26O6	3
363.1216	All datasets	M+Cl	C16H24O7	8
363.158	All datasets	M-H	C16H29O7P	1
365.1373	All datasets	M+Cl	C16H26O7	16
347.1267	All datasets	N/A	N/A	0
361.1423	All datasets	N/A	N/A	0
343.1318	*Hydra*+Extracts	M+Cl	C17H24O5	5
361.1504	*Hydra*+Extracts	M+FA-H	C15H24O7	2
369.1685	*Hydra*+Extracts	M+Cl, M-H	C16H30O7, C20H27NaO5	6
172.0979	Microbe+Extracts	M+FA-H, M-H	C7H13NO, C8H15NO3	14
186.1136	Microbe+Extracts	M+FA-H, M-H	C8H15NO, C9H17NO3	14
187.0976	Microbe+Extracts	M+FA-H, M-H	C8H14O2, C9H16O4	71
200.1292	Microbe+Extracts	M+FA-H, M-H	C10H19NO3, C9H17NO	8
201.0768	Microbe+Extracts	M+FA-H, M-H	C8H12O3, C9H14O5	5
201.1132	Microbe+Extracts	M+FA-H, M-H	C10H18O4, C9H16O2	63
202.1085	Microbe+Extracts	M+FA-H, M-H	C8H15NO2, C9H17NO4	11
207.0121	Microbe+Extracts	M-H	C10H8O3S	2
214.1085	Microbe+Extracts	M+FA-H, M-H	C10H17NO4, C9H15NO2	54
214.1449	Microbe+Extracts	M+FA-H, M-H	C10H19NO, C11H21NO3	4
215.0328	Microbe+Extracts	M+Cl, M-H	C5H13O7P, C6H12O6	60
215.0925	Microbe+Extracts	M+FA-H	C9H14O3	4
231.0874	Microbe+Extracts	M+FA-H, M-H	C10H16O6, C9H14O4	4
239.0804	Microbe+Extracts	M+Cl	C8H16N2O4	10
239.1289	Microbe+Extracts	M+FA-H	C12H18O2	26
240.0644	Microbe+Extracts	M+Cl	C8H15NO5	5
240.1008	Microbe+Extracts	M+Cl	C9H19NO4	1
241.1081	Microbe+Extracts	M+FA-H	C11H16O3	6
242.1762	Microbe+Extracts	M+FA-H, M-H	C12H23NO, C13H25NO3	2
243.0641	Microbe+Extracts	M+Cl	C8H16O6	2
243.1238	Microbe+Extracts	M-H	C12H20O5	1
243.1602	Microbe+Extracts	M+FA-H, M-H	C12H22O2, C13H24O4	71
250.0932	Microbe+Extracts	M+FA-H, M-H	C8H15NO5, C9H17NO7	8
253.1445	Microbe+Extracts	M+FA-H, M-H	C13H20O2, C14H22O4	18
256.0593	Microbe+Extracts	M+Cl, M-H	C7H16NO7P, C8H15NO6	20
257.1031	Microbe+Extracts	M+FA-H, M-H	C11H16O4, C12H18O6	3

257.1394	Microbe+Extracts	M+FA-H	C12H20O3	18
259.1187	Microbe+Extracts	M+FA-H, M-H	C11H18O4, C12H20O6	5
261.1344	Microbe+Extracts	M+FA-H, M-H	C11H20O4, C12H22O6	4
262.0932	Microbe+Extracts	M-H	C10H17NO7	1
263.1168	Microbe+Extracts	M+Cl	C11H20N2O3	7
268.0957	Microbe+Extracts	M+Cl	C10H19NO5	1
269.1312	Microbe+Extracts	M+Cl	C15H22O2	78
269.1394	Microbe+Extracts	M+FA-H	C13H20O3	14
271.1187	Microbe+Extracts	M+FA-H	C12H18O4	7
273.098	Microbe+Extracts	M+FA-H, M-H	C11H16O5, C12H18O7	3
273.1344	Microbe+Extracts	M+FA-H	C12H20O4	7
277.1445	Microbe+Extracts	M+FA-H, M-H	C15H20O2, C16H22O4	58
283.1551	Microbe+Extracts	M+FA-H, M-H	C14H22O3, C15H24O5	9
285.2071	Microbe+Extracts	M+FA-H, M-H	C15H28O2, C16H30O4	52
287.15	Microbe+Extracts	M+FA-H	C13H22O4	2
289.1212	Microbe+Extracts	M+Cl	C14H22O4	2
291.2096	Microbe+Extracts	M+Cl	C16H32O2	32
292.1038	Microbe+Extracts	M+FA-H, M-H	C10H17NO6, C11H19NO8	9
293.1792	Microbe+Extracts	M-H	C14H30O4S	1
295.1398	Microbe+Extracts	M+FA-H	C11H22O6	1
298.0699	Microbe+Extracts	M+Cl, M-H	C10H17NO7, C9H18NO8P	3
299.15	Microbe+Extracts	M+FA-H	C14H22O4	2
301.1293	Microbe+Extracts	M+FA-H, M-H	C13H20O5, C14H22O7	3
301.1657	Microbe+Extracts	M+FA-H, M-H	C14H24O4, C15H26O6	3
302.1245	Microbe+Extracts	M-H	C13H21NO7	1
302.1609	Microbe+Extracts	M+FA-H, M-H	C13H23NO4, C14H25NO6	2
303.1369	Microbe+Extracts	M+Cl	C15H24O4	9
307.2045	Microbe+Extracts	M+Cl	C16H32O3	29
309.1014	Microbe+Extracts	M+Cl, M+FA-H	C11H20O5S, C15H18N2O3	4
309.1707	Microbe+Extracts	M+FA-H, M-H	C16H24O3, C17H26O5	9
309.1741	Microbe+Extracts	M+Cl	C17H26N2O	5
311.2228	Microbe+Extracts	M+FA-H, M-H	C17H30O2, C18H32O4	69
313.1576	Microbe+Extracts	M+Cl	C17H26O3	7
313.2384	Microbe+Extracts	M+FA-H, M-H	C17H32O2, C18H34O4	103
315.1813	Microbe+Extracts	M+FA-H, M-H	C15H26O4, C16H28O6	9
319.2409	Microbe+Extracts	M+Cl	C18H36O2	27
320.1998	Microbe+Extracts	M+Cl	C16H31NO3	1
322.2154	Microbe+Extracts	M+Cl	C16H33NO3	2
323.1267	Microbe+Extracts	M-H	C13H25O7P	1
328.213	Microbe+Extracts	M+FA-H, M-H	C16H29NO3, C17H31NO5	4

329.1525	Microbe+Extracts	M+Cl	C17H26O4	7
333.111	Microbe+Extracts	M+Cl	C15H22O6	5
335.1631	Microbe+Extracts	M+Cl	C16H28O5	3
336.1583	Microbe+Extracts	M+Cl	C15H27NO5	1
337.1787	Microbe+Extracts	M+Cl	C16H30O5	2
341.1372	Microbe+Extracts	M+Cl	C14H26O7	1
343.1682	Microbe+Extracts	M+Cl	C18H28O4	29
343.2126	Microbe+Extracts	M+FA-H, M-H	C17H30O4, C18H32O6	136
344.1998	Microbe+Extracts	M+Cl	C18H31NO3	1
345.1474	Microbe+Extracts	M+Cl	C17H26O5	4
345.1838	Microbe+Extracts	M+Cl	C18H30O4	29
346.2154	Microbe+Extracts	M+Cl	C18H33NO3	1
347.1348	Microbe+Extracts	M+FA-H, M-H	C14H22O7, C15H24O9	2
348.13	Microbe+Extracts	M+FA-H	C13H21NO7	1
348.2311	Microbe+Extracts	M+Cl	C18H35NO3	2
358.2235	Microbe+Extracts	M+FA-H	C17H31NO4	3
359.1631	Microbe+Extracts	M+Cl	C18H28O5	5
360.1947	Microbe+Extracts	M+Cl	C18H31NO4	10
360.2392	Microbe+Extracts	M+FA-H	C17H33NO4	3
361.1787	Microbe+Extracts	M+Cl	C18H30O5	42
362.2104	Microbe+Extracts	M+Cl	C18H33NO4	4
363.1944	Microbe+Extracts	M+Cl	C18H32O5	32
364.226	Microbe+Extracts	M+Cl, M-H	C17H36NO5P, C18H35NO4	3
365.1737	Microbe+Extracts	M-H	C21H25F3O2	1
365.21	Microbe+Extracts	M+Cl	C18H34O5	17
366.2417	Microbe+Extracts	M-H	C17H38NO5P	1
367.1529	Microbe+Extracts	M+Cl, M-H	C15H29O8P, C16H28O7	18
367.1893	Microbe+Extracts	M-H	C16H33O7P	3
375.158	Microbe+Extracts	M+Cl	C18H28O6	3
377.0856	Microbe+Extracts	M+Cl	C12H22O11	60
377.1737	Microbe+Extracts	M+Cl	C18H30O6	5
379.1893	Microbe+Extracts	M+Cl, M-H	C17H33O7P, C18H32O6	135
380.2209	Microbe+Extracts	M+Cl, M+FA-H	C18H35NO5, C20H31O4	3
381.1685	Microbe+Extracts	M+Cl	C17H30O7	1
389.1736	Microbe+Extracts	M+Cl, M-H-H2O	C19H30O6, C25H29FO2Si	3
389.21	Microbe+Extracts	M+Cl	C20H34O5	108
391.1893	Microbe+Extracts	M+Cl	C19H32O6	15
393.2049	Microbe+Extracts	M-H	C18H35O7P	1
394.2002	Microbe+Extracts	M+FA-H	C20H29O5	1
396.2158	Microbe+Extracts	M+FA-H, M-H	C16H34NO5P, C17H36NO7P, C20H31O5	6

405.1897	Microbe+Extracts	M+Cl	C16H34O9	1
409.1998	Microbe+Extracts	M+Cl	C19H34O7	1
411.1791	Microbe+Extracts	M+Cl, M+FA-H	C18H32O8, C21H25F3O2	2
419.2206	Microbe+Extracts	M-H	C20H37O7P	1
423.2155	Microbe+Extracts	M+Cl, M-H	C19H37O8P, C20H36O7	2
431.2206	Microbe+Extracts	M+Cl, M-H	C21H37O7P, C22H36O6	7
441.2527	Microbe+Extracts	M+Cl	C23H38N2O4	1
473.2826	Microbe+Extracts	M+Cl	C29H42O3	2
479.1478	Microbe+Extracts	M+Cl, M+FA-H, M-H	C23H27ClO6, C24H28O8, C24H29ClO8	3
265.1479	Microbe+Extracts	N/A	N/A	0
287.1136	Microbe+Extracts	N/A	N/A	0
293.1161	Microbe+Extracts	N/A	N/A	0
297.153	Microbe+Extracts	N/A	N/A	0
305.1161	Microbe+Extracts	N/A	N/A	0
307.1318	Microbe+Extracts	N/A	N/A	0
309.111	Microbe+Extracts	N/A	N/A	0
321.111	Microbe+Extracts	N/A	N/A	0
321.1474	Microbe+Extracts	N/A	N/A	0
321.2105	Microbe+Extracts	N/A	N/A	0
335.1267	Microbe+Extracts	N/A	N/A	0
337.2054	Microbe+Extracts	N/A	N/A	0
339.1216	Microbe+Extracts	N/A	N/A	0
339.158	Microbe+Extracts	N/A	N/A	0
339.1999	Microbe+Extracts	N/A	N/A	0
349.106	Microbe+Extracts	N/A	N/A	0
353.2003	Microbe+Extracts	N/A	N/A	0
355.2239	Microbe+Extracts	N/A	N/A	0
367.2441	Microbe+Extracts	N/A	N/A	0
371.2552	Microbe+Extracts	N/A	N/A	0
378.2053	Microbe+Extracts	N/A	N/A	0
379.1529	Microbe+Extracts	N/A	N/A	0
381.2316	Microbe+Extracts	N/A	N/A	0
381.2597	Microbe+Extracts	N/A	N/A	0
393.1686	Microbe+Extracts	N/A	N/A	0
395.1842	Microbe+Extracts	N/A	N/A	0
395.2754	Microbe+Extracts	N/A	N/A	0
407.2318	Microbe+Extracts	N/A	N/A	0
449.2159	Microbe+Extracts	N/A	N/A	0

Supplementary Table 4. Putative annotations for the six mass traces that were high in control animals, and present in microbial cultures, as well as the original bioactive extracts.

m/z	Adduct	Name	Formula
365.1373	M+Cl	Picrocrocin	C16H26O7
365.1373	M+Cl	8-Epiiridodial glucoside	C16H26O7
365.1373	M+Cl	Iridodial glucoside	C16H26O7
365.1373	M+Cl	Tetranor-PGFM	C16H26O7
365.1373	M+Cl	(3b,4b,5b)-4,5-Epoxy-p-menth-1-en-3-ol 3-glucoside	C16H26O7
365.1373	M+Cl	(1R,4R,5S)-5-Hydroxyfenchone glucoside	C16H26O7
365.1373	M+Cl	(4S,6R)-p-Mentha-1,8-diene-6,7-diol 7-glucoside	C16H26O7
365.1373	M+Cl	(1R,4S,6R)-6-Hydroxyfenchone glucoside	C16H26O7
365.1373	M+Cl	6-Hydroxy-2-bornanone glucoside	C16H26O7
365.1373	M+Cl	(1S,4R)-10-Hydroxyfenchone glucoside	C16H26O7
365.1373	M+Cl	Portuloside A	C16H26O7
365.1373	M+Cl	Epijasminoside A	C16H26O7
365.1373	M+Cl	Schizonepetoside C	C16H26O7
365.1373	M+Cl	Schizonepetoside D	C16H26O7
365.1373	M+Cl	Schizonepetoside B	C16H26O7
365.1373	M+Cl	Schizonepetoside A	C16H26O7
347.1267	N/A	No compounds found	N/A
361.1423	N/A	No compounds found	N/A
349.1423	M+Cl	(-)-trans-Carveol glucoside	C16H26O6
349.1423	M+Cl	Perilloside A	C16H26O6
349.1423	M+Cl	(+)-trans-Carveol glucoside	C16H26O6
363.1216	M+Cl	Tetranor-PGDM	C16H24O7
363.1216	M+Cl	Tetranor-PGEM	C16H24O7
363.1216	M+Cl	Prostaglandin M	C16H24O7
363.1216	M+Cl	3-Hydroxy-4-isopropylbenzyl alcohol 3-glucoside	C16H24O7
363.1216	M+Cl	Cymorcin monoglucoside	C16H24O7
363.1216	M+Cl	Perilloside B	C16H24O7
363.1216	M+Cl	PGDM	C16H24O7
363.1216	M+Cl	Rhododendrin	C16H24O7
363.158	M-H	(10S)-Juvenile hormone III diol phosphate	C16H29O7P

Supplementary Table 5. List of significantly different mass traces identified in the 5-microbe extracts compared to the microbe-free extracts. FC = Fold change.

Compound Annotation or m/z	FC	P value
159.06522	45.196	0.00219
241.06836	42.112	0.011505
377.21485	30.427	0.0039034
159.03291	29.342	0.038282
218.92487	18.489	0.037108
203.07658	18.062	0.030476
61.06477	16.211	0.018825
157.08592	14.799	0.0011041
239.0891	13.297	0.0090042
127.99582	12.708	0.0004809
161.06589	12.38	0.026745
330.04698	11.71	0.0017695
333.18847	10.826	0.0038577
121.12234	9.5934	0.045459
289.16228	9.5409	0.0026088
358.25928	9.282	0.0061549
194.96333	9.0915	0.0075706
311.18306	9.0425	0.020648
308.22226	8.6565	0.043266
299.27363	8.519	0.0084894
255.06412	8.3876	0.02429
269.09968	8.3333	0.010612
217.05598	8.1324	0.044387
94.99051	7.8469	0.0056242
228.08238	7.7645	0.039843
335.16038	7.733	0.0016424
346.02482	7.519	0.040272
321.18124	7.4887	0.017584
365.19375	7.4079	0.028266
421.24121	7.3514	0.023126
103.11172	7.2749	0.03361
95.04914	7.2699	0.03106
121.08595	7.2302	0.0060323
372.19213	6.9542	0.0076808
153.12739	6.7353	0.021155
269.14958	6.7125	0.0019956
171.13796	6.6987	0.048703
287.27349	6.6612	0.021473
331.17272	6.3317	0.037744
191.17946	6.1279	0.022193
161.01222	5.8939	0.045928

206.60974	5.8622	0.02454
305.14963	5.7644	0.032026
312.16699	5.7065	0.035063
202.18026	5.4756	0.027044
399.26179	5.4685	0.043563
449.23581	5.1363	0.031483
180.89451	5.0748	0.02421
151.14812	5.0012	0.013689
247.13058	4.9666	0.043288
177.16381	4.9459	0.021327
209.19011	4.8284	0.022399
79.07534	4.7616	0.0085236
327.26598	4.7219	0.020177
350.71069	4.6933	0.0046592
231.11296	4.6081	0.017219
267.00288	4.5913	0.0031632
226.0753	4.5499	0.042782
273.16738	4.5011	0.0078083
215.01639	4.4521	0.0054217
256.19187	4.3878	0.0093341
259.16534	4.3138	0.034084
303.1414	4.3132	0.010888
149.02334	4.2935	0.0158
254.21156	4.219	0.048314
311.19657	4.2139	0.02333
128.10701	4.1754	0.030996
245.13599	4.139	0.0047686
481.26181	4.0426	0.029492
215.20069	4.0352	0.017745
184.13327	3.872	0.044534
159.13795	3.8682	0.039852
198.14895	3.8409	0.02997
163.14817	3.8131	0.047985
263.23702	3.738	0.04292
236.97404	3.6686	0.0071499
231.21088	3.4986	0.033481
437.23567	3.4788	0.045879
255.2068	3.4687	0.049746
259.2422	3.4195	0.030844
219.21088	3.2045	0.0059876
251.23708	2.9925	0.024608
212.16468	2.9718	0.0099306
223.20578	2.953	0.025546
233.22648	2.934	0.010763

123.11683	2.7659	0.017555
226.18026	2.7331	0.006592
343.20104	2.6851	0.037737
246.20648	2.6503	0.0079126
109.10119	2.5494	0.0076535
81.06986	2.5238	0.006989
125.09611	2.5114	0.045664
471.30661	2.5094	0.0098604
83.08551	2.48	0.00499
97.06478	2.4399	0.0022341
247.24212	2.4379	0.0023224
243.12034	2.4301	0.037638
257.18613	2.4039	0.01059
84.08076	2.392	0.0057853
433.38142	2.3767	0.038496
191.01671	2.3645	0.046831
95.08553	2.317	0.0077261
125.13249	2.3129	0.021972
73.06477	2.3055	0.043272
85.10117	2.2842	0.0015546
137.1325	2.2831	0.012817
Isovalerate	2.2496	0.0049257
367.2456	2.2029	0.043019
129.05462	2.151	0.0053057
71.08552	2.1469	0.011131
275.11012	2.1383	0.0064594
111.11684	2.1329	0.0099219
474.23464	2.1216	0.011877
393.20987	2.0543	0.038099
256.26351	2.0368	0.0084104
97.10118	2.0263	0.0009323
349.18343	1.688	0.020825
221.07437	1.6573	0.04289
147.06521	1.6473	0.0044027
195.06285	1.6231	0.032849
183.06283	1.5611	0.0049553
gamma-Aminobutyric acid	1.5475	0.019205
427.28082	1.5169	0.035667
329.19333	0.53523	0.046665
425.21463	0.51058	0.03791
415.2543	0.46092	0.04131
296.19682	0.40483	0.025747
132.10192	0.35666	0.010314
199.14418	0.34509	0.033525

273.11839	0.321	0.038474
104.9923	0.30399	0.036902
385.22234	0.29175	0.038335
357.15426	0.27089	0.030332
408.24679	0.2637	0.0054796
254.16473	0.26293	0.016037
353.2298	0.23991	0.042711
181.0948	0.23408	0.018045
453.24523	0.22527	0.03479
422.26207	0.22433	0.018687
269.09443	0.2118	0.024439
389.25094	0.20893	0.0015856
289.09229	0.20068	0.030814
450.29338	0.1942	0.021207
279.10286	0.19106	0.0050733
227.17551	0.19085	0.0029881
210.11791	0.18845	0.026753
327.25463	0.17848	0.039168
419.21328	0.17497	0.046248
86.09641	0.17488	0.044536
263.15304	0.17216	0.0029298
361.20988	0.16751	0.026841
129.10225	0.16329	0.034689
213.15985	0.16285	0.0039114
440.25048	0.16157	0.017233
147.11279	0.15214	0.012095
323.19357	0.15103	0.043893
392.25436	0.13941	0.0083151
L-Proline/2-Pyrrolidinecarboxylic acid	0.13837	0.0044961
439.26508	0.12996	0.019012
186.99546	0.12454	0.023306
433.22819	0.11675	0.047504
437.25065	0.10834	0.0040371
361.24657	0.10301	0.0018655
348.17406	0.1011	0.0094894
120.0808	0.094588	0.029008
185.16484	0.091051	0.030076
314.20741	0.089273	4.36E-05
446.24343	0.088624	0.0067828
371.22894	0.076292	0.0023423
288.19193	0.076028	0.0092515
269.16085	0.072566	0.0095935
143.11791	0.071079	0.0079823
166.08626	0.061151	0.0080638

215.13912	0.055545	0.009785
394.23365	0.054866	0.0011711
338.18391	0.053717	0.0022466
199.18054	0.051347	0.016673
228.1707	0.042135	0.0037189
233.16494	0.037195	0.014852
338.18225	0.03695	0.0017223
229.15478	0.036038	0.0020339
213.12349	0.031589	0.0070103
263.13919	0.026372	0.0014493
286.17625	0.026042	0.0015231
245.18609	0.023201	0.0026526
329.14965	0.015588	0.0057941
326.20921	0.014896	1.49E-05
205.09722	0.013446	0.0057336
326.20755	0.013346	0.00014604
136.06177	0.010713	0.0021802
294.18132	0.0087617	0.00050776
260.19703	0.0067451	0.00028824
279.17052	0.0055888	0.00021284
342.2391	0.0019176	2.55E-05
328.22341	0.0014118	1.39E-05
288.20324	0.00098907	6.74E-05
Adenosine	0.00030202	8.28E-05

Supplementary Table 6. Percent abundance of the OTUs present in the native microbiota extract with manual annotation of the main colonizing species of *Hydra.* The percent abundance (%) does not reflect the abundances on the polyps as the bacteria have very different growth rates *in vivo* compared to *in vivo.*

OTU ID	%	Phylum	Class	Order	Family	Genus
OTU17	57.23	Proteobacteria	Betaproteobacteria	Burkholderiales	Comamonadaceae	
750018	11.04	Proteobacteria	Gammaproteobacteria	Pseudomonadales	Pseudomonadaceae	Pseudomonas
OTU2 (Undibacterium)	8.31	Proteobacteria	Betaproteobacteria	Burkholderiales	Oxalobacteraceae	
750411 (Curvibacter)	4.29	Proteobacteria	Betaproteobacteria	Burkholderiales	Comamonadaceae	
839235	2.85	Proteobacteria	Gammaproteobacteria	Aeromonadales	Aeromonadaceae	
545507 (Acidovorax)	1.65	Proteobacteria	Betaproteobacteria	Burkholderiales	Comamonadaceae	Acidovorax
587804	1.22	Proteobacteria	Betaproteobacteria	Burkholderiales	Comamonadaceae	
OTU6	1.18	Proteobacteria	Gammaproteobacteria	Pseudomonadales	Pseudomonadaceae	
33410	0.99	Proteobacteria	Betaproteobacteria	Burkholderiales	Comamonadaceae	
OTU4	0.82	Proteobacteria	Betaproteobacteria	Burkholderiales	Oxalobacteraceae	
1136510	0.78	Proteobacteria	Betaproteobacteria	Burkholderiales	Comamonadaceae	
OTU1066	0.66	Proteobacteria	Betaproteobacteria	Burkholderiales	Comamonadaceae	
256215	0.58	Proteobacteria	Gammaproteobacteria	Pseudomonadales	Pseudomonadaceae	Pseudomonas
541859	0.55	Proteobacteria	Gammaproteobacteria	Pseudomonadales	Pseudomonadaceae	Pseudomonas
OTU6664	0.43	Proteobacteria	Gammaproteobacteria	Pseudomonadales	Pseudomonadaceae	Pseudomonas
OTU6919	0.52	Proteobacteria	Betaproteobacteria	Burkholderiales	Comamonadaceae	
OTU7933	0.40	Proteobacteria	Betaproteobacteria	Burkholderiales	Comamonadaceae	Acidovorax
OTU20	0.36	Proteobacteria	Gammaproteobacteria	Aeromonadales	Aeromonadaceae	
764682	0.35	Proteobacteria	Gammaproteobacteria	Pseudomonadales	Pseudomonadaceae	Pseudomonas
578606	0.36	Proteobacteria	Gammaproteobacteria	Pseudomonadales	Pseudomonadaceae	Pseudomonas
837574	0.29	Proteobacteria	Gammaproteobacteria	Aeromonadales	Aeromonadaceae	
OTU16015	0.35	Proteobacteria	Betaproteobacteria	Burkholderiales	Comamonadaceae	
OTU14	0.30	Proteobacteria	Betaproteobacteria	Burkholderiales	Comamonadaceae	
OTU16816	0.27	Proteobacteria	Gammaproteobacteria	Pseudomonadales	Pseudomonadaceae	
731748	0.28	Proteobacteria	Betaproteobacteria	Burkholderiales	Comamonadaceae	
141316	0.24	Proteobacteria	Betaproteobacteria	Burkholderiales		

OTU5768	0.25	Proteobacteria	Betaproteobacteria	Burkholderiales	Comamonadaceae	
OTU15407	0.23	Proteobacteria	Betaproteobacteria	Burkholderiales	Comamonadaceae	
4391034 (Pelomonas)	0.22	Proteobacteria	Betaproteobacteria	Burkholderiales	Comamonadaceae	
OTU597	0.24	Proteobacteria	Betaproteobacteria	Burkholderiales	Comamonadaceae	
OTU5533	0.25	Proteobacteria	Gammaproteobacteria	Pseudomonadales	Pseudomonadaceae	Pseudomonas
549837	0.20	Proteobacteria	Gammaproteobacteria	Pseudomonadales	Pseudomonadaceae	Pseudomonas
OTU11809	0.20	Proteobacteria	Gammaproteobacteria	Pseudomonadales	Pseudomonadaceae	Pseudomonas
OTU8046	0.16	Unassigned				
OTU6895	0.14	Proteobacteria	Gammaproteobacteria	Aeromonadales	Aeromonadaceae	
OTU5045	0.16	Proteobacteria	Betaproteobacteria	Burkholderiales	Comamonadaceae	Acidovorax
574721	0.16	Proteobacteria	Betaproteobacteria	Burkholderiales	Comamonadaceae	
OTU7613	0.13	Proteobacteria	Betaproteobacteria	Burkholderiales	Comamonadaceae	
797572	0.10	Proteobacteria	Betaproteobacteria	Burkholderiales	Comamonadaceae	
833853	0.10	Proteobacteria	Betaproteobacteria	Burkholderiales	Comamonadaceae	
OTU16676	0.08	Proteobacteria	Betaproteobacteria	Burkholderiales	Comamonadaceae	
336824	0.09	Proteobacteria	Betaproteobacteria	Burkholderiales	Comamonadaceae	
OTU12776	0.07	Proteobacteria	Betaproteobacteria	Burkholderiales	Comamonadaceae	
OTU13535	0.07	Proteobacteria	Gammaproteobacteria	Aeromonadales	Aeromonadaceae	
141042	0.06	Proteobacteria	Betaproteobacteria	Burkholderiales	Comamonadaceae	
4408559	0.07	Proteobacteria	Betaproteobacteria	Burkholderiales	Comamonadaceae	
OTU14782	0.05	Proteobacteria	Betaproteobacteria	Burkholderiales		
513078	0.04	Proteobacteria	Gammaproteobacteria	Pseudomonadales	Pseudomonadaceae	Pseudomonas
OTU5866	0.04	Proteobacteria	Gammaproteobacteria	Aeromonadales	Aeromonadaceae	
OTU11843	0.05	Proteobacteria	Betaproteobacteria	Burkholderiales	Comamonadaceae	
OTU14860	0.04	Proteobacteria	Gammaproteobacteria	Pseudomonadales	Pseudomonadaceae	Pseudomonas
OTU4254	0.04	Proteobacteria	Betaproteobacteria	Burkholderiales	Comamonadaceae	
OTU11087	0.04	Proteobacteria	Betaproteobacteria	Burkholderiales	Oxalobacteraceae	
OTU1278	0.04	Proteobacteria	Betaproteobacteria	Burkholderiales	Comamonadaceae	
OTU10168	0.04	Proteobacteria	Gammaproteobacteria	Pseudomonadales	Pseudomonadaceae	Pseudomonas
719367	0.04	Proteobacteria	Betaproteobacteria	Burkholderiales	Comamonadaceae	

354682	0.04	Proteobacteria	Betaproteobacteria	Burkholderiales	Comamonadaceae	
OTU16170	0.04	Proteobacteria	Betaproteobacteria	Burkholderiales	Comamonadaceae	Rhodoferax
OTU2749	0.03	Proteobacteria	Betaproteobacteria	Burkholderiales		
2742255	0.03	Proteobacteria	Betaproteobacteria	Burkholderiales	Comamonadaceae	
674815	0.03	Proteobacteria	Betaproteobacteria	Burkholderiales	Comamonadaceae	
OTU10046	0.03	Proteobacteria	Gammaproteobacteria			
OTU13513	0.03	Proteobacteria	Betaproteobacteria	Burkholderiales	Comamonadaceae	
OTU2254	0.03	Proteobacteria	Betaproteobacteria	Burkholderiales	Comamonadaceae	
OTU8617	0.03	Proteobacteria	Gammaproteobacteria	Aeromonadales	Aeromonadaceae	